



OIL EXPLORATION PERMIT EP 325
EXMOUTH GULF
WESTERN AUSTRALIA

PUBLIC ENVIRONMENTAL REPORT

VOLUME 3 — OIL SPILL TRAJECTORY ANALYSIS

DoE Information Centre



016589

Prepared by Steedman Limited

622.323(26)

LEP

Vol. 3

July 1988

o r a R e s o u r c e s N L

622.323(26)
LEP
copy B
901276B
16019

LIBRARY / INFORMATION CENTRE
DEPARTMENT OF ENVIRONMENT
168 ST GEORGE'S TERRACE
PERTH

Prediction of Oil Spill
Envelopes for the Proposed
Whalebone Prospect and Rivoli Prospect
Exploration Wells, Exmouth Gulf

prepared for
LeProvost, Semeniuk & Chalmer
Environmental Consultants

by
K.L. Russell

Checked by
J.R. Andrewartha and S.J. Buchan

ENVIRONMENTAL PROTECTION AUTHORITY
1 MOUNT STREET, PERTH

Steedman Limited
July 15, 1988
Job No AS769
Report No R395
Copy No.



STEEDMAN LIMITED

(Incorporated in Western Australia)

APPLIED SCIENCE AND ENGINEERING

July 15 1988

"Bindarra House"
384 Rokeby Road
Subiaco 6008
Western Australia
Ph. (09) 381 8522
Telex: AA93934
Fax: 381 4484

LeProvost Semeniuk & Chalmer
Environmental Consultants
181 York Street
SUBIACO WA 6008

Attention: Mr Ian LeProvost

Dear Sir

OIL SPILL ENVELOPE PREDICTION
WHALEBONE AND RIVOLI PROSPECTS
EXMOUTH GULF

Further to your letter of March 28, 1988, we submit our report (R395) titled "Prediction of Oil spill envelopes for the Proposed Whalebone Prospect and Rivoli Prospect Exploration Wells, Exmouth Gulf".

The report considers the most likely areas that would be affected by an oil spill from the proposed Whalebone Prospect and Rivoli Prospect well locations after 6, 12, 24 and 48 hours for eighteen different scenarios of wind and tide.

Available information was assembled to provide a description of the winds and oceanography in Exmouth Gulf. Two shallow water linear numerical circulation models were used to generate surface currents due to the action of both tides and wind. An oil spill advection model utilized the surface currents to predict oil slick movements and thereby defined the most likely areas affected.

If you require additional information or further interpretation regarding this report, please do not hesitate to contact us.

Yours faithfully
STEEDMAN LIMITED

K L Russell

KLR:SPT:AS769:88432

TABLE OF CONTENTS

1.	INTRODUCTION	1
1.1	Overview	1
1.2	Report Format	2
1.3	Scope of Work	2
2.	WINDS	3
2.1	Synoptic Scale Meteorology	3
2.2	Available Surface Wind Data	3
2.3	Ambient Wind Conditions	4
2.4	Extreme Wind Conditions	5
2.5	Light Wind Conditions	7
3.	OCEANOGRAPHY	8
3.1	Currents	8
3.2	Waves	10
3.3	Water Levels	10
4.	NUMERICAL CIRCULATION MODELS	13
4.1	Selection	13
4.2	Model Grid and Bathymetry	14
4.3	Open Boundary Conditions	14
4.4	2D Model Calibration	15
4.5	Model Results	16
4.6	Coastal Boundary Flow	17
5.	ESTIMATION OF OIL SPILL ENVELOPES	19
5.1	Oil Spill Movement	19
5.2	Oil Spill Model	21
5.3	Model Results	23
6.	CONCLUSIONS	26
7.	REFERENCES.....	28

Tables

Figures

Appendices

LIST OF APPENDICES

- A : Average Monthly Wind Speed and Direction Percentage Occurrence
Matrices for Learmonth Meteorological Office and Exmouth Navy Alpha
for the months November through April
- B : Theory of Wind and Tide Driven Depth-Averaged Coastal Circulation
- C : Extension of Depth-Averaged Circulation to Include Vertical
Structure

LIST OF TABLES

- Table 2.1 Wind data available in the Exmouth Gulf region.
- Table 2.2 Wind speed and direction percentage occurrence matrix for Learmonth Meteorological Office. Data covers the months November to April for 1975/76 to 1984/85.
- Table 2.3 Wind speed and direction percentage occurrence matrix for Exmouth Navy Alpha station. Data covers the months November to April for 1972/73 to 1975/76.
- Table 2.4 Combined wind speed persistence and exceedence matrix for Learmonth Meteorological Office. Data covers the months November to April for 1975/76 to 1984/85.
- Table 2.5 Combined wind speed persistence and exceedence matrix for Exmouth Navy Alpha station. Data covers the months November to April for 1972/73 to 1975/76.
- Table 2.6 Storm types, estimated principal months of occurrence and typical wind speeds and directions.
- Table 3.1 Percentage occurrence matrix of significant wave height and period of wind waves at Whalebone Prospect for the months November to April. Wave heights and period were estimated using the Sverdrup Munk Bretschneider (SMB) relationship. Note that the matrix entries are in tenths of a percent.
- Table 3.2 Percentage occurrence matrix of significant wave height and period of wind waves at Rivoli Prospect for the months November to April. Wave heights and period were estimated using the Sverdrup Munk Bretschneider (SMB) relationship. Note that the matrix entries are in tenths of a percent.
- Table 4.1 Tidal constants for several locations in the vicinity of the model grid.
- Table 4.2 Estimated harmonic constants for the model corners, used to provide tidal forcing along the open sea boundaries.

LIST OF FIGURES

- Figure 1.1 Location diagram showing the position of Exmouth Gulf on the North West Shelf.
- Figure 1.2 Location diagram showing the position of Whalebone and Rivoli Prospects in Exmouth Gulf.
- Figure 2.1 Typical summer and winter synoptic situations over north-western Australia.
- Figure 2.2 Surface synoptic charts showing typical conditions of (a) a tropical cyclone and (b) a pressure gradient storm affecting Exmouth Gulf.
- Figure 2.3 Example of tropical cyclone tracks, July 1973 to 1974 (from Lourenz, 1981).
- Figure 2.4 Average decadal incidence of tropical cyclones in 5° squares (all months) July 1959 to June 1980 (from Lourenz, 1981).
- Figure 4.1 Grid and coastline used with the numerical circulation model.
- Figure 4.2 Contours of digitized bathymetry used with the numerical circulation model. The digitized 'real' coastline is also shown.
- Figure 4.3 Spring tidal depth-average currents, at 3 hourly intervals, predicted by the 2D circulation model. Hour 84 corresponds to 1200 24.11.88.
- Figure 4.4 Spring tidal surface elevation contours, at 3 hourly intervals predicted by the 2D circulation model. Hour 84 corresponds to 1200 24.11.88 and contour interval is 0.05 m.
- Figure 4.5 Neap tidal depth-average currents, at 3 hourly intervals, predicted by the 2D circulation model. Hour 73 corresponds to 0100 3.11.88.
- Figure 4.6 Neap tidal surface elevation contours, at 3 hourly intervals, predicted by the 2D circulation model. Hour 73 corresponds to 0100 3.11.88 and contour interval is 0.05 m.
- Figure 4.7 Surface currents predicted by the 2.5D circulation model for a steady 10 m s^{-1} wind from the
(a) north
(b) north-east
(c) east
(d) south-east.

LIST OF FIGURES (Cont'd)

- Figure 4.8 Surface currents predicted by the 2.5D circulation model for a steady 10 m s^{-1} wind from the
 (a) south
 (b) south-west
 (c) west
 (d) north-west.
- Figure 4.9 Schematic representation of the depth structure of currents forced by cross-shore winds (adapted from Csanady, 1982). The x direction is long-shore.
- Figure 4.10 Schematic representation of the depth structure of currents forced by long-shore winds (adapted from Csanady, 1982). The y direction is cross-shore.
- Figure 5.1 Schematic diagram of oil spill trajectory.
- Figure 5.2 Oil spill envelopes for release times of 6, 12, 24 and 48 hours for the case of spring tides only for Whalebone Prospect.
- Figure 5.3 Oil spill envelopes for release times of 6, 12, 24 and 48 hours for the case of neap tides only for Whalebone Prospect.
- Figure 5.4 Oil spill envelopes for release times of 6, 12, 24 and 48 hours for the case of a 10 m s^{-1} northerly wind during spring tides for Whalebone Prospect.
- Figure 5.5 Oil spill envelopes for release times of 6, 12, 24 and 48 hours for the case of a 10 m s^{-1} northerly wind during neap tides for Whalebone Prospect.
- Figure 5.6 Oil spill envelopes for release times of 6, 12, 24 and 48 hours for the case of a 10 m s^{-1} north-easterly wind during spring tides for Whalebone Prospect.
- Figure 5.7 Oil spill envelopes for release times of 6, 12, 24 and 48 hours for the case of a 10 m s^{-1} north-easterly wind during neap tides for Whalebone Prospect.
- Figure 5.8 Oil spill envelopes for release times of 6, 12, 24 and 48 hours for the case of a 10 m s^{-1} easterly wind during spring tides for Whalebone Prospect.
- Figure 5.9 Oil spill envelopes for release times of 6, 12, 24 and 48 hours for the case of a 10 m s^{-1} easterly wind during neap tides for Whalebone Prospect.
- Figure 5.10 Oil spill envelopes for release times of 6, 12, 24 and 48 hours for the case of a 10 m s^{-1} south-easterly wind during spring tides for Whalebone Prospect.

LIST OF FIGURES (Cont'd)

- Figure 5.11 Oil spill envelopes for release times of 6, 12, 24 and 48 hours for the case of a 10 m s^{-1} south-easterly wind during neap tides for Whalebone Prospect.
- Figure 5.12 Oil spill envelopes for release times of 6, 12, 24 and 48 hours for the case of a 10 m s^{-1} southerly wind during spring tides for Whalebone Prospect.
- Figure 5.13 Oil spill envelopes for release times of 6, 12, 24 and 48 hours for the case of a 10 m s^{-1} southerly wind during neap tides for Whalebone Prospect.
- Figure 5.14 Oil spill envelopes for release times of 6, 12, 24 and 48 hours for the case of a 10 m s^{-1} south-westerly wind during spring tides for Whalebone Prospect.
- Figure 5.15 Oil spill envelopes for release times of 6, 12, 24 and 48 hours for the case of a 10 m s^{-1} south-westerly wind during neap tides for Whalebone Prospect.
- Figure 5.16 Oil spill envelopes for release times of 6, 12, 24 and 48 hours for the case of a 10 m s^{-1} westerly wind during spring tides for Whalebone Prospect.
- Figure 5.17 Oil spill envelopes for release times of 6, 12, 24 and 48 hours for the case of a 10 m s^{-1} westerly wind during neap tides for Whalebone Prospect.
- Figure 5.18 Oil spill envelopes for release times of 6, 12, 24 and 48 hours for the case of a 10 m s^{-1} north-westerly wind during spring tides for Whalebone Prospect.
- Figure 5.19 Oil spill envelopes for release times of 6, 12, 24 and 48 hours for the case of a 10 m s^{-1} north-westerly wind during neap tides for Whalebone Prospect.
- Figure 5.20 Oil spill envelopes for release times of 6, 12, 24 and 48 hours for the case of spring tides only for Rivoli Prospect.
- Figure 5.21 Oil spill envelopes for release times of 6, 12, 24 and 48 hours for the case of neap tides only for Rivoli Prospect.
- Figure 5.22 Oil spill envelopes for release times of 6, 12, 24 and 48 hours for the case of a 10 m s^{-1} northerly wind during spring tides for Rivoli Prospect.
- Figure 5.23 Oil spill envelopes for release times of 6, 12, 24 and 48 hours for the case of a 10 m s^{-1} northerly wind during neap tides for Rivoli Prospect.
- Figure 5.24 Oil spill envelopes for release times of 6, 12, 24 and 48 hours for the case of a 10 m s^{-1} north-easterly wind during spring tides for Rivoli Prospect.

LIST OF FIGURES (Cont'd)

- Figure 5.25 Oil spill envelopes for release times of 6, 12, 24 and 48 hours for the case of a 10 m s^{-1} north-easterly wind during neap tides for Rivoli Prospect.
- Figure 5.26 Oil spill envelopes for release times of 6, 12, 24 and 48 hours for the case of a 10 m s^{-1} easterly wind during spring tides for Rivoli Prospect.
- Figure 5.27 Oil spill envelopes for release times of 6, 12, 24 and 48 hours for the case of a 10 m s^{-1} easterly wind during neap tides for Rivoli Prospect.
- Figure 5.28 Oil spill envelopes for release times of 6, 12, 24 and 48 hours for the case of a 10 m s^{-1} south-easterly wind during spring tides for Rivoli Prospect.
- Figure 5.29 Oil spill envelopes for release times of 6, 12, 24 and 48 hours for the case of a 10 m s^{-1} south-easterly wind during neap tides for Rivoli Prospect.
- Figure 5.30 Oil spill envelopes for release times of 6, 12, 24 and 48 hours for the case of a 10 m s^{-1} southerly wind during spring tides for Rivoli Prospect.
- Figure 5.31 Oil spill envelopes for release times of 6, 12, 24 and 48 hours for the case of a 10 m s^{-1} southerly wind during neap tides for Rivoli Prospect.
- Figure 5.32 Oil spill envelopes for release times of 6, 12, 24 and 48 hours for the case of a 10 m s^{-1} south-westerly wind during spring tides for Rivoli Prospect.
- Figure 5.33 Oil spill envelopes for release times of 6, 12, 24 and 48 hours for the case of a 10 m s^{-1} south-westerly wind during neap tides for Rivoli Prospect.
- Figure 5.34 Oil spill envelopes for release times of 6, 12, 24 and 48 hours for the case of a 10 m s^{-1} westerly wind during spring tides for Rivoli Prospect.
- Figure 5.35 Oil spill envelopes for release times of 6, 12, 24 and 48 hours for the case of a 10 m s^{-1} westerly wind during neap tides for Rivoli Prospect.
- Figure 5.36 Oil spill envelopes for release times of 6, 12, 24 and 48 hours for the case of a 10 m s^{-1} north-westerly wind during spring tides for Rivoli Prospect.
- Figure 5.37 Oil spill envelopes for release times of 6, 12, 24 and 48 hours for the case of a 10 m s^{-1} north-westerly wind during neap tides for Rivoli Prospect.

1. INTRODUCTION

1.1 Overview

Minora Resources N.L. are presently assessing the feasibility of exploration drilling operations in Exmouth Gulf, at the two locations, Whalebone Prospect and Rivoli Prospect (see figures 1.1 and 1.2). Drilling would take place between November 1988 and February 1989. LeProvost, Semeniuk and Chalmer have been engaged to prepare a Stage 2 Notice of Intent. As part of the Notice of Intent, contingency plans for oil spills must be made, due to the environmentally sensitive nature of many areas both within and immediately outside the Gulf. Steedman Limited were subcontracted to consider what possible oil spill trajectories could occur.

This report considers the best available information and, as far as practical, estimates the most likely trajectory paths. The method adopted is one of considering "worst case" scenarios rather than following a complete probabilistic approach.

Recent studies on continental shelves and coastal waters have shown the dominant role of winds and weather systems in forcing the motion of these waters. In particular, wind effects are well recognised as a major factor in oil slick motion (Murray, 1982). Weather systems of nearly all sizes and time scales may have strong effects on oil slick movement and oil dispersal. Currents driven by these systems are influenced by the surface wind stress and the rotation of the Earth, which causes them to veer to the left of the wind (in the southern hemisphere). Near the shore in shallow water, these effects are constrained by the coast, forcing the flow to be approximately parallel to the coast.

In the near field region of an oil spill, tidal currents are also of importance. On the North West Shelf the large semi-diurnal tidal range (Australian National Tide Tables 1988, 1987) produces very strong tidal currents. These currents are controlled in Exmouth Gulf area by the irregular coastline, islands and reef systems and the variable bathymetry.

Modelling of oil spill movement has only recently progressed beyond an elementary stage. In open waters, away from the coast, many effective models still utilise empirical rules to predict oil movement. Many are based on using the "3% of the wind speed" rule for surface currents. More complex models which realistically incorporate evaporation, surface tension and turbulent mixing have yet to be fully developed (Murray, 1982). Additional and more difficult problems occur near the coastal boundaries, which are usually the important areas of environmental concern.

The detail of the advanced oil spill models cannot reasonably be incorporated for the Exmouth Gulf region, as many of the parameters are completely unknown. Consequently some simplification must be made. In this study it is assumed that the oil travels with the ocean coastal currents, the oil slick is conservative (i.e. no loss through

evaporation or chemical transformation), both the horizontal and vertical turbulent diffusive processes may be neglected, and the wind driven and tidal currents dominate the oil slick transport through the coastal waters. In general these assumptions will lead to an over-estimate of the distance of travel of the slick, since the slick tends to maintain the same direction as, but lower speed than, the underlying water (Loucks and Laurence, 1971).

Meteorological and physical oceanographic data in the area are limited and no systematic surveys of surface circulation patterns suitable for oil spill travel estimates have been undertaken. However, information shows that wind driven circulation and tidal currents will dominate the trajectory of any oil spill from the proposed well locations in Exmouth Gulf.

1.2 Report Format

Chapters 2 and 3 of this report are concerned with the meteorological and oceanographic characteristics of the development area, addressing both the ambient and extreme conditions typical of the area. Particular attention is directed at the nature of the surface winds which drive the coastal circulation. Measured data provide estimates of the wind distribution for the period of interest, November to April.

Chapter 4 describes the numerical circulation models used to predict the wind and tide-driven currents in the Exmouth Gulf area. Chapter 5 describes the oil spill model which uses the currents provided by the circulation models to estimate maximum oil spill envelopes for particular scenarios of wind and tide. The report is concluded in chapter 6.

1.3 Scope of Work

The scope of work for this study is summarised as follows:

- (i) to provide a description of the wind and oceanographic characteristics for the region around the proposed well locations sufficient to estimate the oil spill trajectories;
- (ii) generate surface currents from measured Exmouth Gulf winds using shallow-water linear numerical models;
- (iii) estimate selected oil spill trajectory envelopes due to the action of wind and tide;
- (iv) prepare a report detailing the techniques applied, results and conclusions of the study.

2. WINDS

2.1 Synoptic Scale Meteorology

The normal wind regime over the study area is controlled largely by the northward/southward movement of the Subtropical High Pressure Belt, which is a series of discrete anticyclones which encircles the hemisphere. These high pressure cells are continuously moving (throughout the year) from west to east across the southern regions of Australia.

In winter, the axis of the anticyclonic belt lies across the Australian continent between 25° to 30°S. In summer the axis moves south of the Australian continent and lies between 35°S to 40°S. Figure 2.1 shows the typical winter and summer synoptic situations and the positions of the Subtropical High Pressure Belt.

With the Subtropical High Pressure Belt lying between 35°S and 40°S in the summer, intense solar heating over the north of continental Australia causes a zone of low pressure to develop. On average this semi-permanent low pressure area is centred inland from the north-west coast of Australia and has a trough running roughly parallel to the coast. Over the northern part of Western Australia surface winds are generally westerly as a transequatorial monsoon flow develops in response to this low pressure area.

2.2 Available Surface Wind Data

Recorded wind speed and direction data and statistics are available from the Bureau of Meteorology archives for several locations about Exmouth Gulf. Details of the available data are shown in table 2.1.

The records for Learmonth (Met. Office) and Exmouth (Navy Alpha) were obtained from the Bureau to compile the most representative database for the region of interest. As shown in table 2.1, three hourly records are available for both locations. Approximately 6 years of data were obtained for Navy Alpha, and almost 11 years of data for Learmonth (up to the end of 1985). The data resolution is : wind speed, 1 knot (0.5 m s^{-1}); and wind direction, 22.5 degrees.

Analysis of these data was undertaken to determine some climatic characteristics for the region. Firstly, wind speed and direction occurrence statistics were calculated for all the complete November to April periods contained in the data sets. They are shown in matrix form in tables 2.2 and 2.3 for Learmonth and Exmouth respectively. Matrices for each month between November and April are given in appendix A.

The results show that winds are generally stronger at Exmouth Navy Alpha (e.g. the 10% exceedence wind speeds at Exmouth Navy Alpha and Learmonth are approximately 11 m s^{-1} and 9 m s^{-1} , respectively). At both stations, wind directions range mainly between the south, south-west and west octants. Predominant octants differ however - south-west at Learmonth and south at Exmouth.

Persistence analysis was also carried out for the two locations in order to provide an indication of variation of wind conditions in the shorter term. Tables 2.4 and 2.5 show the combined persistence and exceedence matrices for Learmonth and Exmouth respectively for the months of interest. Results show, for example that wind speed exceed 10 m s^{-1} for periods of 1 day or more for 0.7% and 1.7% of the time at Learmonth and Exmouth Navy Alpha respectively.

In terms of application to the proposed well locations, Whalebone and Rivoli Prospects, it is considered the wind statistics from Exmouth Navy Alpha should be used. There are several reasons for this:

- (i) the Navy Alpha station is closer to the sites of interest,
- (ii) the Navy Alpha station is closer to the water and therefore more representative of the marine environment,
- (iii) wind speeds at the Navy Alpha station are generally greater than those at Learmonth, adding a degree of conservatism, and
- (iv) in terms of data quality and frequency, there is no reason to prefer one data set over the other.

2.3 Ambient Wind Conditions

A description of the seasonal characteristics follows. The period of interest spans the months November, 1988 to April, 1989. Most of this period falls in the summer season, excepting April which will most likely be a transition month.

Summer Season (October to March):

In summer, Exmouth Gulf is south-west of the mean low pressure area over northern Australia. The winds in the area during summer are from the south and south-west and are recirculated continental air which moves seawards to the south of the heat low, then is recirculated over the area of interest towards the Australian mainland. The term pseudo-monsoon (Gentilli, 1971) has been used to describe the situation.

The semi-permanent heat low over north-western Australia controls the air flow over the area. In general, air will flow into this low pressure area (with a general clockwise circulation). This results in a south and south-westerly flow of air over Exmouth Gulf. Wind speeds will typically range between 2 and 10 m s^{-1} and occasionally reach 15 m s^{-1} .

Often this air mass has travelled over warm tropical waters, and therefore may be moist and unstable. This flow is the dominant feature during summer. It is occasionally interrupted by a period of easterly winds associated with a particularly intense high pressure cell in the Subtropical High Pressure Belt, or by a period of variable but often strong winds associated with the passage of a tropical cyclone.

The sea breeze effect in the area often results in stronger southerly winds during the afternoon (see below).

Winter Season (May to August):

During the winter period, Exmouth Gulf lies on the northern periphery of the high pressure cells. As winds flow outwards from the high pressure cell in an anticlockwise direction, the area of interest is dominated by a flow of easterly and south-easterly air. Successive high pressure cells separated by cols (relatively low pressure area between two high pressure cells) and troughs do little to disturb the direction of the outflow as they move eastward, but they can have a marked effect on the speed of the winds. The wind speed increases in response to increasing pressure gradient, and decreases as the pressure gradient relaxes. These south-east trades are cool and dry winds originating over continental Australia.

Intensification of the pressure gradients, generally caused by an intense high pressure system in the Great Australian Bight area, results in easterly gales.

Transition Months (April and September):

During each of these transition months, the heat low is transitory instead of semi-permanent and the air flow in the area depends on the dominant pressure feature, i.e. either the heat low or the subtropical high pressure belt. During these periods both summer (S, SW) and winter (S, SE, E) air flows may be expected.

The change from summer to winter conditions is generally quite sharp with only a short transition period.

Sea Breezes

Superimposed upon the synoptic winds are local winds, particularly land and sea breezes.

During the summer months in particular, and generally throughout the year, the differential heating and cooling of the sea and land during the daily cycle results in local sea breezes (sea to land) in the afternoon and land breezes (land to sea) overnight.

In the Exmouth Gulf area a two stage sea breeze often occurs. Initially a local sea breeze will set in from the Gulf itself and later in the day the general west coast sea breeze (southerly) will override the local breeze.

2.4 Extreme Wind Conditions

There are four types of storms which occur in the area. Storms are short term transient events whose effects are generally limited to periods of up to several days, but they are capable of producing extreme wind speeds and wave heights compared with ambient conditions (e.g. Gentilli, 1971).

The types of storms, their principal months of occurrence, typical wind speeds and durations, extreme wind speeds and directions are summarised in table 2.6. A description of the storm types is given below.

Tropical Cyclones:

Tropical cyclone is the general term for a cyclone that originates over the tropical oceans. At maturity, the tropical cyclone is one of the most intense storms. Torrential rainfall is often associated with the storms.

Climatic Surveys (e.g. U.S. Navy, 1976; Gentilli, 1971) show that tropical cyclones (Hurricanes) form a distinct population of storms, which produce the most extreme wind speeds in the region. Gomes and Vickery (1976), Southern and Scott (1976), Holland (1980), and Lourensz (1981) have discussed the nature, the important characteristics and the occurrence of these storms about the Australian continent.

Tropical cyclones occur in the summer period and form south of the equator in the eastern Indian Ocean area, and the Timor and Arafura seas. Figure 2.2a shows the typical influence of a tropical cyclone on the surface pressure chart. Cyclone tracks show most of the storms pass the area of interest heading west, south-west or south (e.g. figure 2.3). Figure 2.4 (from Lourensz, 1981) shows the decadal frequency of occurrence of tropical cyclones in 5° lat./long. 'squares' in the period July 1959 to June 1980 (all months). From these satellite based data Lourensz (1981) estimates the frequency of occurrence of these storms in the Exmouth Gulf area is 15 storms per decade (i.e. 1.5 storms per annum).

The life cycle of tropical cyclones usually progresses through four stages of development, namely:

- (a) tropical low pressure area;
- (b) tropical cyclone where the winds exceed 7 m s^{-1} ;
- (c) severe tropical cyclone where the winds exceed 33 m s^{-1} ;
- (d) dissipating, or weakening storm.

In the Exmouth area nearly all storms are either in the tropical cyclone or severe tropical cyclone stage.

Trade Wind Surge:

In Exmouth Gulf, storm winds which are caused by strong pressure gradients, occur in the winter as a result of surges in the south-easterly wind regime. The normal moderate winds will strengthen to about 12 to 16 m s^{-1} and extreme wind speeds up to 30 m s^{-1} may occur. The storms are the result of an intense high pressure cell in the Subtropical High Pressure Belt passing to the east across the southern portion of Western Australia (figure 2.2b). Typically these surges last 3 to 5 days.

Squalls:

Squalls are associated with thunderstorms occurring in the summer period. The squall results from the strong downdrafts in the cumulonimbus cloud. They are of relatively short duration and are usually accompanied by heavy rain, lightning and thunder. In some cases, squalls are associated with cumulonimbus clouds of only a few kilometres in diameter. In such cases, the strong winds are usually 15 to 25 m s^{-1} and of approximately one half hour duration.

In other, less frequent cases, the cumulonimbus clouds may cover a considerably greater area occasionally forming into lines of 100 to 200 km in length and 20 to 40 km in width. In these cases, the winds associated with the squalls may be in excess of 20 m s^{-1} for several hours, and in extreme cases may reach 25 to 35 m s^{-1} with instantaneous gusts up to 45 or 50 m s^{-1} . The high wind velocities in the squalls present a danger to operations, but they are of insufficient duration to be of major importance to surface current movements.

Tornadoes and Water Spouts:

Tornadoes and water spouts occur in the area associated with thunderstorm activity and tropical cyclones of the summer season. No reported information exists on their frequency of occurrence or intensity. In general very high winds (say 50 m s^{-1}) could be expected. As these events are of fairly short duration, and affect only a very localised area, they do not generate surface currents of any consequence.

2.5 Light Wind Conditions

Light winds are defined as those winds which are less than 5 m s^{-1} and correspond to a Beaufort Force 3 or less, generating slight to moderate seas. Light wind conditions may occur at any time during the year.

Statistics contained in tables 2.2 and 2.3 show that winds less than 5 m s^{-1} occur in the November to April period for approximately 40% and 36% of the time on average at Learmonth and Navy Alpha respectively. Variations on a monthly basis are significant (see appendix A). Percentage occurrences of light winds at Learmonth range between 30 and 63% and at Exmouth Navy Alpha they range between 30 and 41%. At both locations, light winds occur for less than 40% of the time during the months November through February.

Light wind conditions can persist for 48 hours or more for up to 19% and 24% of the time at Learmonth and Navy Alpha respectively. Detailed persistence statistics for these two locations are contained in tables 2.4 and 2.5.

During light wind periods, the surface wind currents will become less significant and the tidal and ocean drift currents will dominate the water movement.

3. OCEANOGRAPHY

3.1 Currents

No systematic study of the circulation in Exmouth Gulf exists and general knowledge of the water movement in these areas is limited (White, 1975). Results from studies of other coastal embayments, suggest that several types of current regimes will be operating within Exmouth Gulf. This section attempts to draw together the available data and theory to describe the water movement in the Gulf.

Limited measurements have been taken in the Gulf region (e.g. RAN, 1952; R.K. Steedman & Associates, 1982). These measurements are not of sufficient duration or close enough to the sites of interest to characterise the current regime.

The currents can be divided into several classes and they are listed in order of speed magnitude as follows:

- (i) tidal;
- (ii) wind driven circulation;
- (iii) Indian Ocean circulation (across the Gulf entrance);
- (iv) thermohaline.

Details of these divisions are discussed below. The exact nature of each of these currents is complex and in reality they interact with each other (e.g. non-linearities are discussed by Fofonoff, 1962 and Krauss, 1973). In order to arrive at some estimates of the broad current pattern for engineering and environmental considerations, some simplifications are necessary. Without entering into the analysis of the full equations of motion (e.g. Fofonoff, 1962) we assume that the current systems are simply superimposed.

Tidal Currents:

The tidal currents are the most significant instantaneous current component of the area (RAN, 1954). Velocities greater than 0.65 m s^{-1} (1.3 knots) have been recorded at the spring tide within Exmouth Gulf (RAN, 1954). These currents enter and leave the Gulf in the north-west, between North West Cape and the Muiron Islands.

The magnitude of the tidal velocity can be roughly estimated by considering Exmouth Gulf as a rectangular basin of uniform depth and breadth. As described by R.K. Steedman & Associates (1978), results compare favourably with measured values of 0.65 m s^{-1} .

Numerical modelling (see section 4) of the tidally-driven circulation in Exmouth Gulf shows comparable values for the currents. Modelled spring tidal currents range up to 0.7 m s^{-1} near Whalebone Prospect and 0.5 m s^{-1} near Rivoli Prospect. Currents at neap tides are estimated to range up to 0.3 m s^{-1} and 0.15 m s^{-1} at the two respective locations. Modelling also shows that the tidal currents flow slightly east of north during ebbs and west of south during flood tide at the sites of interest. As we move further north to North West

Cape and beyond, the direction of the tidal flow changes to accommodate the Muiron Islands. Flood and ebb tides flow to east-south-east and west-north-west between the Cape and Muiron Islands.

The semi-diurnal nature of the tides in this region cause a total of two flood and two ebb tide speed peaks on most days.

Wind-Driven Circulation:

In general terms, the wind applies a surface stress to the ocean surface which is proportional to the square of the wind speed, forcing movement of the surface layers. The balance between the Coriolis force, inertia, pressure gradient, surface and bottom stress controls the wind-driven circulation.

In the absence of detailed measurements, numerical modelling has been undertaken in order to estimate the wind-driven circulation at the sites of interest and in the surrounding Gulf waters. Details of the modelling techniques used are described in section 4 and also appendices B and C. Modelling indicates that surface currents between 0.05 m s^{-1} and 0.4 m s^{-1} can be expected for 10 m s^{-1} wind speeds at the sites of interest. The range of speeds quoted accounts for the differing circulation patterns induced by different wind directions. Current speeds will also vary in the local region about the sites of interest (see section 4). For storm conditions, wind-driven currents can be substantially larger. For example, under the influence of tropical cyclone wind speeds of up to 30 to 40 m s^{-1} , wind-driven surface currents may reach 1 m s^{-1} in the region of interest.

Longshore Drift Resulting from Indian Ocean Circulation:

Little quantitative data is available on the longshore drift resulting from the Indian Ocean circulation impinging on the continental shelf adjacent Exmouth Gulf. The U.S. Navy Marine Climatic Atlas (U.S. Navy, 1976) indicates a south-westerly flow (up to 0.4 m s^{-1}) in the period January to September, and a reversal for the balance of the year. No other published data is available to estimate the Indian Ocean circulation. For most of the year, the longshore current flows into the Gulf from the north-east and across the entrance to North West Cape (U.S. Navy, 1976).

It is anticipated that a north-easterly Indian Ocean flow will have little effect on the mean circulation inside the Gulf, mainly affecting the circulation at the entrance, whereas a south-westerly flow will penetrate into the Gulf down the east coast. In the region of interest, it is estimated the current components resulting from Indian Ocean circulation are in the range 0 to 0.1 m s^{-1} .

The influx of Indian Ocean water into the Gulf is important for the maintenance of the existing water quality and is thought to follow a clockwise pattern. At Whalebone and Rivoli Prospects it is estimated that very little east-west component exists and mainly a northward flowing component of the longshore Indian Ocean circulation is present.

Thermohaline Circulation:

Variations in salinity and temperature of the water mass in Exmouth Gulf can cause what is known as thermohaline circulation. As discussed by R.K. Steedman & Associates (1978) factors such as the temperature and salinity gradients, precipitation, evaporation and coefficients of eddy diffusivity will influence the nature of this circulation. It was estimated by R.K. Steedman & Associates (1978) that magnitudes of the induced thermohaline circulation will be less than 0.01 m s^{-1} , and it is not considered further.

3.2 Waves

The orientation and extent of Exmouth Gulf has a significant effect upon the waves within the Gulf. In most directions the fetch is limited by the surrounding coast. The longest fetch is to the north (figure 1.2).

An examination of the wind statistics for Learmonth and Exmouth Navy Alpha (tables 2.2 and 2.3) for the period of interest show that northerly winds are relatively infrequent (i.e. 3.6% and 3.3% of the time during the November to April period respectively). Consequently the fetch for sea wave generation is generally limited to the dimensions of Exmouth Gulf.

In the absence of measured wave data in the Gulf, the wind generated wave climate has been estimated using the empirical Sverdrup Munk Bretschneider (SMB) relationship (Bretschneider, 1966; CERC, 1984). Significant wave height and period occurrence matrices are shown in tables 3.1 and 3.2 for Whalebone and Rivoli Prospects, for the November to April period. Significant wave heights and periods are estimated to be generally less than 1 m and 5 seconds.

Swell waves do not commonly propagate into the Western half of the Gulf as it is unusual for swell to be generated to the north or north-east of the Gulf. The exception is during tropical cyclones.

Waves will be significantly larger during strong storm events, in particular, tropical cyclones. Previous studies (Steedman and Russell, 1986) suggest that tropical cyclones may generate wind waves up to 2 m and swell waves up to 4 or 5 m which will propagate into the Gulf.

3.3 Water Levels

Longer period water level variations (i.e. periods greater than 1 hour) are the combination of several environmental phenomena, including the astronomical tides, atmospheric pressure variations and shelf waves.

By far the most significant component is the astronomical tide. Astronomical tide heights in the North West Australian shelf region are well known (Easton, 1970; Holloway, 1983; Department of Marine and

Harbours, personal communications 1986; Australian National Tide Tables 1988, 1987; and various measurement programmes undertaken for companies working in the area, e.g. R.K. Steedman & Associates, 1982; Steedman Limited, 1987). In Exmouth Gulf, two standard ports exist, at Point Murat and at Learmonth (figure 1.2).

The tides in Exmouth Gulf are characteristically semi-diurnal with a small diurnal inequality. This is caused by the dominance of the principal lunar (M_2) and principal solar (S_2) constituents. Tidal range increases towards the head of the Gulf.

At Point Murat, the mean spring range is 1.7 m while at Learmonth, it is 2.1 m. Tide measurements undertaken by the Department of Marine and Harbours at Badjirrajirra Creek (figure 1.2) indicated a mean spring range of 2.0 m. Values of the major tidal constituents M_2 , S_2 , O_1 , K_1 , are given in table 4.1 for the above three locations. Times and elevations for daily high and low tides for the two standard ports can be obtained from the Australian National Tide Tables 1988 (1987).

Long term variations, such as the seasonal astronomical variations in mean sea level, occur in the area. The mean level in the months March to June is approximately 0.1 m above the annual mean sea level. For the months August to November, the mean level is approximately 0.1 m below the annual mean sea level.

Astronomical tides at Whalebone Prospect location will be similar to those at Point Murat. At Rivoli Prospect, the character of the astronomical tides will lie between those of Point Murat and Learmonth. This is borne out by results from the tidally-driven numerical circulation model that was run for Exmouth Gulf (see section 4).

Meteorological effects on water levels are two-fold. Water level variations can be caused by atmospheric pressure variations and also by wind forcing. Variations due to atmospheric pressure are generally small - a 5 mb fluctuation would result in a water level change of approximately 0.05 m. The inverse barometer effect, as it is known, is more important in the case of tropical cyclones, where central pressure reductions of up to 50 to 100 mb can cause water levels to rise by 0.5 to 1.0 m.

Water level variations due to wind forcing are also generally small in Exmouth Gulf. They depend on the balance of forces such as surface wind stress, bottom stress, Coriolis force, inertia and pressure gradient.

Numerical modelling shows (section 4) water level differences over the width of the gulf are about 0.05 m for a 10 m s^{-1} wind (easterly or westerly). Again, this effect is more important during the stronger wind forcing associated with storms. For example, numerical modelling has shown (Steedman and Russell, 1986) that known cyclones have surges of up to 0.4 m for wind speeds up to 35 m s^{-1} at Exmouth (similar results would be expected at Rivoli Prospect and Whalebone Prospect).

Shelf waves cause water level variations at the coastline of 0.1 to 0.5 m over periods of 5 to 30 days (Provis and Radok, 1979; Holloway et al., 1981). The variations are unpredictable and their cause is not known.

Other shelf waves have been related to tropical cyclones (Fandry et al, 1984).

4. NUMERICAL CIRCULATION MODELS

4.1 Selection

The subject of coastal circulation is well developed, both theoretically and experimentally (e.g. see texts by Csanady, 1982; Nihoul, 1979 and 1982; Bowden, 1983). Theoretical models, based on the equations of motion, have been related to observed currents, sea level variations and water properties. Parameters such as average current movement and water levels can be estimated within reasonable bounds of error.

The dynamics of the shallow coastal waters in Exmouth Gulf and environs are generally poorly observed and understood. By contrast, the tidal water level elevations at the coastal stations are reasonably well known.

Observations suggest that both wind-driven circulation and tidal motion will dominate the water movement, and hence any oil spill transport.

As a first approximation, it was judged that a linear vertically integrated numerical model would best simulate tidal movement in this area. This type of model has been applied to a variety of locations along the North West Shelf and coastline (e.g. Mills, 1985; Steedman and Russell, 1986; Steedman Limited, 1986; Andrewartha, 1987). The main source of friction to tidal flow is via the bottom stress and hence a depth-integrated model should define, reasonably well, surface currents due to tides.

This is not the case for wind-driven flow where both surface and bottom stress are important. Hence it was decided the appropriate model should have the capability of describing the vertical structure through the water column, in particular the surface layer currents.

The models chosen for this study therefore, are a depth-integrated (2D) model for tide-driven cases as described in appendix B (Heaps, 1969; Fandry, 1982), and a "2.5D" model for wind-driven cases, as described in appendix C (Jelesnianski, 1970; Fandry, 1983).

The latter is able to model currents at any given depth. However, to produce time-varying currents at several grid points, as required for tracking oil spills, requires enormous computing time and storage resources. As this was not practical the model could only be run with uniform wind fields, constant in time, to produce steady-state current fields. Thus, the wind cases to be studied needed to be represented in terms of a constant wind strength from a given direction.

To model tide-plus-wind driven cases it was decided to superimpose the surface currents predicted by the wind-only 2.5D model onto the tidal currents predicted by the 2D model. This procedure is at worst conservative since at times of strong tidal currents, the effect of the wind stress is probably diminished (Provis and Lennon, 1983).

The circulation models require as input a digitised gridded bathymetry plus coastline, and a specification of the open boundary conditions. The details of these requirements plus calibration of the 2D model are given in the following three sections.

The role of the circulation models was to provide a time varying surface current, for different case studies (section 4.5), to be used as input to the oil spill trajectory model (chapter 5).

4.2 Model Grid and Bathymetry

Bathymetric and grid data were already available for the region of interest from a previous modelling study (Steedman and Russell, 1986). As these data satisfied the requirements of this study (i.e. the spatial resolution is adequate and the region of interest is covered), they formed the basis of the bathymetry and grid for this study.

The uniform grid chosen for use with the numerical circulation models is shown in figure 4.1. Each of the grid points shown represents a point where both depth and surface elevation are defined (see appendix B).

The grid contains 23 x 36 points in which the x and y grid spacings are given by $\Delta x = \Delta y = 3.15$ km. The 3.15 km grid spacing is unable to resolve the fine coastal and island detail, and so judgements were made as to how to represent the coastline and islands.

The depth at each grid point was originally estimated to the nearest 1 metre using available charts. Most information was gained from chart AUS 744. In assigning grid depths from chart estimates, a value of approximately 2 m was added to adjust the Chart Datum values to mean sea level (MSL), as required by the model.

Bathymetry contours relative to MSL, used by the circulation models, are plotted in figure 4.2.

4.3 Open Boundary Conditions

To complete the integration of the equations of motion, the open sea boundary conditions need to be specified. The boundary conditions are described in more detail in appendix B. It should be noted that the full dynamical equations cannot be solved on the boundaries. The open boundary conditions represent the best available estimate of what actually occurs at these boundaries, however the results within one or two grid points of these boundaries may not be accurate.

In the case of tide-only flow, the tidal surface elevations are specified at all grid points along the open boundaries, at each time step. This procedure serves a dual role by also providing the tidal forcing for the model.

In the case of wind-driven flow, the boundary values of surface elevation and current flow are initialized to be zero, and then various options may be chosen to specify the normal flow across the

boundaries as the model run progresses. For this study, appropriate boundary conditions for wind-only driven flow were found to be zero-normal-flow-gradient on the northern boundaries, and the radiation condition on the west and east boundary.

For the model area being considered here it was decided that only the 4 major constituents M_2 , S_2 , K_1 and O_1 would be needed to adequately represent the tide. The model requires as input the amplitudes and phases of these 4 constituents at the open boundary corners. The values used were based on previous modelling work (Steedman and Russell, 1986).

In setting these tidal constants, reference was made to published values from several different sources, for various nearby locations. The Australian National Tide Tables 1988 (1987) provides the constants for coastal ports and some offshore locations i.e. Norwegian Bay, Point Murat, Learmonth, Serrurier Island and Onslow. Schwiderski (1979, 1981a, 1981b, 1981c) provided estimates at six nearby locations, while further information was gained from measurements made by Department of Marine and Harbours (personal communications, 1986) at Badjirrajirra Creek.

The tidal constants gained from the above sources are listed in table 4.1. While those of K_1 and O_1 are reasonably uniform across the region, the constants for M_2 and S_2 vary considerably. One reason for this is the fact that the constants have all been derived from different lengths of tide data. The tide tables do not specify source data lengths. In many cases these would have been too short to accurately resolve all constituents.

The variability of the constants is also indicative of the dynamics of the tides in and around Exmouth Gulf. This included the substantial amplification of the M_2 and S_2 amplitudes towards the head of the Gulf. The complex variations in the tidal constants preclude accurate estimation of constants for the open boundary grid points.

The technique chosen was to subjectively weigh up all the data in table 4.1 and hence manually estimate constants for the 4 corners of the model grid. The constants at intermediate grid points on open boundaries were then obtained by linear interpolation. Amplitudes were chosen principally from those for Point Murat, Learmonth, Serrurier Island and Onslow whilst phases were estimated from all the available data. The tidal constants estimated for the 4 corners of the grid are given in table 4.2.

4.4 2D Model Calibration

Following specification of the bathymetry and open boundary conditions, certain other parameters need to be specified to run the models (see appendix B). These parameters have been chosen as follows:-

Time step	(Δt) = 40 sec
Bottom friction coefficient (k)	= 0.003.

Other studies suggest that the bottom friction coefficient may be better represented as varying over the grid (Ramming and Kowalik, 1980; Andrewartha, 1987), however there is insufficient data to assess the importance of a variable bottom friction coefficient.

Available data for calibration of the 2.5D model (used to generate surface wind-driven currents) is non-existent in Exmouth Gulf. Calibration of the 2D model (used to generate tidal currents) was limited as there is only data at three locations within the model domain, and the tidal current and height information at each location is insufficient.

Comparison of predicted and modelled tide heights for Exmouth Gulf is described by Steedman and Russell (1986) and is not repeated here. The results show that tide heights and phases compare very well.

Velocities of 0.65 m s^{-1} and greater reported by the RAN (1954) at spring tides compare reasonably well with modelled spring tidal currents (see figure 4.3 and the more detailed description of the modelled tidal currents in section 4.5) which range up to 0.7 m s^{-1} . It has to be remembered that the modelled tidal currents are depth averaged, whilst the observed values do not necessarily correspond to the depth average value. Vertical variation in the tidal currents is not large, however, so the discrepancy should not be significant.

4.5 Model Results

This section provides examples of surface elevations, depth-integrated currents and surface currents predicted by the numerical circulation models for input to the oil spill model described in chapter 5. For tide and wind-driven flow, the examples include time history output at specific locations, current vectors at all grid points and contours of surface elevation across the grid.

2D Circulation Model Results

The periods chosen to represent the extreme types of tidal flow found near the two proposed well locations in Exmouth Gulf and thus to be used for the tide-driven model runs are as follows:

Spring tides : 0000 21.11.88 to 0000 27.11.88
Neap tides : 0000 31.10.88 to 0000 06.11.88.

Six days were chosen for each run because the circulation model requires 48 hours to 'warm-up' and the oil spill model requires 96 hours of current data for advection of the oil (see section 5.2).

Figures 4.3 and 4.4 contain examples of depth-averaged currents and surface elevations from spring tidal forcing, and figures 4.5 and 4.6 present those for neap tidal forcing. Maximum current speeds are attained approximately midway between high and low spring water. This

maximum speed varies considerably across the grid due to the islands and changes in depth. Maximum depth-averaged tidal currents are predicted to be approximately 0.7 m s^{-1} in the region of interest.

2.5D Circulation Model Results

As mentioned in section 4.1, computer constraints restricted running of the 2.5D circulation model to the steady state case, using a wind field both constant in time, and uniform across the grid. Because we are only modelling 'worst case' scenarios here, rather than pursuing a probabilistic approach which would take into account the frequency of occurrence of all wind patterns it was decided to model 8 wind cases.

Reference to measured wind data (tables 2.2 to 2.5 and appendix A) shows that at Barrow Island the wind seldom blows for any length of time above 10 m s^{-1} (except during the storms mentioned in section 2.4 and which are not being considered here). Wind speeds greater than 10 m s^{-1} at Exmouth Navy Alpha only persist for more than 24 hours for 1.7% of the time. During the period November to April, winds are predominantly southerly, south-westerly or westerly.

On the basis of the above information the 8 cases for study were chosen to be simply a 10 m s^{-1} wind blowing from the cardinal directions north, north-east, east, south-east, south, south-west, west and north-west.

Apart from the model parameters given in section 4.4, and the open boundary conditions described in section 4.3, there remains one input parameter which needs to be specified to run the 2.5D model in a wind-driven mode. That parameter is the wind drag coefficient which, for a 10 m s^{-1} wind, was chosen to be (see appendix B):

$$\text{Wind drag coefficient } (c_d) = 1.2 \times 10^{-3}.$$

The 2.5D model was run for 65 hours to ensure the steady state value was attained for each of the 8 cases described above. The current vector fields at hour 65 were determined for a depth of -1.0 m . The results for the 8 cases are given in figure 4.7 and 4.8. In open waters, the surface currents would be expected to flow to the left of the wind (in the southern hemisphere). However, the Gulf topography places additional constraints on the flow, with the result that the surface currents flow generally to the right of the wind. They generally vary in magnitude from 0.2 to 1.0 m s^{-1} . Typically the currents are at least 3% of the wind speed (0.3 m s^{-1}) or larger.

Note that the near-shore surface currents predicted by the 2.5D model are subject to the constraints described in the following section.

4.6 Coastal Boundary Flow

It is worthwhile examining the flow at the coastal boundaries in more detail.

The coastal boundary conditions of the numerical model (appendix B) simply assume there is zero normal depth-averaged flow at the coast.

Of course this condition does not accurately represent this region, where both wind-driven surface currents and ocean wave drift can bring pollutants ashore.

Csanady (1982) summarises the so-called Ekman adjustment drift theory which describes both the horizontal and vertical structure of the flow at the coastal boundary. Figure 4.9 shows the cross-shore and longshore current structure close to the coast for a cross-shore wind. The flow in the y direction may be either onshore or offshore. The Coriolis force (southern hemisphere) will left turn the current from the wind, and hence develop the surface longshore component. In both the cross and longshore directions the mass balance is achieved by an opposite bottom flow. Similarly, a longshore wind will induce an onshore or offshore surface flow with a bottom counter flow (figure 4.10).

Clearly the vertically-integrated model does not describe this structure. However, the vertically-integrated 2D model should be reasonably accurate at distances greater than one or two grid points from the coast.

Also, the 2.5D model is not accurate in a narrow region close to the coast (see appendix C, section 1.5).

5. ESTIMATION OF OIL SPILL ENVELOPES

5.1 Oil Spill Movement

The transportation processes of oil in coastal regimes have been well summarised, e.g. Hunter (1980) and Murray (1982). Generally the transport of oil at, or near, the sea surface is governed by:

- (i) tidal, wind-driven and drift currents of the water mass,
- (ii) localised wind-driven motion at the air-sea interface, which may be caused by such mechanisms as surface gravity waves and the direction of the surface wind stress on the oil patch;
- (iii) spreading and mixing processes, such as surface tension, surface wave activity, horizontal turbulence;
- (iv) loss of oil constituents through evaporation, chemical change or some biological degradation.

The mean position, or centre of mass, of the patch is controlled by (i) and (ii), while the spreading is controlled by (iii) and (iv).

From the conservation of mass, the average vertically-integrated transport equation describing the distribution of the oil is given by

$$\frac{\partial c}{\partial t} + u \frac{\partial c}{\partial x} + v \frac{\partial c}{\partial y} = \kappa \left(\frac{\partial^2 c}{\partial x^2} + \frac{\partial^2 c}{\partial y^2} \right) + Q \quad , \quad (5.1)$$

where

c is the concentration of the oil (kg m^{-3});

κ is the horizontal eddy diffusivity (assumed isotropic);

Q represents any source or sink terms;

and u, v , are the vertically-averaged velocities.

These variables may be scaled using

$$\begin{aligned} c^* &= c/C & , \\ (x^*, y^*) &= (x/L, y/L) & , \\ (u^*, v^*) &= (u/U, v/U) & , \\ t^* &= t/T & , \end{aligned} \quad (5.2)$$

where L is the characteristic horizontal dimension (taken here as the length of the tidal excursion), U is the characteristic velocity, C is the average concentration, and T is the time scale of interest. Substituting (5.2) into (5.1) gives the non-dimensional equation

$$\frac{t_d}{T} \frac{\partial c^*}{\partial t^*} + Pe \left(u^* \frac{\partial c^*}{\partial x^*} + v^* \frac{\partial c^*}{\partial y^*} \right) = \frac{\partial^2 c^*}{\partial x^{2*}} + \frac{\partial^2 c^*}{\partial y^{2*}}, \quad (5.3)$$

where the Peclet number $Pe = UL/k$ is a measure of the relative importance of advection to diffusion, and the diffusive time scale is $t_d = L^2/k$. Increasing the eddy diffusivity decreases the Peclet number.

The magnitude of the appropriate scaling parameters will govern the relative importance of advection to diffusion.

For short distances about the source, e.g. one tidal excursion:

Let $L \approx 10$ km, the length of the tidal excursion,

$T \approx 0.5 \times 10^5$ sec, time of one tidal cycle,

$U \approx 0.3$ m s⁻¹, average tidal speed (figures 4.3 and 4.5),

$k \approx 10$ m² s⁻¹, see Okubo (1974),

then, $Pe \approx 300$ and advection clearly dominates diffusion (right hand side of equation (5.3)).

For larger distances within the scale of the model which might be covered by drift currents

say $L \approx 50$ km

and $U \approx 0.05$ m s⁻¹

then $T \approx 10^6$ sec

$k \approx 50$ m² s⁻¹, Okubo (1974),

then, $Pe \approx 50$ and hence advection would still dominate.

For very large distances and lower current speeds, the Peclet number reduces even further and diffusion begins to dominate advection. However, that is not the case with this study where short to moderate distances are appropriate.

Therefore it is reasonable as a first approximation near the source to neglect the diffusive terms in the transport equation, and assume a time-dependent advection scheme only. In addition the difficulties in parameterising the other spreading terms (items iii and iv above), and the difficulty of describing the flow against the coastline (section 4.6), would lead to unavoidable gross simplifications.

It is now assumed that advection only will be carried out by a superposition of the time-dependent tidal currents for spring and neap tides (section 4.5) with the steady-state wind-driven currents (section 4.5).

5.2 Oil Spill Model

The position p of the centre of mass of a patch of oil at time t , after being released from p_0 at the time t_0 , is given by the integral

$$p(t) = p_0 + \int_{t_0}^t \omega(p(\tau), \tau) d\tau \quad (5.4)$$

where

$$p_0 = p(t_0)$$

$$p(t) = (x(t), y(t)) \quad (5.5)$$

$$\omega(p(t), t) = (u(p(t), t), v(p(t), t))$$

where x and y are the excursion positions and u and v are the x and y components of water velocity.

To simulate the advection of patches or 'particles' with the oil spill model, a new particle is released from p_0 at discrete time intervals ΔT . Each particle is advected every time step of the circulation model, Δt , by the value of the current velocity determined by the circulation model for that grid location. By this method, equation (5.4) is approximated by:

$$p(t) = p_0 + \sum_{i=0}^{N-1} \omega(p_i, t_i) \Delta t \quad (5.6)$$

where $\omega(p_i, t_i)$ is the velocity of the particle at location $p_i = p(t_i)$ at time $t_i = t_0 + i\Delta t$, and N is the number of time steps from t_0 to t .

The distance travelled by a particle along its trajectory, after time t , is given by the line integral

$$\chi(t) = \int_{p_0}^{p(t)} ds \quad (5.7)$$

where ds is arc length.

Equation (5.7) can be rewritten as an ordinary integral in time as

$$\begin{aligned} \chi(t) &= \int_{t_0}^t [x'(\tau)^2 + y'(\tau)^2]^{1/2} d\tau \\ &= \int_{t_0}^t [u(p(\tau), \tau)^2 + v(p(\tau), \tau)^2]^{1/2} d\tau \\ &= \int_{t_0}^t |\omega(p(\tau), \tau)| d\tau \end{aligned} \quad (5.8)$$

Equation (5.8) is approximated by the oil spill model as:

$$X(t) = \sum_{i=0}^{N-1} [u(p_i, t_i)^2 + v(p_i, t_i)^2]^k \Delta t \quad (5.9)$$

Oil spill envelopes are required for release times of 6, 12, 24 and 48 hours. The problem could therefore be phrased as "where could an oil patch find itself after 6, 12, 24 or 48 hours from release?"

To this end, the model was allowed to 'warm up' for T_1 hours with no advection, and then particles were released at intervals of ΔT hours for a further T_2 hours (i.e. $T_2/\Delta T$ particles were released during each run).

The model was then allowed to run for a further 48 hours to allow the last particle to advect for the maximum release time of 48 hours. Total run time for each case was therefore $T_1 + T_2 + 48$ hours.

By allowing the release of several particles over a period T_2 , the combined trajectories of all these particles produces an envelope which encompasses all possible scenarios for oil released at any time over the period T_2 . Thus, period T_2 should be chosen at least greater than one tidal cycle.

To define the envelope area, the position of each particle is recorded each time a new particle is released. Thus, points along each trajectory are resolved to within a time of ΔT .

It should be noted that particle positions were recorded as fractions of the main model grid and that velocities were interpolated to give the appropriate value for those particle positions.

Note also that although $T_2/\Delta T$ particles are released from the source, and there exist therefore the same number of trajectories to plot, the entire length of each trajectory is not plotted. The actual amount plotted depends on the release time defining the particular envelope of concern i.e. 6, 12, 24 or 48 hours.

For example, consider the first particle to be released at the beginning of time T_2 . The trajectory of this particle continues to develop up to time $T_2 + 48$. However, only the 6 hours closest to the source should be plotted for the 6 hour envelope, and only the first 12 hours for the 12 hour envelope etc. Thus the only entire trajectory to be plotted is that of the last particle to be released and then only for the 48 hour envelope. Figure 5.1 is a schematic diagram showing how much of each trajectory is plotted.

For the maximum release time of 48 hours, the corresponding envelope can contain several thousand points. To avoid plotting such a densely packed set of points, the oil spill area was subdivided into a fine grid, and only 1 point plotted per envelope cell if the envelope ever traversed that cell. Thus each envelope area is an 'evenly-shaded'

plot which defines all possible areas through which an oil spill could have travelled. A given oil spill, released for any duration within time T_2 of the particular case study should therefore be confined within the shaded area, but will not necessarily span the entire area.

5.3 Model Results

Model input parameters described in the previous section were chosen to be:

Particle release coords., (x_0, y_0)	
for Whalebone Prospect	= (6.0, 25.0)
for Rivoli Prospect	= (6.0, 20.5)
Particle advection interval	$\Delta t = 40$ sec
Particle release interval,	$\Delta T = 0.5$ hours
Model 'warm-up' period,	$T_1 = 48$ hours
Particle release duration,	$T_2 = 48$ hours
No. of envelope cells per grid cell	= 5.

The release period T_2 was chosen to be 48 hours since this encompasses 4 tidal cycles, and also provides for a sufficient number of releases (96) to ensure a good spread of trajectory points for plotting.

Eighteen simulation runs were carried out for currents corresponding to spring tides only, neap tides only, plus each of these 2 cases acting coincidentally with the 8 wind cases described in section 4.5. Envelopes showing the maximum extent of an oil spill given by the model for spill durations of 6, 12, 24 and 48 hours, for each of the 18 case studies are given in figures 5.2 to 5.19 for Whalebone Prospect and figures 5.20 to 5.37 for Rivoli Prospect. A description of the results for each location follows.

Whalebone Prospect

In the case of spring tides only, figure 5.2 shows that the envelope is somewhat elliptical in shape due to the oscillatory nature of the current flow. Since the principal axis of the current ellipse changes from a NNE-SSW alignment south of Whalebone Prospect to NNW-SSE in the mouth of the Gulf, the envelope is distorted from a true ellipse. The length of the envelope is about 25 km in length after 48 hours, compared with a length of 14 km for the neap tide only case (figure 5.3).

For the tide-plus-wind simulations, the wind component is seen to dominate the movement of the oil spill. This is particularly the case where the wind-driven current is parallel to, and hence masks, the tidal oscillations. In such instances the envelopes are long and narrow and drawn out in the direction of the wind-driven currents (e.g. see figures 5.18 and 5.19).

In the case where the wind-driven current is directed at an angle to the tidal currents, the result is a distorted envelope with 'bulges' due to the tidal oscillations. This behaviour is shown in figures 5.6 and 5.8 for spring tides acting with westerly and northerly winds respectively. Overall, spring tide-plus-wind situations produce

broader envelopes than neap tide-plus-wind situations. Envelope lengths are comparable for a given release duration. These lengths depend somewhat on wind direction, but range from approximately 6 to 20 km for 6 hour releases, to 30 to 45 km for 24 hour releases. The envelopes either encounter land or extend beyond the model boundaries within 48 hours. Note that these distances relate to a sustained wind of 10 m s^{-1} over the given period.

Envelopes for the northerly, north-easterly and easterly winds affect the coastline from Exmouth to North West Cape and beyond, i.e. Exmouth to North West Cape, Bundegi reefs to the Cape and beyond, and Point Murat to the Cape respectively (see figures 5.4 to 5.9).

For the south-easterly, southerly and south-westerly winds the envelopes exit the Gulf to the north between the Cape and the Muiron Islands, to the north-east and to the east-north-east (see figures 5.10 to 5.15). Envelopes for the westerly and north-westerly winds intersect the coastline from Tent Point to the south and from Point Lefroy to Gales Bay, respectively (see figures 5.16 to 5.19).

The envelopes show that all of the coastline in Exmouth Gulf is at risk in the event of an oil spill from the proposed Whalebone Prospect well location. The time taken for oil to travel to the coastline under sustained 10 m s^{-1} winds varies from about 6 hours for Exmouth to North West Cape to somewhat more than 24 hours for the north-eastern coast and almost 48 hours to the head of the Gulf (e.g. Gales Bay).

Several comments are relevant to these results. Firstly, they apply to constant wind directions, whereas in reality the wind directions change daily (refer to section 2), with small variations over shorter time scales (i.e. minutes). Secondly, only the eight cardinal directions are represented. For intermediate directions, the envelopes will cover different parts of the Gulf (e.g. for a wind direction of south-south-east, the envelope would quite likely affect the Muiron Islands).

It should be noted that several islands and reefs, especially on the eastern and north-eastern side of the Gulf are too small to be represented by the model grid. Also there are a number of islands beyond the north-eastern boundary of the grid. All of these areas would be at risk for specific wind directions, particularly southerlies, south-westerlies and westerlies.

In the case where envelopes intersect the coastline, no further movement (i.e. along the coast) is predicted. Although such movement will likely occur in reality, the models used do not account for the currents very close to the coast that cause this effect (see section 4.6). It should also be noted that currents within one or two grid points of the boundaries may not be accurate as the full dynamical equations cannot be solved on the boundaries. The open boundary conditions (appendix B) represent the best available estimate of what actually occurs at the boundaries.

Rivoli Prospect

The general comments made about the results for Whalebone Prospect also apply to the results for Rivoli Prospect.

For spring and neap tides only, figures 5.20 and 5.21 again show envelopes that are ellipical in shape. However, because Rivoli Prospect is further into the Gulf than Whalebone prospect, the ellipses are nearly straight lines aligned NNE-SSW with almost no minor axis. The envelope lengths after 48 hours are about 15 km and 10 km for spring and neap tides, respectively.

Figures 5.22 to 5.27 show that envelopes for the northerly, north-easterly and easterly winds intersect the coastline in the vicinity of Exmouth, between Exmouth and Bundegi Reefs and between Bundegi Reefs and Point Murat.

For the south-easterly and southerly winds, figures 5.28 to 5.31 show that the envelopes exit the gulf to the north between North West Cape and the Muirons and the north-east respectively. The envelope for the south-east wind does just intersect the coastline near Point Murat.

Envelopes for the south-westerly, westerly and north-westerly winds affect the coastline between Locker Point and Tent Point, near Hope Point, and from Point Lefroy to Gales Bay, respectively (see figures 5.32 to 5.37).

The envelopes indicate that for sustained wind speeds of 10 m s^{-1} , oil could travel from the proposed Rivoli Prospect well location to almost any point of the Gulf coastline or the Muiron Islands in about 24 hours. It would take a little longer to reach the head of the Gulf.

6. CONCLUSIONS

The following conclusions are drawn:

1. For Exmouth Gulf, some of the ambient climatology is reasonably well known, from land and coastal observations and measurements including winds and water levels. Other aspects, such as wave climate and water currents have not been measured systematically and are not well known. In the absence of measurements, numerical modelling of the wind driven and tidal currents provides the best estimates of the Gulf circulation which will transport any oil spill away from the exploration well sites.
2. Both vertically integrated (2D) and depth-dependent (2.5D) numerical circulation models have been applied to Exmouth Gulf. The 2D model was used to consider tidally-driven time varying currents, while the 2.5D model was used to provide wind-driven currents under a constant wind speed.
3. There is inadequate current meter and water level data for Exmouth Gulf to properly calibrate the models. However the limited observations compare favourably with model output (i.e. tide constituents are within 5% and tidal currents are within 10%). The models have also been used at other locations, including the North West Shelf, where measurements have shown good agreement with modelled output. It is considered that these models provide the best available estimates of the important currents for oil spill modelling in Exmouth Gulf.
4. The oil spill model used makes several assumptions. It is assumed that no oil is lost through evaporation, or chemical, or physical degradation, and that the oil moves with the surface currents. Horizontal diffusion of the oil patches is shown to be insignificant compared with advection so it is omitted. In addition, near-shore drift along the coastline induced by waves and beach slope has not been modelled. Although these effects could be modelled, they would add considerable complexity to the models. It is not considered that the results of this study would be significantly improved by the additional modelling.
5. A total of eighteen oil spill scenarios were studied, for each of the two proposed well locations, Whalebone and Rivoli Prospects. These included spring and neap tide only cases, as well as each of these tides acting concurrently with a steady 10 m s^{-1} wind from each of the eight cardinal wind directions (north, north-east, east, south-east, south, south-west, west and north-west). For each of the 36 scenarios, the envelopes of the maximum oil excursion distance in 6, 12, 24 and 48 hours were determined.

6. Generally, for the tide only cases, the oil spill envelopes were confined to elliptical regions lying NNE-SSW, with much less spreading occurring along the minor axis of the ellipse for Rivoli Prospect than for Whalebone Prospect due to the unidirectionality of the currents there. Maximum excursions under tides only were predicted as 25 km about Whalebone Prospect and 15 km about Rivoli Prospect.
7. For the combined wind and tidally driven cases, the envelopes are drawn out in a long shape which reflects the predominant influence of the wind-driven currents. These envelopes are broader for spring tides, may reach 20 km width depending on the wind direction with the main axis of the tidal ellipse.
8. These envelopes also indicate that most of the Exmouth Gulf coastline would be at risk in under 48 hours in the event of an oil spill from either location, assuming sustained wind speeds of 10 m s^{-1} were experienced. It should be noted that wind speeds only exceed 10 m s^{-1} for periods of more than 1 day for 1.7% of the time during the November to April period, so the modelled oil spill travel times to the coastline are less than what could be expected under most wind conditions. When evaluating these results, the assumptions made in the oil spill model should also be borne in mind (refer in particular to item 3 and 4 above).

The times taken for the oil spill trajectories from the two locations to intersect the coastline vary slightly. The main differences occur along the east and south coastline where envelopes from Rivoli Prospect reach most coastal points in 24 hours or less, while it takes them a little longer from Whalebone Prospect (in the order of 30 hours or less).

9. Due to the proximity of the proposed well locations to the west coast of the Gulf, oil spills will take less time to reach this coastline (e.g. about 6 hours under sustained 10 m s^{-1} northerly, north-easterly or easterly winds) than the eastern and southern coastlines. However, the low occurrence of winds from directions other than the south, south-west or west sectors (a total of 24% over the November to April period) means that the coastline from Giralda Bay in the head of the Gulf to North West Cape (the west side of the Gulf) is much less likely to be affected than other parts of the Gulf.

The most likely direction for oil spill travel is towards the north-east under a southerly wind (with a probability of about 35%), exiting the Gulf between the Muiron Islands and Locker Point. Under a sustained 10 m s^{-1} wind, the oil would take 24 hours or more to reach the Muirons, the main coastline (in the vicinity of Locker Point) or any intermediate islands (such as Serrurier Island).

7. REFERENCES

- Andrewartha, J.R., 1987. Prediction of Oil Spill Envelopes for Barrow Island Tanker Terminal. Unpublished Steedman Limited report (R356) prepared for West Australian Petroleum Pty. Ltd.
- Australian National Tide Tables 1988, 1987. Australian Government Publishing Service (Canberra).
- Bowden, K.F., 1983. Physical Oceanography of Coastal Waters. Ellis Horwood Limited (Chichester).
- Bretschneider, C.L., 1966. Wave Generation by Wind, Deep and Shallow Water. In Estuary and Coastline Hydrodynamics (A.T. Ippen, editor). McGraw-Hill Book Company, pp 133-196.
- CERC, 1984. Shore Protection Manual, U.S. Army Coastal Engineering Research Centre. U.S. Government Printing Office, Washington D.C.
- Csanady, G.T., 1982. Circulation in the Coastal Ocean. D. Reidel Publishing Company (Holland).
- Easton, A.K., 1970. The tides of the continent of Australia. Research Paper No. 37 Horace Lamb Centre for Oceanographical Research, Flinders University of South Australia.
- Fandry, C.B., 1982. A numerical model of the wind-driven transient motion in Bass Strait. J. Geophys. Res., 87, 499-517.
- Fandry, C.B., 1983. Model for the three-dimensional structure of wind-driven and tidal circulation in Bass Strait. Aust. J. Mar. Freshw. Res., 34, 121-141.
- Fandry, C.B., L.M. Leslie and R.K. Steedman, 1984. Kelvin-type coastal surges generated by tropical cyclones. J. Phys. Oceanogr., 14, 582-593.
- Fofonoff, N.P., 1962. Dynamics of Ocean Currents, The Sea, Vol. 1, 323-395. Interscience Publishers, John Wiley & Sons (New York).
- Gentilli, J. (ed.), 1971. Climates of Australia and New Zealand. World Survey of Climatotology Vol. 13. Elsevier Publishing Co. (Amsterdam).
- Gomes, L. and B.J. Vickery, 1976. Tropical cyclone gust speeds along the Australian coast. Civil Engin. Trans. The Inst. Engin. Aust. DE18, 40-49.
- Heaps, N.S., 1969. A two dimensional numerical sea model. Phil. Trans. Roy. Soc., A265, 98-137.
- Holland, G.J., 1980. An analytic model of the wind and pressure profiles in hurricanes. Month. Weat. Rev., 108, 1212-1218.

- Holloway, P., I. Barnes, I. Webster and J. Imberger, 1981. Dynamics of the North West Shelf. Unpublished report by Environmental Dynamics, Department of Civil Engineering, University of Western Australia. Report no. ED-81-008.
- Holloway, P.E., 1983. Tides on the Australian North West Shelf. Aust. J. Mar. Freshw. Res., 34, 213-230.
- Hunter, J.R., 1980. An interactive computer model of oil slick motions. Oceanology International '80, pp. 42-80.
- Jelesnianski, C.P., 1970. Bottom stress time history in linearized equations of motion for storm surges. Mon. Weather Rev., 98, 462-478.
- Krauss, W., 1973. Methods and Results of Theoretical Oceanography I, Dynamics of the Homogeneous and Quasihomogeneous Ocean. Gebruder Borntraeger (Berlin).
- Loucks, R.H. and D.J. Lawrence, 1971. Reconnaissance of the 1970 oil spill in the Gulf of St Lawrence. Mar. Pollut. Bull. NS 2 (6), 92-94.
- Lourensz, R.S., 1981. Tropical cyclones in the Australian Region, July 1909 to June 1980. Department of Science and Technology, Bureau of Meteorology. Australian Government Publishing Service (Canberra).
- Mills, D.A., 1985. A numerical hydrodynamic model applied to tidal dynamics in the Dampier Archipelago. Department of Conservation and Environment, Perth, Western Australia, Bulletin 190.
- Murray, S.P., 1982. The effects of weather systems, currents and coastal processes on major oil spills at sea. In Pollutant Transfer and Transport in the Sea, editor G. Kullenberg, Vol. II, 169-227. CRC Press, Inc. (Florida).
- Nihoul, J.C.J. (ed.), 1979. Marine Forecasting. Predictability and Modelling in Ocean Hydrodynamics. Proc. 10th International Liege Colloquium on Ocean Hydrodynamics. Elsevier Scientific Publishing Co. pp. 493.
- Nihoul, J.C.J. (ed.), 1982. Hydrodynamics of Semi-enclosed Seas. Proc. 13th International Liege Colloquium on Ocean Dynamics. Elsevier Scientific Publishing Co. pp. 555.
- Okubo, A., 1974. Some speculations on oceanic diffusion diagrams. Rapp. p.-v. Reun. Cons. Int. Explor. Mer., 167, 77-85.
- Provis, D.G., and R. Radok, 1979. Sea-level oscillations along the Australian coast. Aust. J. Mar. Freshwater Res., 30, 295-301.
- Provis, D.G. and G.W. Lennon, 1983. Eddy Viscosity and Tidal Cycles in a Shallow Sea. Estuarine, Coastal and Shelf Science, 16, 351-361.

- Ramming, H.G. and Kowalik, Z., 1980. Numerical Modelling of Marine Hydrodynamics, Applications to Dynamic Physical Processes. Elsevier, Amsterdam.
- Royal Australian Navy, 1952. Tidal Stream and Current Journal, Exmouth, W.A. Supplied by the Hydrographic Service, R.A.N.
- Royal Australian Navy, 1954. Tidal Stream and Current Journal, Exmouth, W.A. Supplied by the Hydrographic Service, R.A.N.
- Schwiderski, E.W., 1979. Global Ocean Tides, Part II. The semi-diurnal principal lunar tide (M_2), Atlas of tidal charts and maps. Naval Surface Weapons Centre, Virginia, Rep. No. NSWC TR 79-914.
- Schwiderski, E.W., 1981a. Global Ocean Tides, Part III. The semi-diurnal principal solar tide (S_2), Atlas of tidal charts and maps. Naval Surface Weapons Centre, Virginia, Rep. No. NSWC TR 81-122.
- Schwiderski, E.W., 1981b. Global Ocean Tides, Part IV. The diurnal luni-solar declination tide (K_1), Atlas of tidal charts and maps. Naval Surface Weapons Centre, Virginia, Rep. No. NSWC TR 81-142.
- Schwiderski, E.W. 1981c. Global Ocean Tides, Part V. The diurnal principal lunar tide (O_1), Atlas of tidal charts and maps. Naval Surface Weapons Centre, Virginia, Rep. No. NSWC TR 81-144
- Southern, R.L. and A.N. Scott, 1976. The genesis and characteristics of tropical cyclones (with special reference to North West Australia). In Proc. Symp. The Impact of Tropical cyclones on Oil and Mineral Development in North West Australia; A.H. Ennor Chairman. Australian Government Publishing Service (Canberra), pp. 1-31.
- Steedman, R.K. and Associates, 1978. Physical and Oceanographic Processes, Exmouth Gulf, Western Australia. Unpublished report prepared for West Australian Petroleum Pty Ltd.
- Steedman, R.K. and Associates, 1982. Water Current and Tide Measurements, Rig Site Survey, Stations 1 and 2 near Serrurier No. 1, Exmouth Area. Unpublished report (R172) prepared for Esso Australia Limited.
- Steedman Limited, 1986. Prediction of Oil Spill Trajectories for Saladin Location. Unpublished report (R306) prepared for LeProvost, Semeniuk & Chalmer, Perth, Western Australia.
- Steedman Limited, 1987. Oceanographic and Meteorological Measurements Saladin Area, January - April 1987. Unpublished report (R348) prepared for West Australian Petroleum Pty Ltd.

U.S. Navy, 1976. Marine Climatic Atlas of the World, Volume III, Indian Ocean. Produced by the Naval Weather Service Detachment (Ashville N.C.).

White, T.F. St. C., 1975. Population Dynamics of the tiger prawn, *Penaeus Esculentus*. Ph.D. Thesis.

Tables

Measurement Station	Latitude (S)	Longitude (E)	Anemometer height AGL (m)	Measurement period	Measurement type	Data frequency (obs/day)
Vlaming Head (lighthouse)	21°49'	114°06'	unknown	1913-1967	Manual	2
Exmouth Composite	21°56'	114°07'	unknown	1967-1975	Synchrotach anemometer	2
Exmouth Navy Alpha	21°49'	114°10'	10	1971-1976	Synchrotach anemometer	8
Learmonth Met. Office	22°14'	114°05'	10	1975-1988	Dines anemometer	8
Learmonth Navy Charlie	22°20'	114°03'	10	1968-1971	Synchrotach anemometer	2
Onslow Met. Office	21°40'	114°07'	10	1940-1975	Dines anemometer	8
Onslow Post Office	21°38'	115°06'	10	1975-1988	Esterline anemometer	2

Table 2.1 Wind data available in the Exmouth Gulf region.

JOB NO. 769

LOCATION: LEARMONTH

WIND SPEED-DIRECTION PERCENTAGE OCCURRENCE MATRIX

=====

LATITUDE: 22 14' 30" S LONGITUDE: 114 5' 36" E

ELEV AHD: ELEV AGL: 10.0 M.

PERIOD: NOVEMBER - APRIL, 1975/76 TO 84/85

		WIND SPEED (M/S)								TOTALS
		0.1	2.1	4.1	6.1	8.1	10.1	12.1	14.1	
		TO	TO	TO	TO	TO	TO	TO	AND	
		2.0	4.0	6.0	8.0	10.0	12.0	14.0	OVER	
D I R E C T I O N	N	.4	1.0	1.2	.8	.2	.1			3.6
	NE	.3	1.3	2.9	1.9	.7	.2	.1	.1	7.6
	E	.4	2.0	3.1	.9	.2	.1			6.7
	SE	.3	1.0	1.2	.6	.3	.1			3.6
	S	.8	2.5	3.6	3.5	1.4	.3			12.2
	SW	1.8	6.6	11.8	15.1	8.9	2.3	.3		46.8
	W	.8	2.0	3.1	4.7	2.2	.5			13.3
	NW	.2	.5	.4	.5	.1				1.8
TOTALS		5.0	16.8	27.2	28.1	14.0	3.7	.5	.2	
OCCURRENCE OF CALMS					4.3%					

STATISTICAL SUMMARY

=====

14496 DATA POINTS USED

	MEAN	MAX	S.D.
U - COMP	1.7	-17.0	3.6
V - COMP	2.9	18.5	4.0
WIND SPEED	5.8	20.6	2.5

NOTE:

1. SPEEDS IN GROUP 0.1 TO 2.0 IMPLIES $0.0 < S \leq 2.0$, ETC
2. DIRECTION GROUPS 22.5 DEG EITHER SIDE OF SPECIFIED DIRECTION
3. DATA SAMPLE INTERVAL IS 180 MINUTES
4. U - COMP IS +VE EAST, V - COMP IS +VE NORTH
5. DATA SAMPLED 0-2100

Table 2.2 Wind speed and direction percentage occurrence matrix for Learmonth Meteorological Office. Data covers the months November to April for 1975/76 to 1984/85.

STEEDMAN LIMITED

JOB NO. 769

LOCATION: EXMOUTH

WIND SPEED-DIRECTION PERCENTAGE OCCURRENCE MATRIX

=====

LATITUDE: 21 49' 0" S LONGITUDE: 114 10' 0" E

ELEV AHD: ELEV AGL: 10.0 M.

PERIOD: NOVEMBER - APRIL, 1972/73 TO 1975/76

		WIND SPEED (M/S)								TOTALS
		0.1	2.1	4.1	6.1	8.1	10.1	12.1	14.1	
		TO	TO	TO	TO	TO	TO	TO	AND	
		2.0	4.0	6.0	8.0	10.0	12.0	14.0	OVER	
D I R E C T I O N	N		.9	1.0	.8	.3	.1		.2	3.3
	NE	.2	1.2	1.6	1.0	.4	.3	.1	.2	4.8
	E	.1	.7	.8	.8	.4	.4	.2	.2	3.6
	SE	.2	1.3	2.2	1.0	.2	.3	.2	.1	5.4
	S	.5	2.6	6.5	8.7	7.4	6.1	2.3	.5	34.7
	SW	.9	3.8	4.3	4.2	2.0	1.8	.3		17.4
	W	.8	2.3	2.8	4.4	3.1	1.4	.3	.1	15.3
	NW	.2	1.1	1.7	2.9	.9	.2	.1	.1	7.1
TOTALS		3.0	13.9	20.9	23.6	14.8	10.5	3.4	1.4	

OCCURRENCE OF CALMS 8.5%

STATISTICAL SUMMARY

=====

5066 DATA POINTS USED

	MEAN	MAX	S.D.
U - COMP	1.2	-26.1	4.2
V - COMP	3.5	-31.3	5.1
WIND SPEED	6.8	33.9	3.2

NOTE:

1. SPEEDS IN GROUP 0.1 TO 2.0 IMPLIES $0.0 < S \leq 2.0$, ETC
2. DIRECTION GROUPS 22.5 DEG EITHER SIDE OF SPECIFIED DIRECTION
3. DATA SAMPLE INTERVAL IS 180 MINUTES
4. U - COMP IS +VE EAST, V - COMP IS +VE NORTH
5. DATA SAMPLED 0-2100

Table 2.3 Wind speed and direction percentage occurrence matrix for Exmouth Navy Alpha station. Data covers the months November to April for 1972/73 to 1975/76.

Wind speed persistence exceedence

Location : LEARMONTH
 Latitude : 22 14' 30"
 Longitude : 114 5' 36"
 Data period : NOVEMBER - APRIL, 1975/76 TO 1984/85

Percent Duration													
M/S	Hours duration						Days duration						
	> 6	>12	>18	>24	>30	>36	> 2	> 4	> 6	> 8	>10	>12	TOTAL HOURS
=> 2.00	90.0	88.4	83.6	77.8	75.0	73.6	68.2	50.9	36.8	30.2	19.9	15.8	39168
=> 4.00	71.5	63.9	52.9	45.5	42.8	39.9	33.9	16.8	6.7	2.3			31083
=> 6.00	41.4	30.0	21.7	14.8	12.4	10.8	6.5	.9	.4				17991
=> 8.00	13.9	7.0	3.3	1.6	1.1	.8							6033
=>10.00	2.5	1.1	.6	.4	.3	.2							1098
=>12.00	.4	.2	.2	.1	.1								159
=>14.00	.2	.1	.1	.1									78
=>16.00													18
=>18.00													6
=>20.00													0
=>22.00													0
=>24.00													0
=>26.00													0
=>28.00													0
=>30.00													0

Table 2.4

Combined wind speed persistence and exceedence matrix for Learmonth Meteorological Office. Data covers the months November to April for 1975/76 to 1984/85.

Wind speed persistence exceedence

Location : EXMOUTH
 Latitude : 21 49' 0"
 Longitude : 114 10' 0"
 Data period : NOVEMBER - APRIL, 1972/73 TO 1975/76

Percent Duration													
M/S	Hours duration						Days duration						TOTAL HOURS
	> 6	>12	>18	>24	>30	>36	> 2	> 4	> 6	> 8	>10	>12	
=> 2.00	88.9	87.5	82.8	74.2	68.9	67.2	56.3	29.2	14.2	5.0	1.4		15402
=> 4.00	74.9	67.7	55.2	45.2	41.4	37.9	31.0	11.6	2.7				12984
=> 6.00	52.8	38.7	27.6	21.7	17.9	15.8	11.5	1.4					9153
=> 8.00	27.2	15.8	8.5	5.6	4.6	3.0	2.5						4710
=>10.00	12.2	5.7	2.8	1.7	1.3	.7	.3						2121
=>12.00	3.2	1.5	1.0	.8	.8	.3							561
=>14.00	.9	.6	.5	.4	.3	.3							153
=>16.00	.5	.4	.3	.3	.2	.2							93
=>18.00	.3	.2	.2										51
=>20.00	.2	.2	.1										30
=>22.00	.1	.1											24
=>24.00	.1	.1											15
=>26.00	.1	.1											12
=>28.00	.1	.1											12
=>30.00	.1												9

Table 2.5 Combined wind speed persistence and exceedence matrix for Exmouth Navy Alpha station. Data covers the months November to April for 1972/73 to 1975/76.

Storm Type	Principal Months of Occurrence	Typical Wind Speed and Duration	Typical Extreme Wind Speeds	Typical Wind Direction
Tropical Cyclone	November - April	15 - 30 m s ⁻¹ 4 - 16 hours	30 - 50 m s ⁻¹	All directions (dependent on eye location)
Trade Wind Surge	May - September	10 - 15 m s ⁻¹ 24 - 72 hours	20 - 30 m s ⁻¹	South-east
Squalls	November - April	15 - 25 m s ⁻¹ 1 - 2 hours	25 - 30 m s ⁻¹	All directions
Tornadoes	November - April	unknown but say 40 m s ⁻¹ 1 - 5 minutes	Unknown, but say 50 m s ⁻¹	All directions

Table 2.6 Storm types, estimated principal months of occurrence and typical wind speeds and directions.

Table 3.1

Percentage occurrence matrix of significant wave height and period of wind waves at Whalebone Prospect for the months November to April. Wave heights and period were estimated using the Sverdrup Munk Bretschneider (SMB) relationship. Note that the matrix entries are in tenths of a percent.

WAVE PERIOD VS. WAVE HEIGHT
PERCENTAGE OCCURRENCE MATRIX

PREPARED FOR: LEPROVOST SEMENIUK & CHALMER
COMPUTED BY : STEEDMAN LIMITED

LOCATION : WHALEBONE PROSPECT LAT: 21 51' 0" S. LONG: 114 13' 0" E. WATER DEPTH: 20.0 M.
PERIOD : NOVEMBER TO APRIL, 1972/73 TO 1975/76

WAVE HEIGHT (M.)	WAVE PERIOD (SEC)																			TOTAL
	0-+	1-+	2-+	3-+	4-+	5-+	6-+	7-+	8-+	9-+	10-+	11-+	12-+	13-+	14-+	15-+	16-+	17-+	18-+	
0.0-0.1	159+	28+																		187
0.1-0.2		72+																		72
0.2-0.3		56+	34+																	90
0.3-0.4			101+																	101
0.4-0.5			87+																	87
0.5-0.6			69+																	69
0.6-0.7			8+	45+																52
0.7-0.8				38+																38
0.8-0.9				54+																54
0.9-1.0				22+																22
1.0-1.1				47+																47
1.1-1.2					17+															17
1.2-1.3					34+															34
1.3-1.4					15+															15
1.4-1.5					17+															17
1.5-1.6					11+															11
1.6-1.7					4+															4
1.7-1.8					1+	3+														3
1.8-1.9						2+														2
1.9-2.0						1+	1+													1
2.0-+						1+	1+													2
TOTALS	159	156	299	206	99	7	1	0	0	0	0	0	0	0	0	0	0	0	0	0
EXCEEDANCE	1000	767	611	312	106	7	1	0	0	0	0	0	0	0	0	0	0	0	0	0

NO. OF DATA POINTS = 5800.
PERCENTAGE CALM = 7.4

NOTES: WIND DATA FROM EXMOUTH

Table 3.2

Percentage occurrence matrix of significant wave height and period of wind waves at Rivoli Prospect for the months November to April. Wave heights and period were estimated using the Sverdrup Munk Bretschneider (SMB) relationship. Note that the matrix entries are in tenths of a percent.

WAVE PERIOD VS. WAVE HEIGHT
PERCENTAGE OCCURRENCE MATRIX

PREPARED FOR: LEPROVOST SEMENIUK & CHALMER
COMPUTED BY: STEEDMAN LIMITED

LOCATION : RIVOLI PROSPECT LAT: 21 58' 0" S. LONG: 114 13' 0" E. WATER DEPTH: 20.0 M.
PERIOD : NOVEMBER TO APRIL, 1972/73 TO 1975/76

WAVE HEIGHT (M.)	WAVE PERIOD (SEC)																			TOTAL
	0-+	1-+	2-+	3-+	4-+	5-+	6-+	7-+	8-+	9-+	10-+	11-+	12-+	13-+	14-+	15-+	16-+	17-+	18-+	
.0-1.1	155+	27+																		181
.1-1.2		66+																		66
.2-1.3		33+	45+																	78
.3-1.4			95+																	95
.4-1.5			106+																	106
.5-1.6			75+	1+																75
.6-1.7			3+	67+																70
.7-1.8				60+																60
.8-1.9				33+																33
.9-1.0				49+																49
1.0-1.1				39+																39
1.1-1.2				1+	16+															17
1.2-1.3					25+															25
1.3-1.4					15+															15
1.4-1.5					8+															8
1.5-1.6					3+															3
1.6-1.7					2+															2
1.7-1.8						1+														1
1.8-1.9						1+														1
1.9-2.0						1+														1
2.0-+						2+	1+	1+												3
TOTALS	155	125	322	248	70	4	1	1	0	0	0	0	0	0	0	0	0	0	0	
EXCEEDANCE	1000	771	646	524	45	6	1	1	0	0	0	0	0	0	0	0	0	0	0	

NO. OF DATA POINTS = 5800.
PERCENTAGE CALM = 7.4

NOTES: WIND DATA FROM EXMOUTH

Location	Latitude °S	Longitude °E	Reference	M ₂		S ₂		K ₁		O ₁	
				A (m)	g (deg)	A (m)	g (deg)	A (m)	g (deg)	A (m)	g (deg)
Norwegian Bay	22°34'	113°42'	ANTT	0.30	280	0.17	354	0.19	280	0.12	279
Point Murat	21°49'	114°11'	"	0.49	314	0.27	26	0.18	302	0.13	281
Learmonth	22°11'	114°05'	"	0.66	312	0.36	24	0.19	292	0.14	281
Serrurier Island	21°36'	114°41'	"	0.48	290	0.26	5	0.18	288	0.12	269
Onslow	21°38'	115°06'	"	0.57	300	0.30	11	0.19	298	0.12	283
-	21°00'	113°00'	Sch.	0.40	281	0.19	341	0.18	286	0.13	270
-	21°00'	114°00'	"	0.46	286	0.23	344	0.19	287	0.14	270
-	21°00'	115°00'	"	0.55	291	0.28	346	0.19	288	0.14	269
-	21°00'	116°00'	"	0.71	292	0.44	349	0.20	288	0.14	272
-	22°00'	113°00'	"	0.35	282	0.17	341	0.18	286	0.13	271
-	23°00'	113°00'	"	0.31	282	0.16	341	0.18	287	0.13	272
Badjirrajirra	22°07'	114°05'	DMH	0.66	312	0.35	27	0.22	298	0.14	279

Note: ANTT Australian National Tide Tables 1988 (1987)

Sch. Schwiderski (1979, 1981a, 1981b, 1981c)

DMH Department of Marine and Harbours (1986)

Table 4.1 Tidal constants for several locations in the vicinity of the model grid.

Location	M_2		S_2		K_1		O_1	
	A (m)	g (deg)	A (m)	g (deg)	A (m)	g (deg)	A (m)	g (deg)
SW Corner	0.44	312	0.22	26	0.17	300	0.13	279
NW Corner	0.35	287	0.18	350	0.16	288	0.12	272
NE Corner	0.48	290	0.23	0	0.17	288	0.12	271
SE Corner	0.53	302	0.26	20	0.18	295	0.14	282

Table 4.2 Estimated harmonic constants for the model corners, used to provide tidal forcing along the open sea boundaries.

Figures

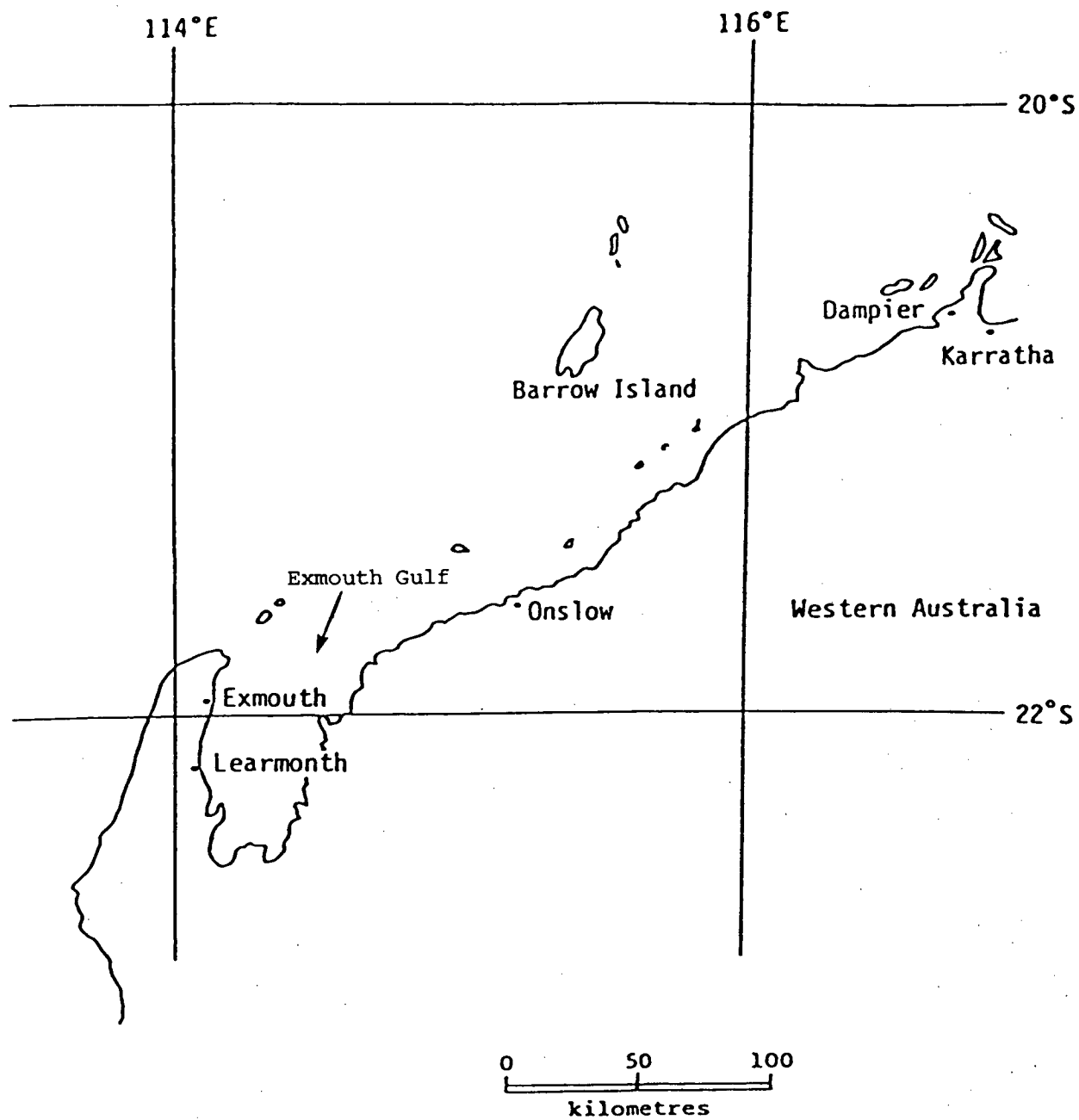


Figure 1.1 Location diagram showing the position of Exmouth Gulf on the North West Shelf.

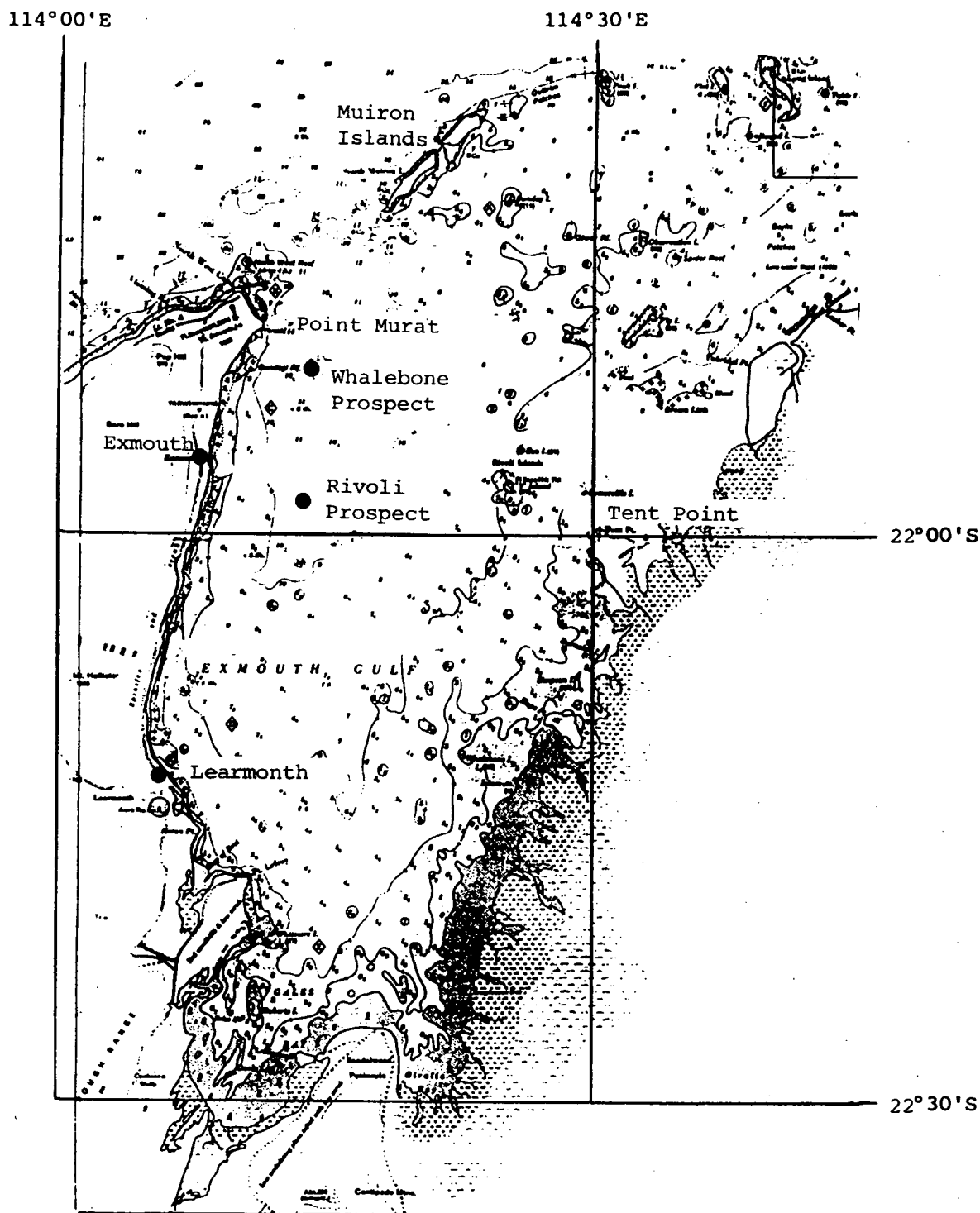
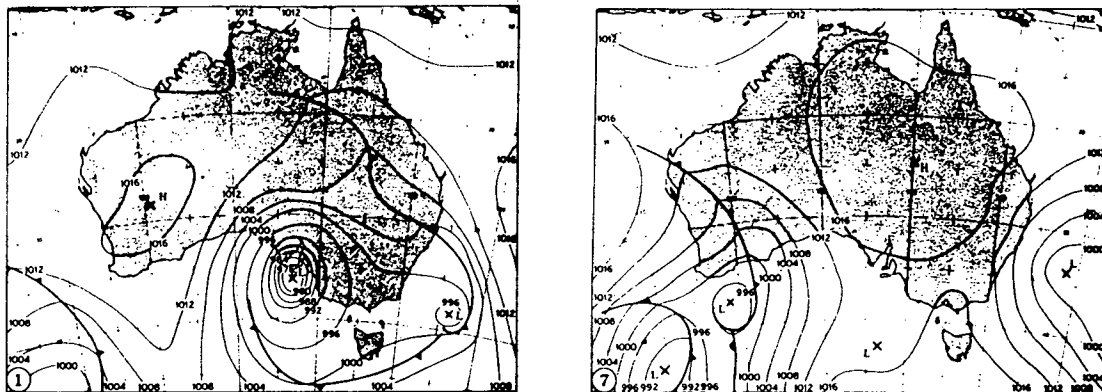
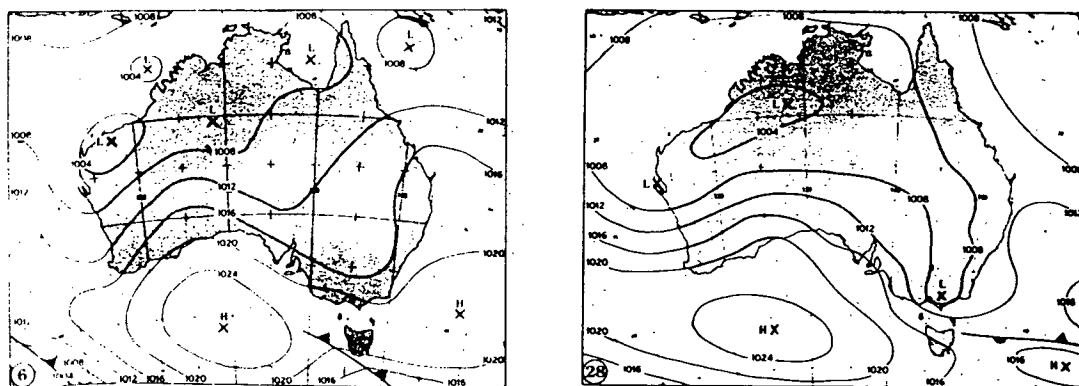


Figure 1.2 Location diagram showing the position of Whalebone and Rivoli Prospects in Exmouth Gulf.

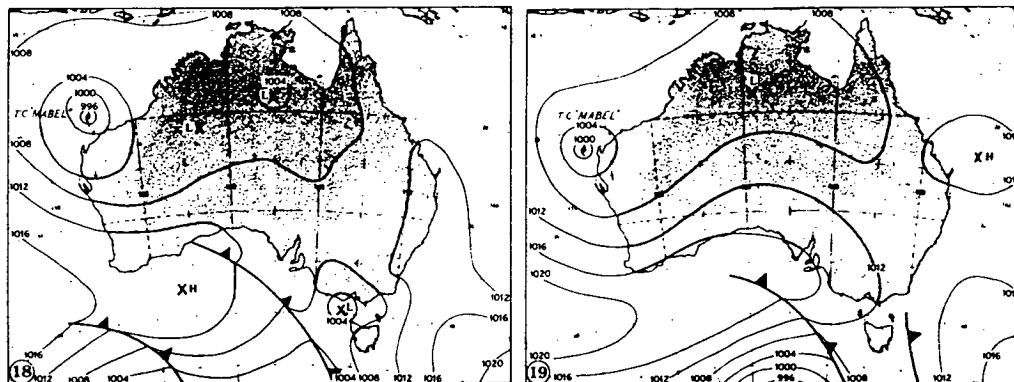


(a) Typical Winter synoptic charts, June 1 and 7, 1981

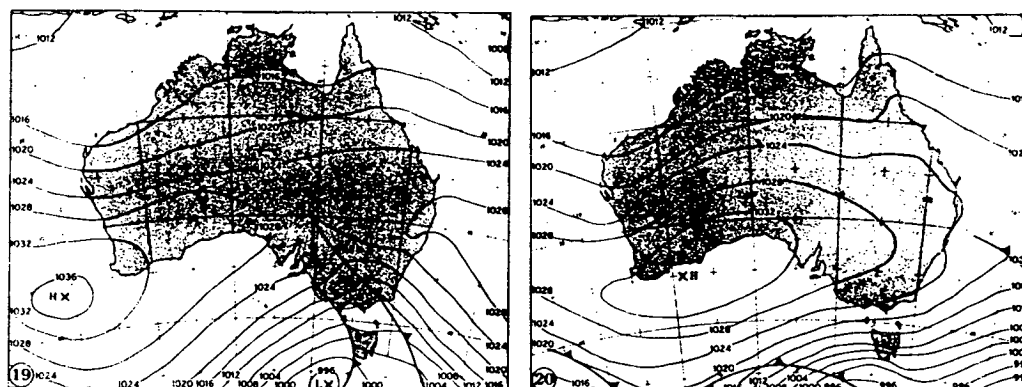


(b) Typical Summer synoptic charts, January 6 and 28, 1981

Figure 2.1 Typical summer and winter synoptic situations over north-western Australia.



(a) tropical cyclone Mabel, January 18 and 19, 1981



(b) trade wind surge example, May 19 and 20, 1982.

Figure 2.2 Surface synoptic charts showing typical conditions of (a) a tropical cyclone and (b) a pressure gradient storm affecting Exmouth Gulf.

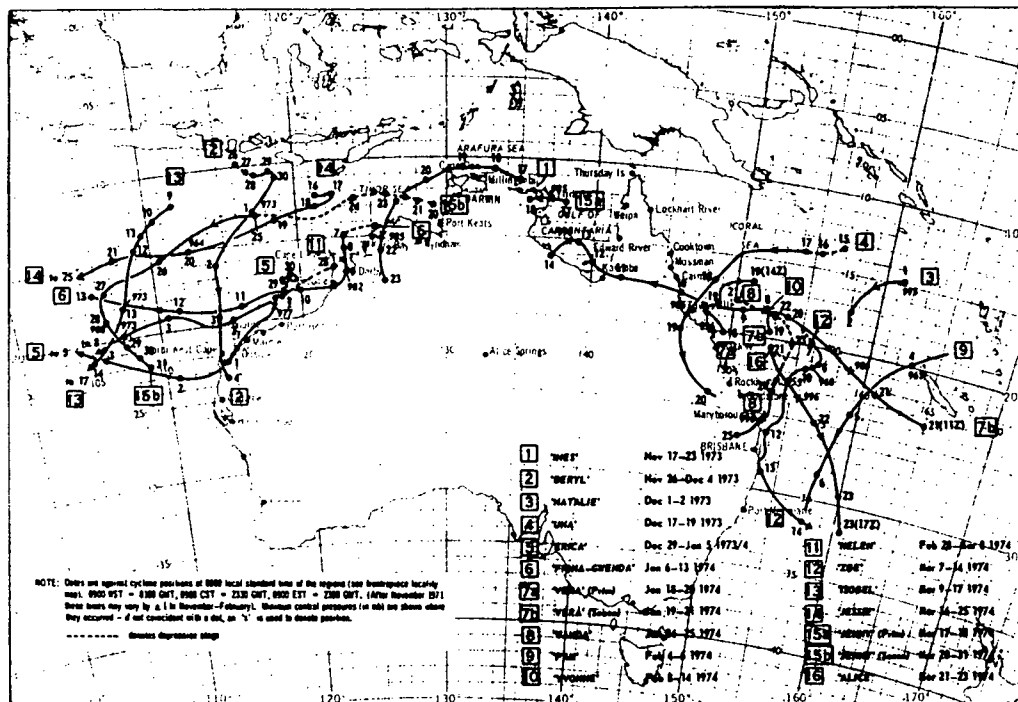


Figure 2.3 Example of tropical cyclone tracks, July 1973 to 1974 (from Lourenz, 1981).

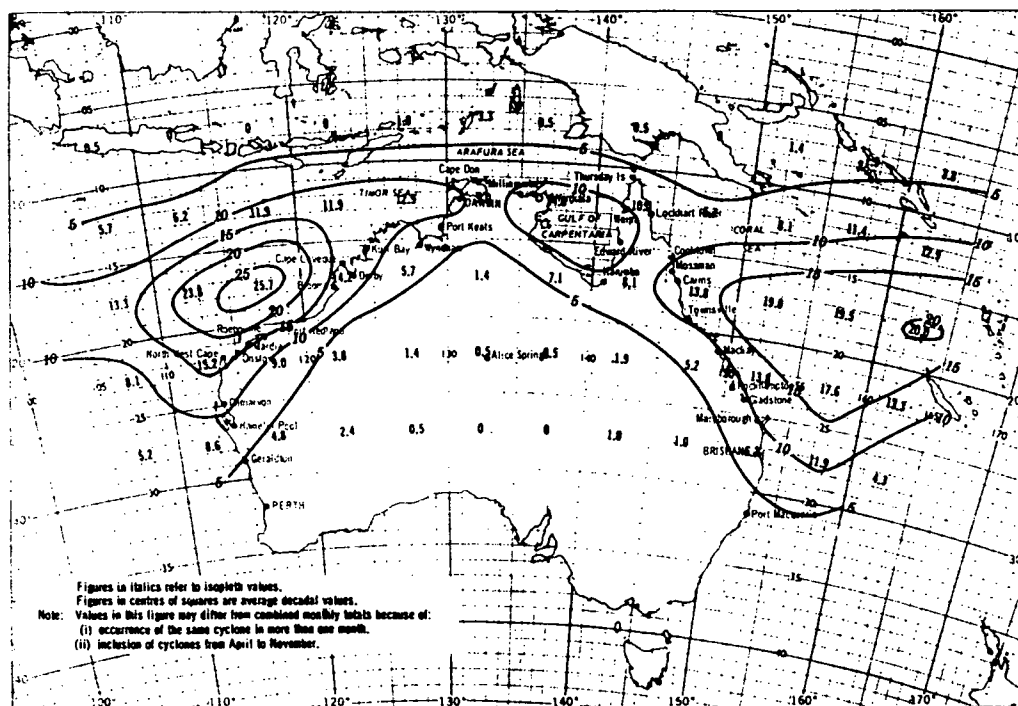


Figure 2.4 Average decadal incidence of tropical cyclones in 5° squares (all months) July 1959 to June 1980 (from Lourenz, 1981).

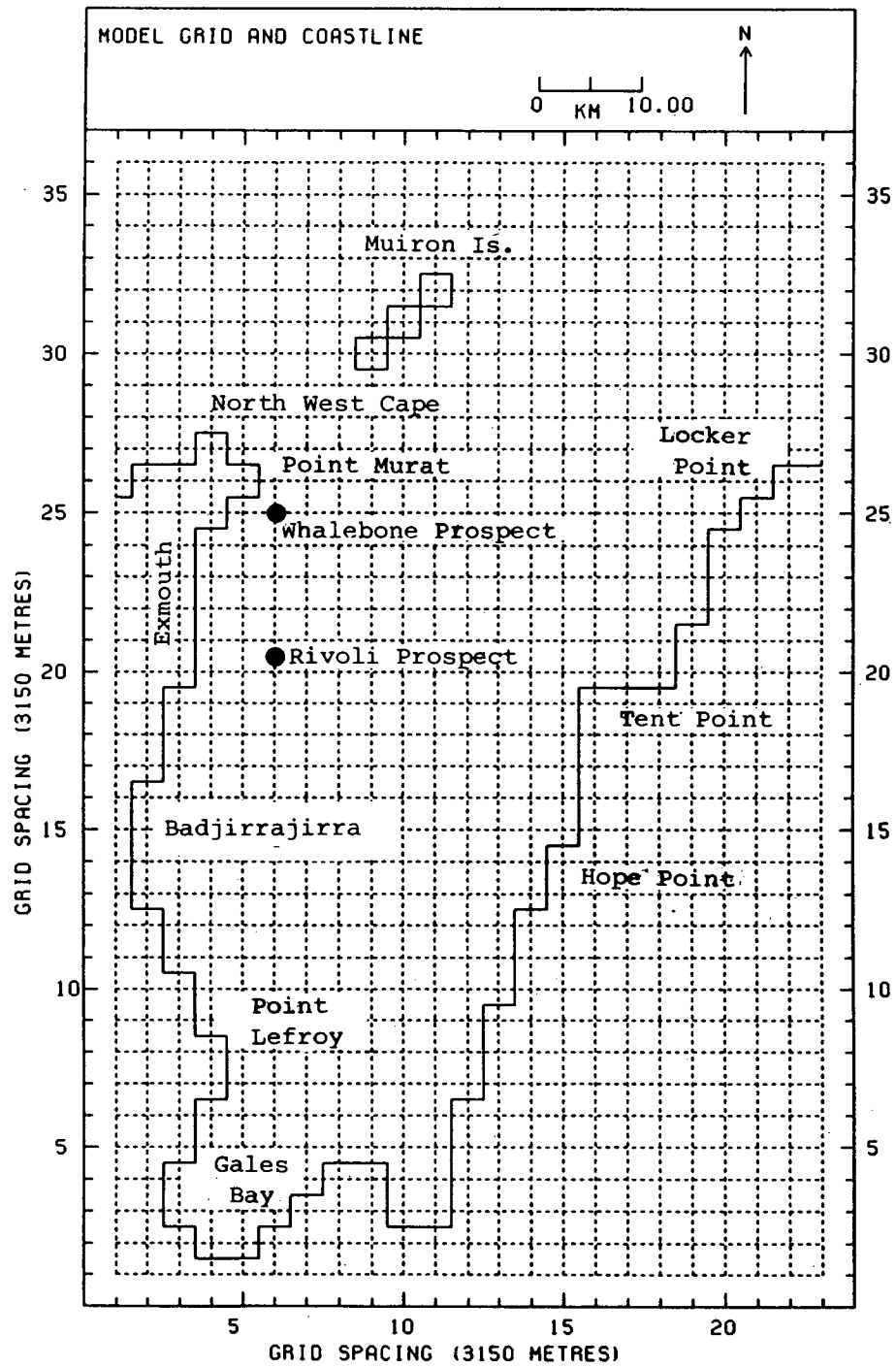


Figure 4.1 Grid and coastline used with the numerical circulation model.



Figure 4.2 Contours of digitized bathymetry used with the numerical circulation model. The digitized 'real' coastline is also shown.

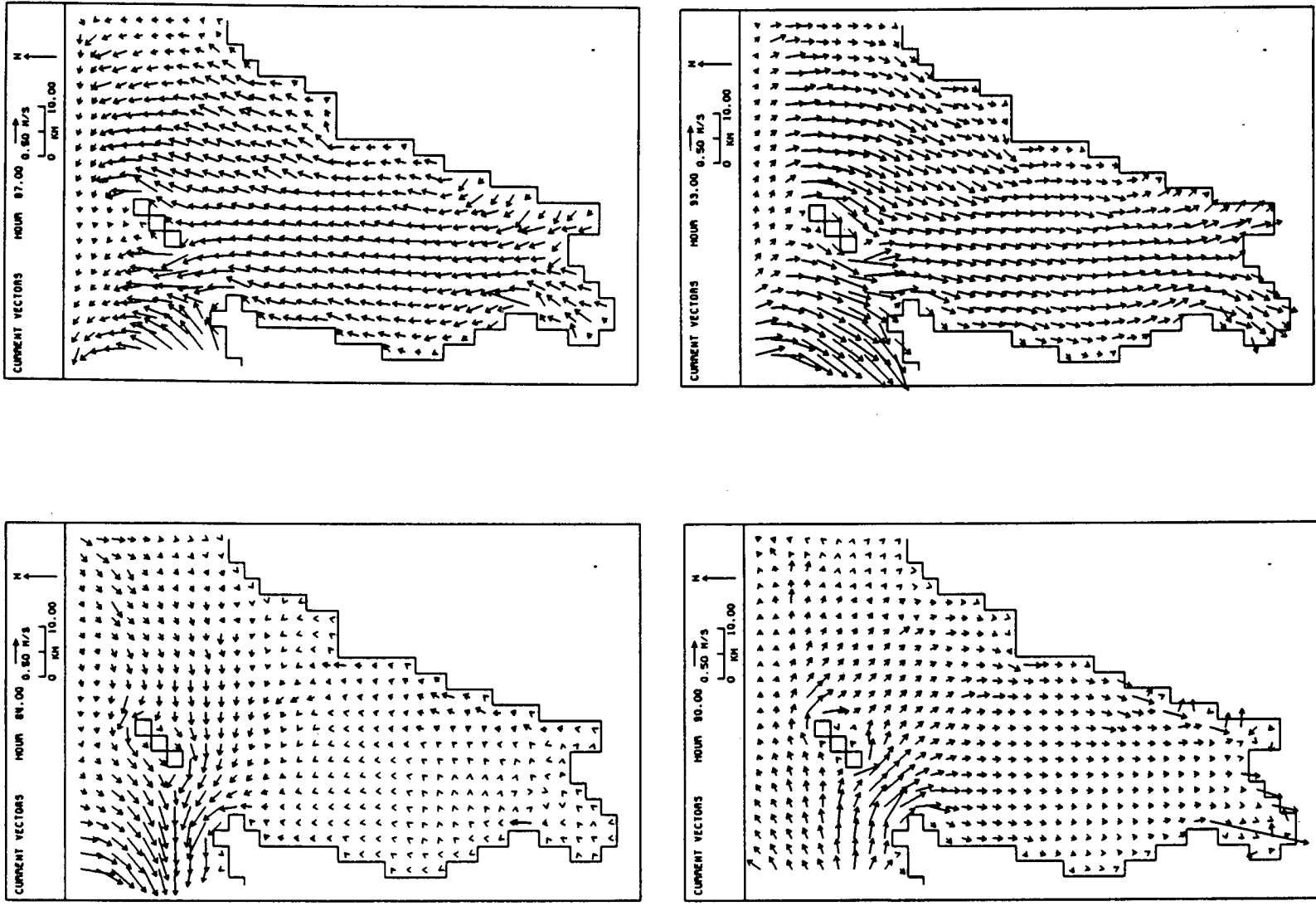


Figure 4.3 Spring tidal depth-average currents, at 3 hourly intervals, predicted by the 2D circulation model. Hour 84 corresponds to 1200 24.11.88.

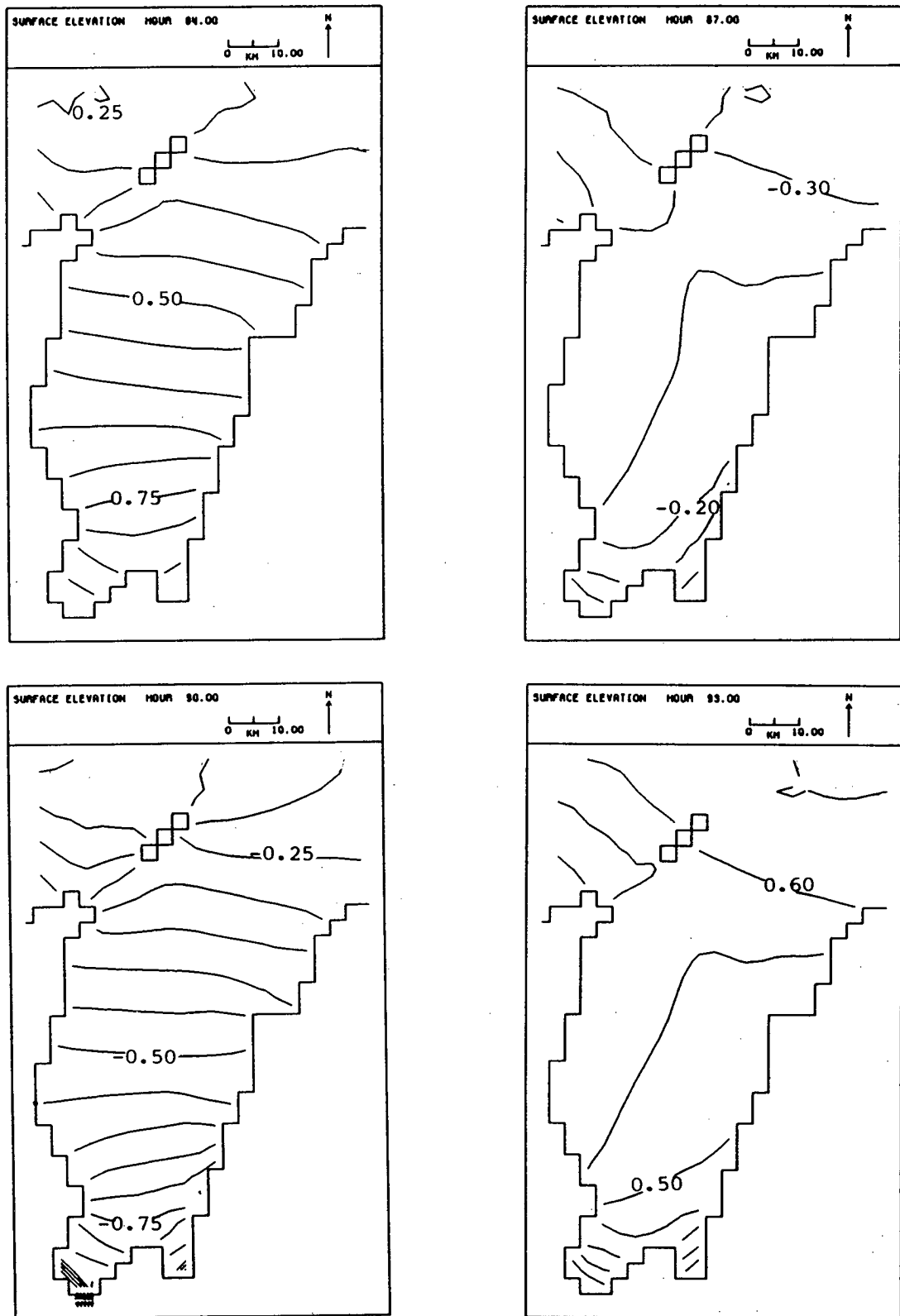


Figure 4.4 Spring tidal surface elevation contours, at 3 hourly intervals predicted by the 2D circulation model. Hour 84 corresponds to 1200 24.11.88 and contour interval is 0.05 m.

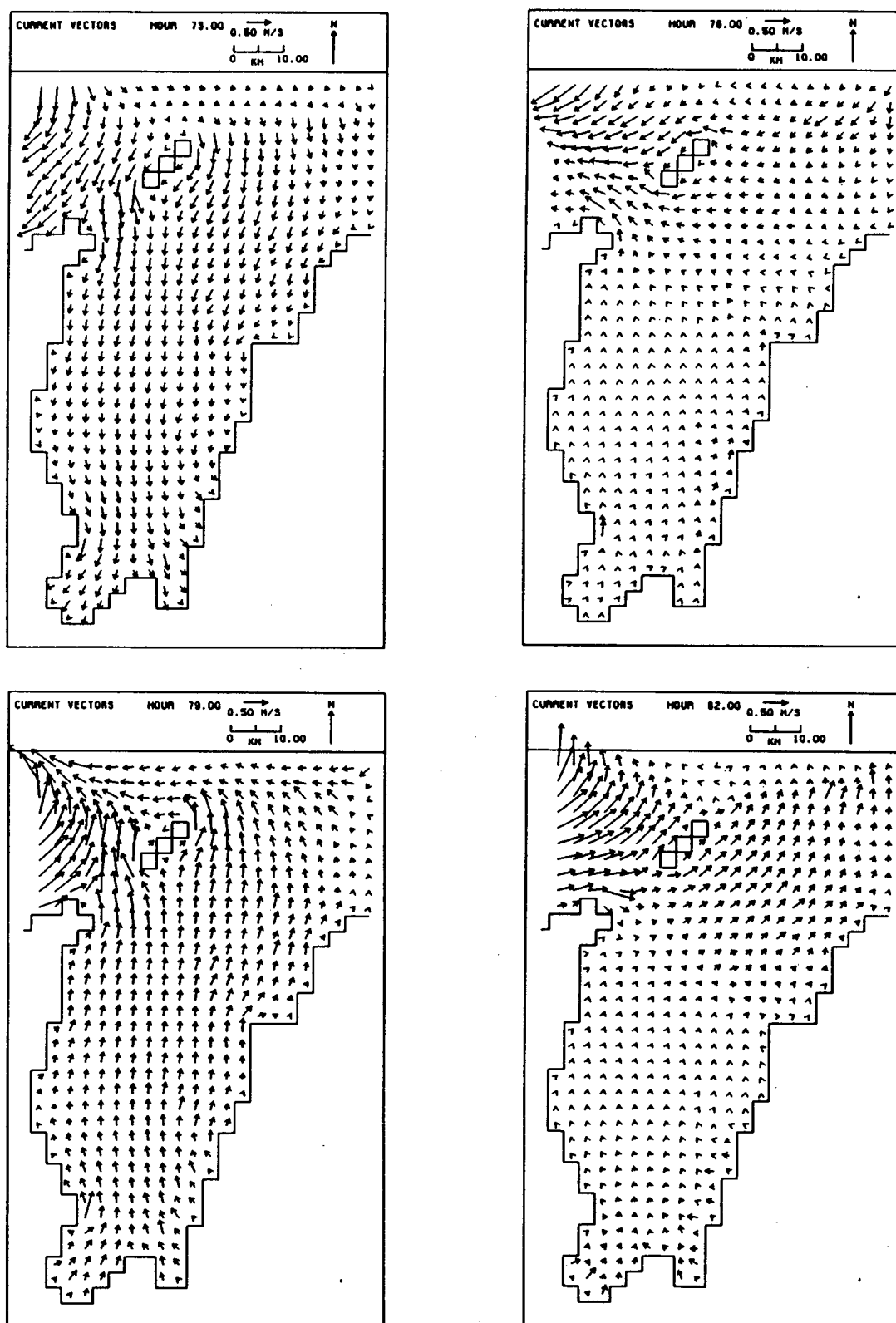


Figure 4.5 Neap tidal depth-average currents, at 3 hourly intervals, predicted by the 2D circulation model. Hour 73 corresponds to 0100 3.11.88.

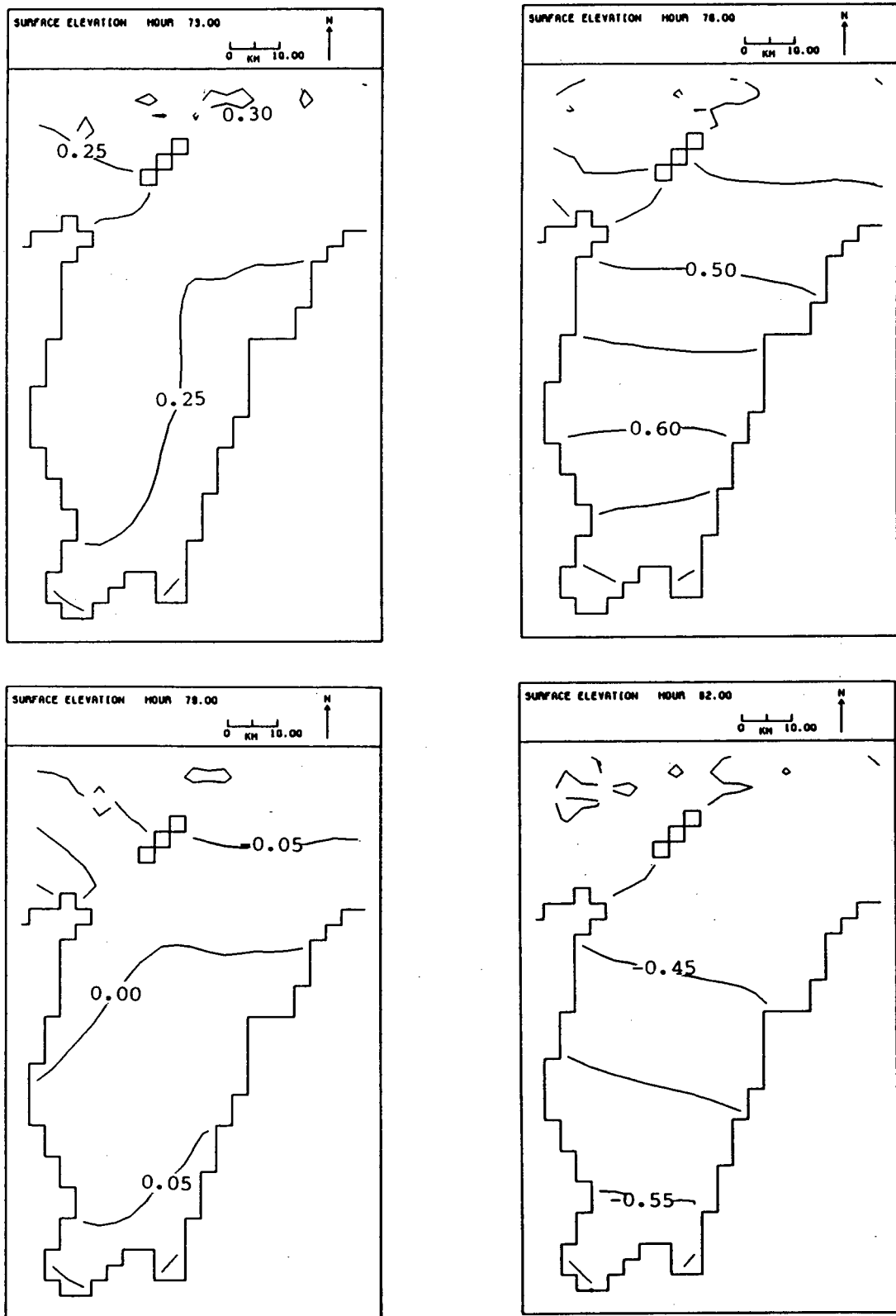


Figure 4.6 Neap tidal surface elevation contours, at 3 hourly intervals, predicted by the 2D circulation model. Hour 73 corresponds to 0100 3.11.88 and contour interval is 0.05 m.

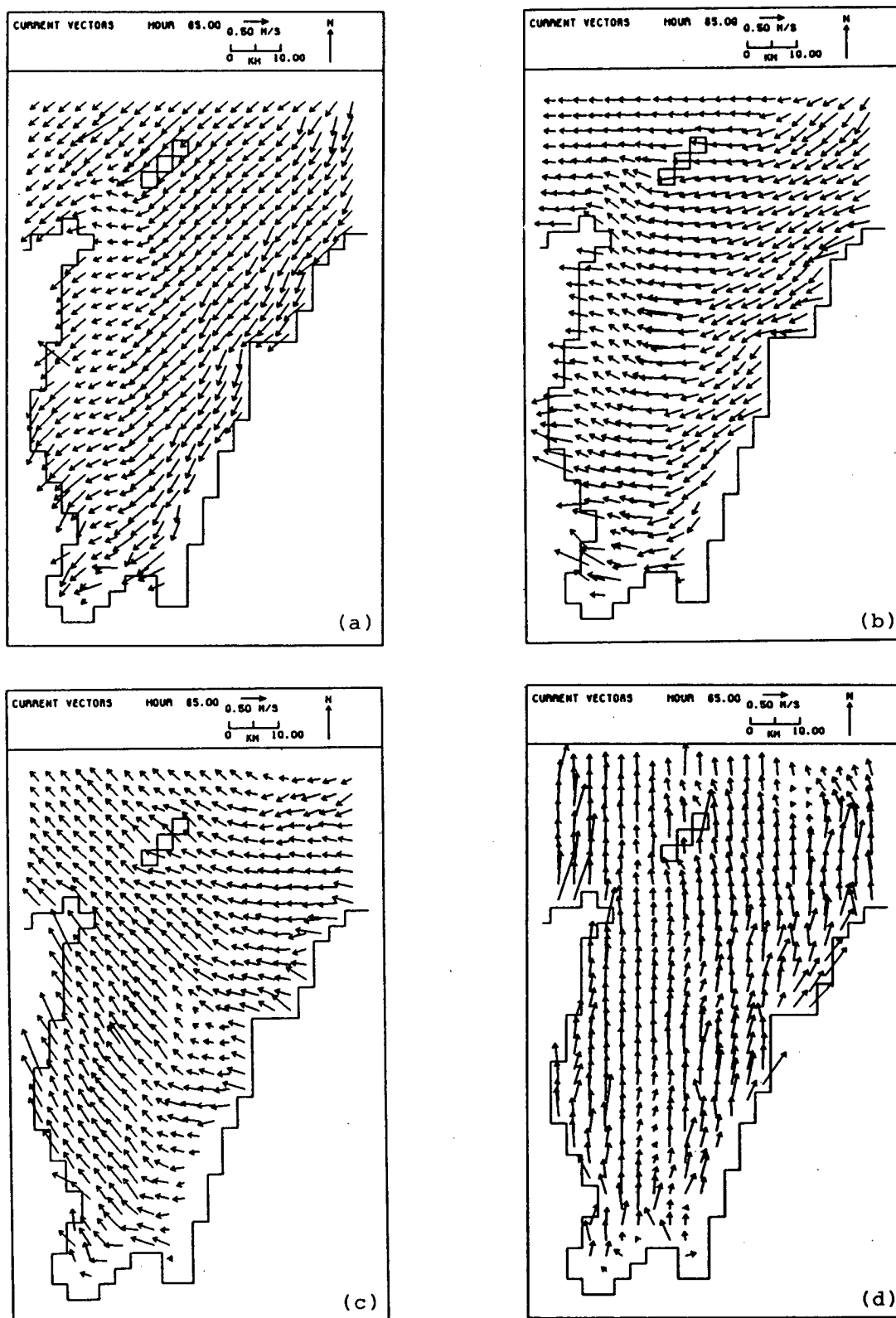


Figure 4.7 Surface currents predicted by the 2.5D circulation model for a steady 10 m s^{-1} wind from the
(a) north
(b) north-east
(c) east
(d) south-east.

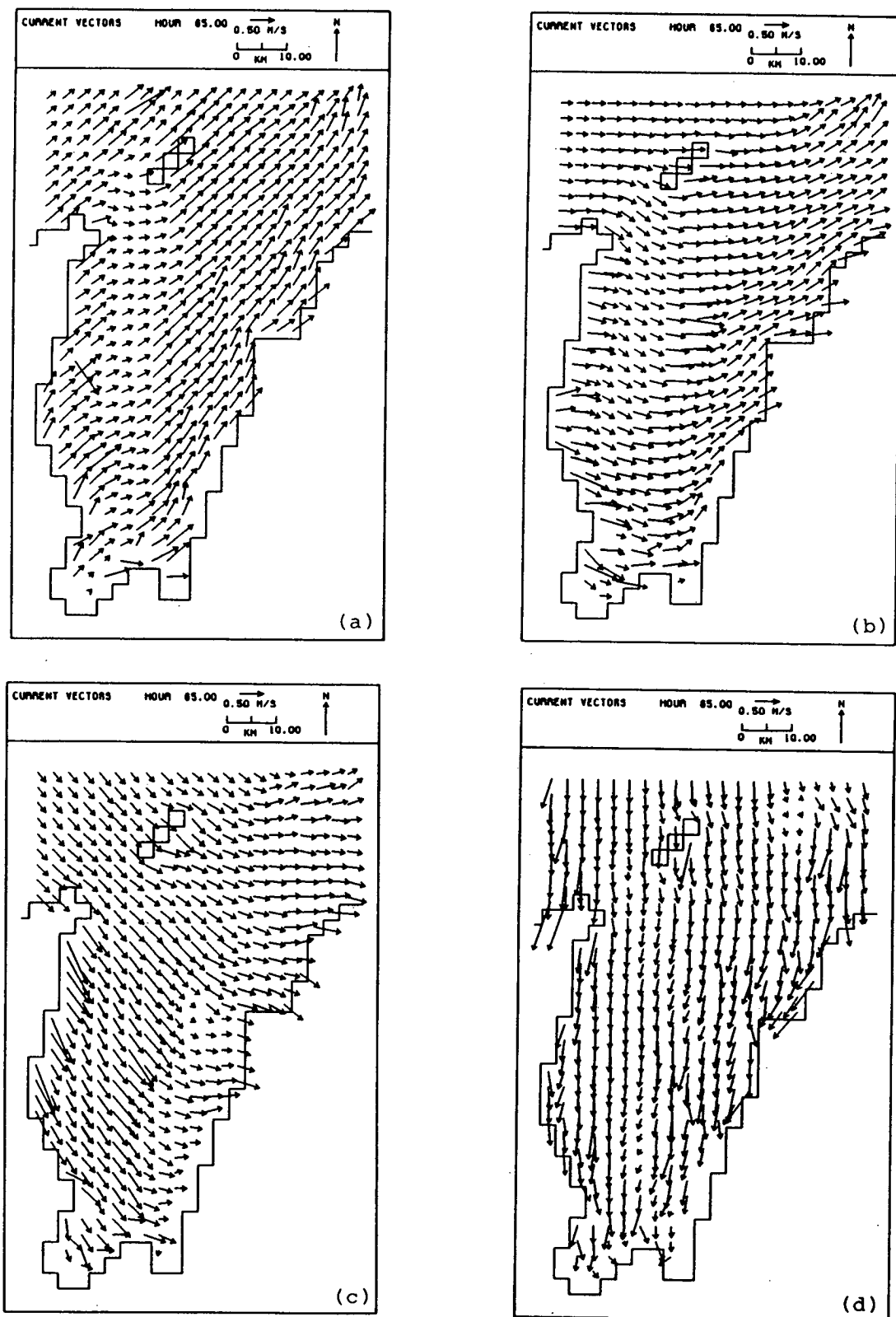


Figure 4.8 Surface currents predicted by the 2.5D circulation model for a steady 10 m s^{-1} wind from the
(a) south
(b) south-west
(c) west
(d) north-west.

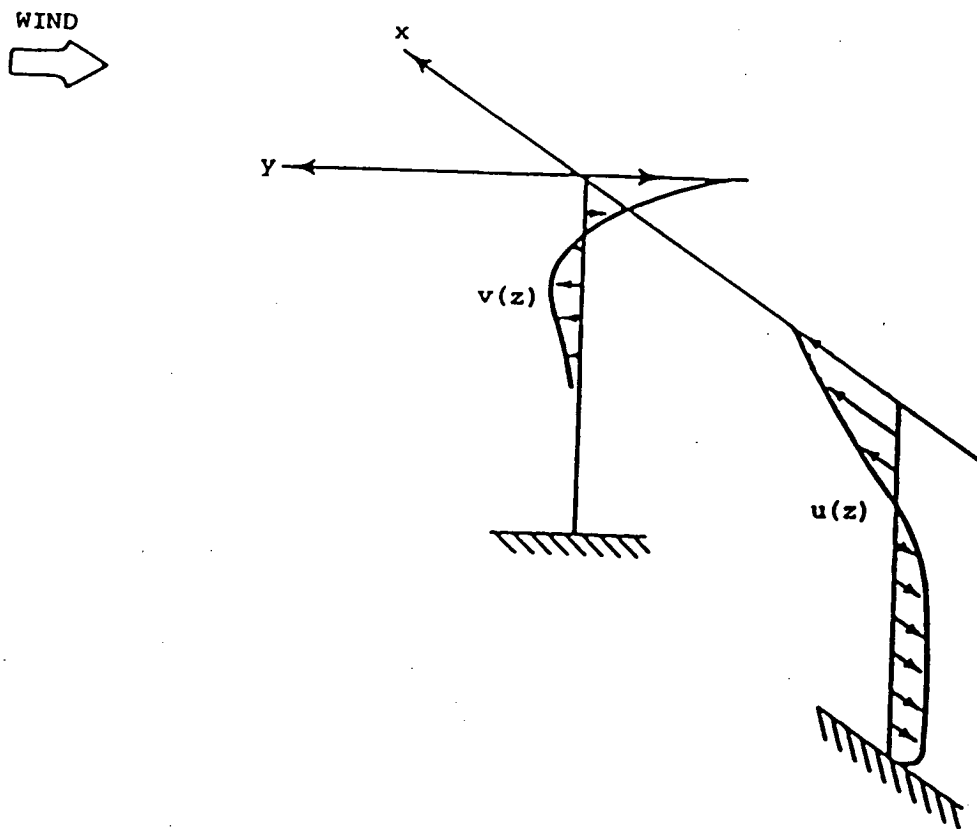


Figure 4.9 Schematic representation of the depth structure of currents forced by cross-shore winds (adapted from Csanady, 1982). The x direction is long-shore.

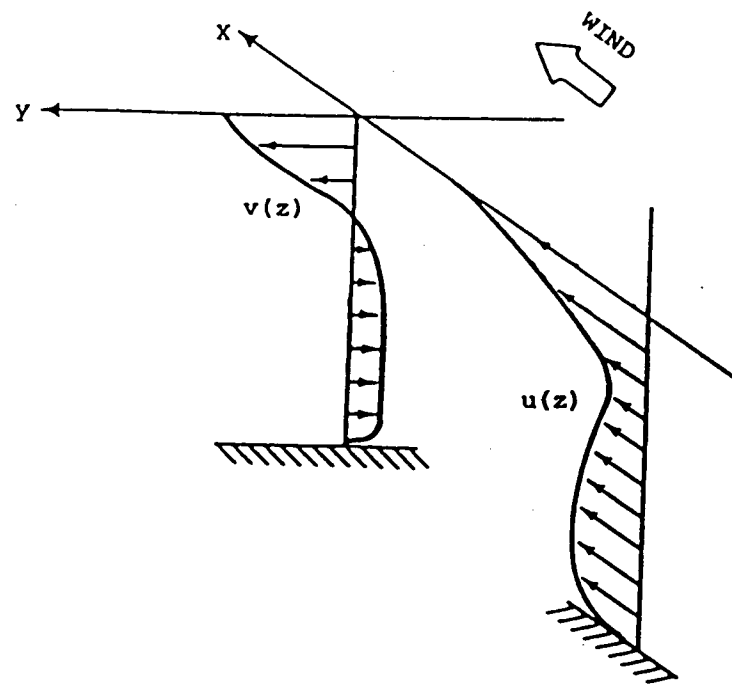
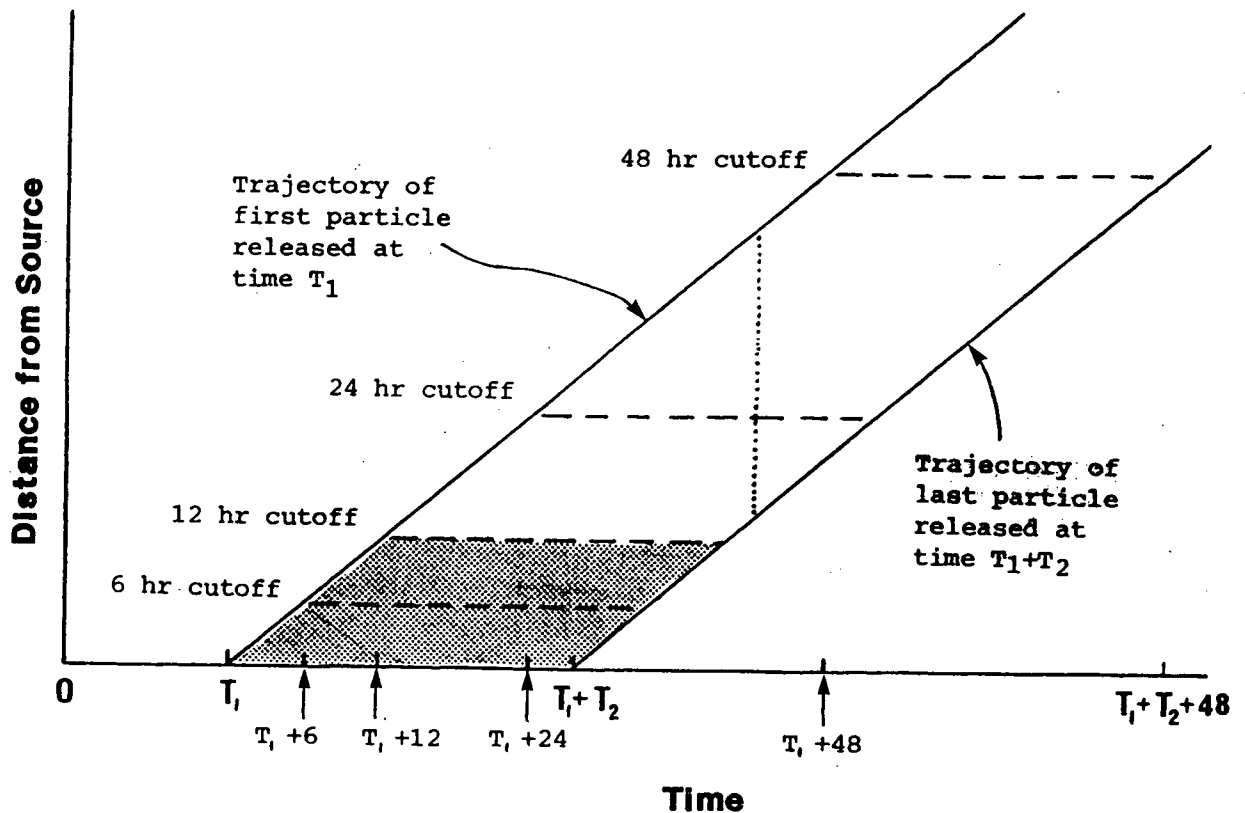


Figure 4.10 Schematic representation of the depth structure of currents forced by long-shore winds (adapted from Csanady, 1982). The y direction is cross-shore.



— A sloping line represents the trajectory of a particle released at a time given by its intersection with the time axis. Shown are the trajectories of the first and last particles released.

----- These lines represent the maximum excursions of particles for 6, 12, 24 & 48 release times. ie they indicate the the upper bound on the number of particles to be plotted for that particular envelope.

..... The length of a vertical section is proportional to the number of particles released at that time. It remains unchanged after time $T_1 + T_2$


 The shaded area represents the 12 hr release envelope.

Figure 5.1 Schematic diagram of oil spill trajectory.

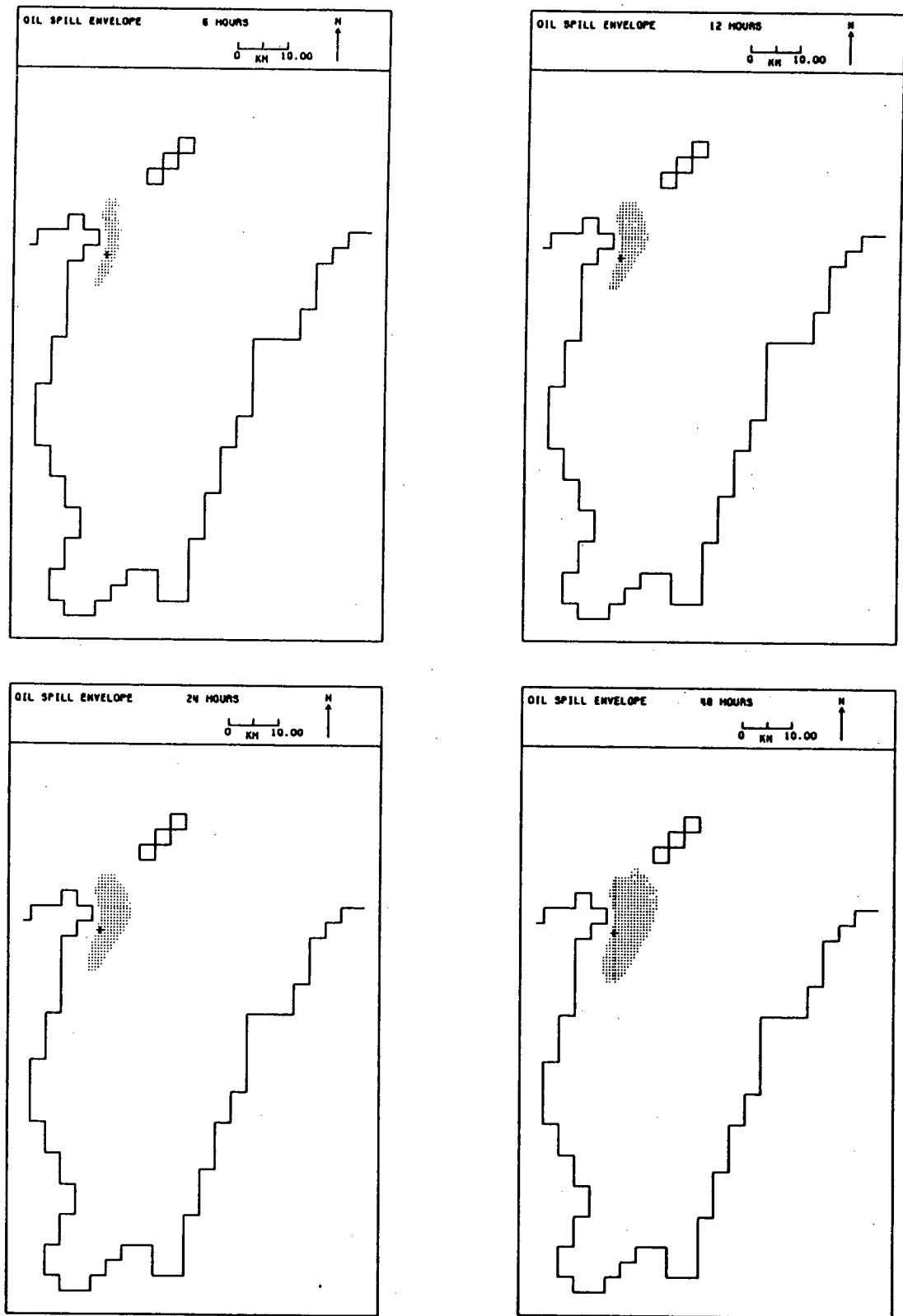


Figure 5.2 Oil spill envelopes for release times of 6, 12, 24 and 48 hours for the case of spring tides only for Whalebone Prospect.

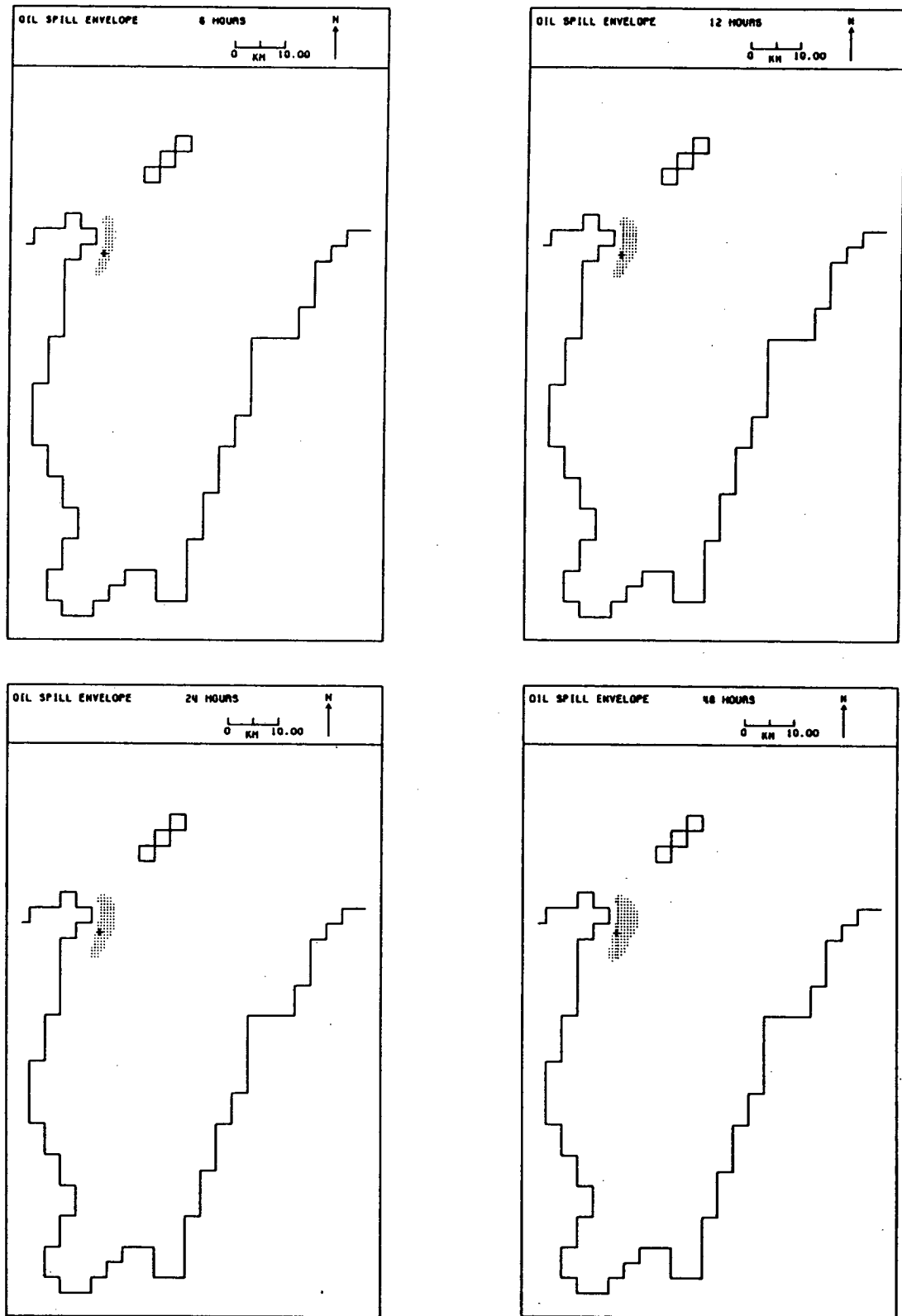


Figure 5.3 Oil spill envelopes for release times of 6, 12, 24 and 48 hours for the case of neap tides only for Whalebone Prospect.

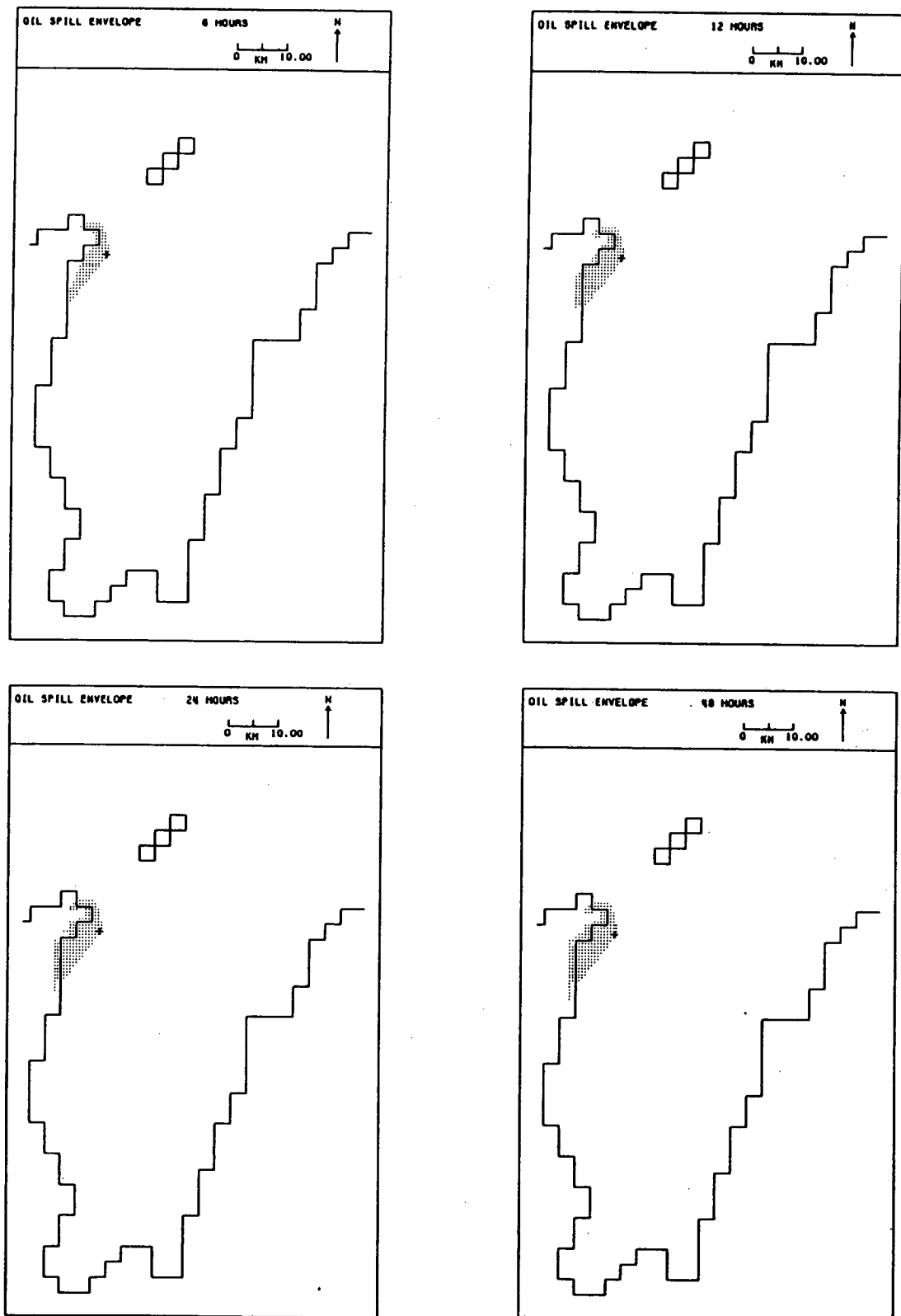


Figure 5.4 Oil spill envelopes for release times of 6, 12, 24 and 48 hours for the case of a 10 m s^{-1} northerly wind during spring tides for Whalebone Prospect.

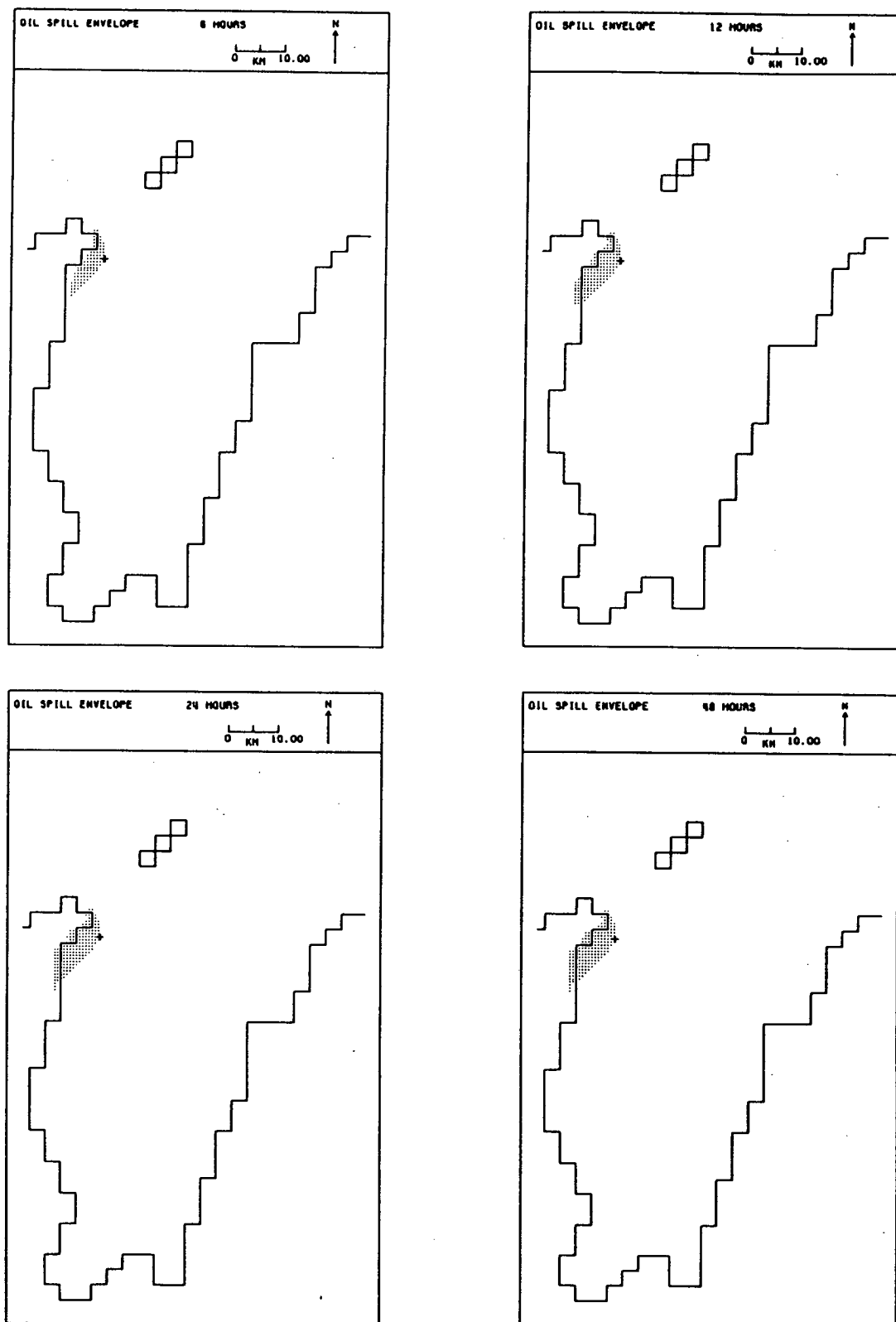


Figure 5.5 Oil spill envelopes for release times of 6, 12, 24 and 48 hours for the case of a 10 m s^{-1} northerly wind during neap tides for Whalebone Prospect.

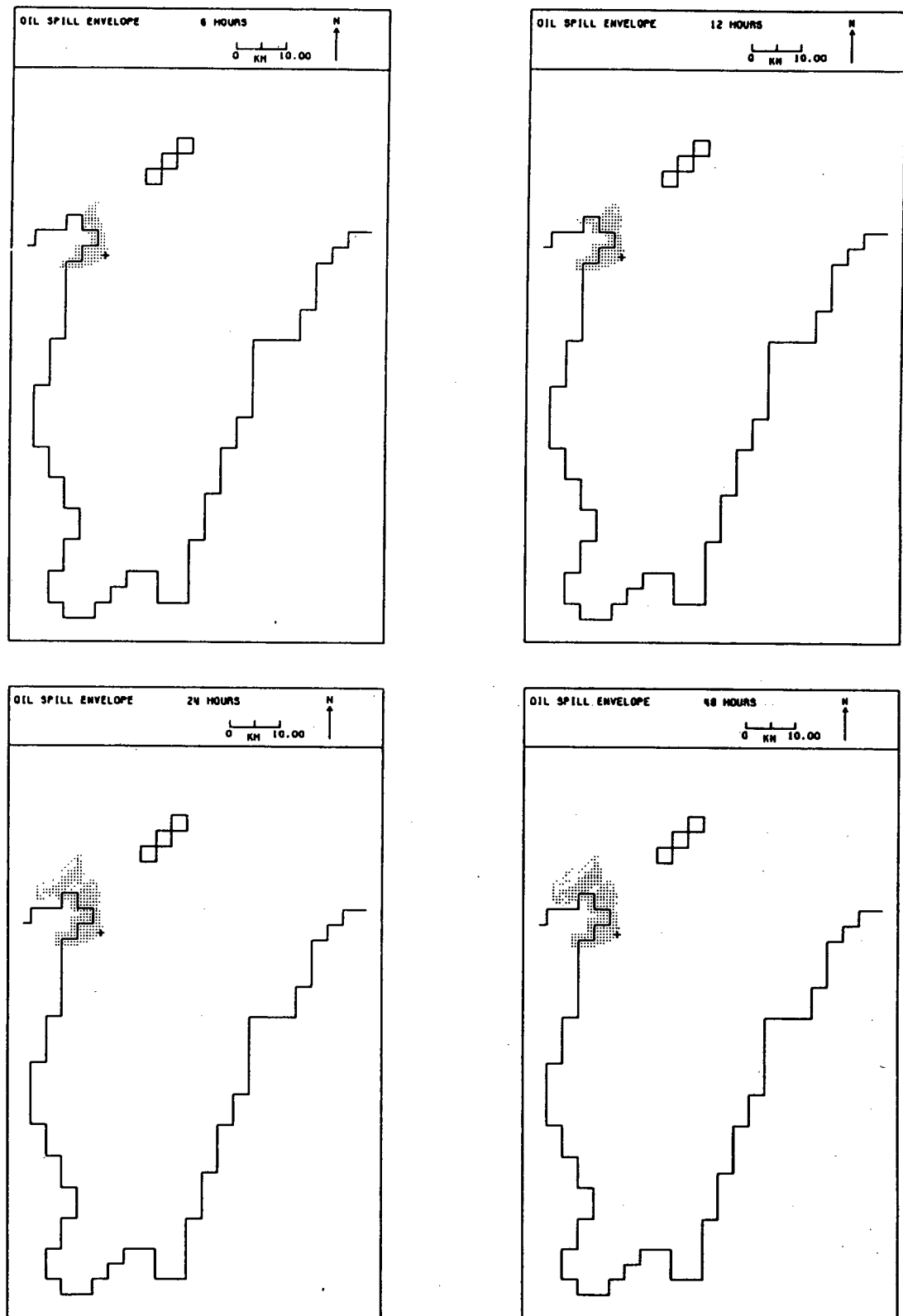


Figure 5.6 Oil spill envelopes for release times of 6, 12, 24 and 48 hours for the case of a 10 m s^{-1} north-easterly wind during spring tides for Whalebone Prospect.

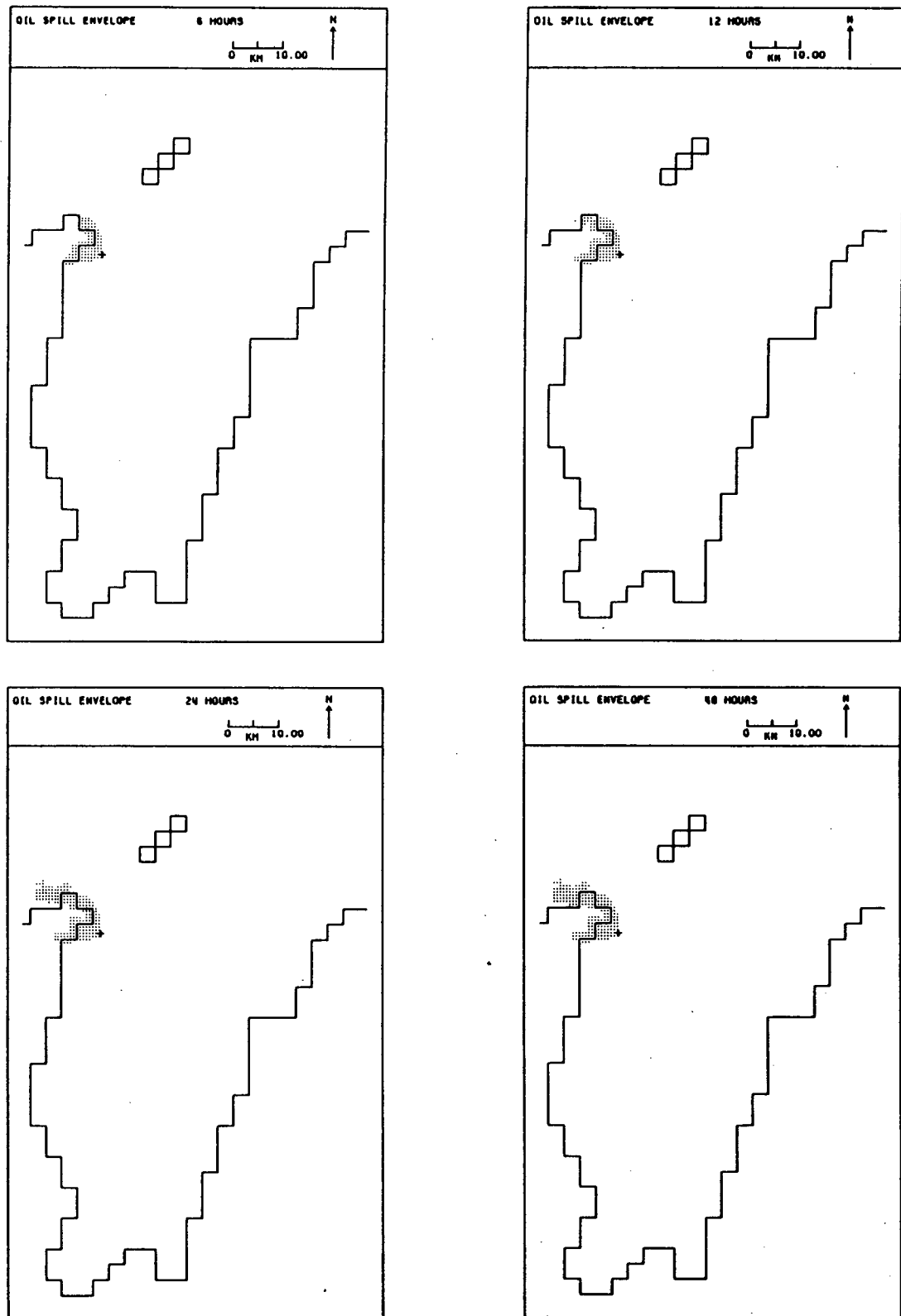


Figure 5.7 Oil spill envelopes for release times of 6, 12, 24 and 48 hours for the case of a 10 m s^{-1} north-easterly wind during neap tides for Whalebone Prospect.



Figure 5.8 Oil spill envelopes for release times of 6, 12, 24 and 48 hours for the case of a 10 m s^{-1} easterly wind during spring tides for Whalebone Prospect.

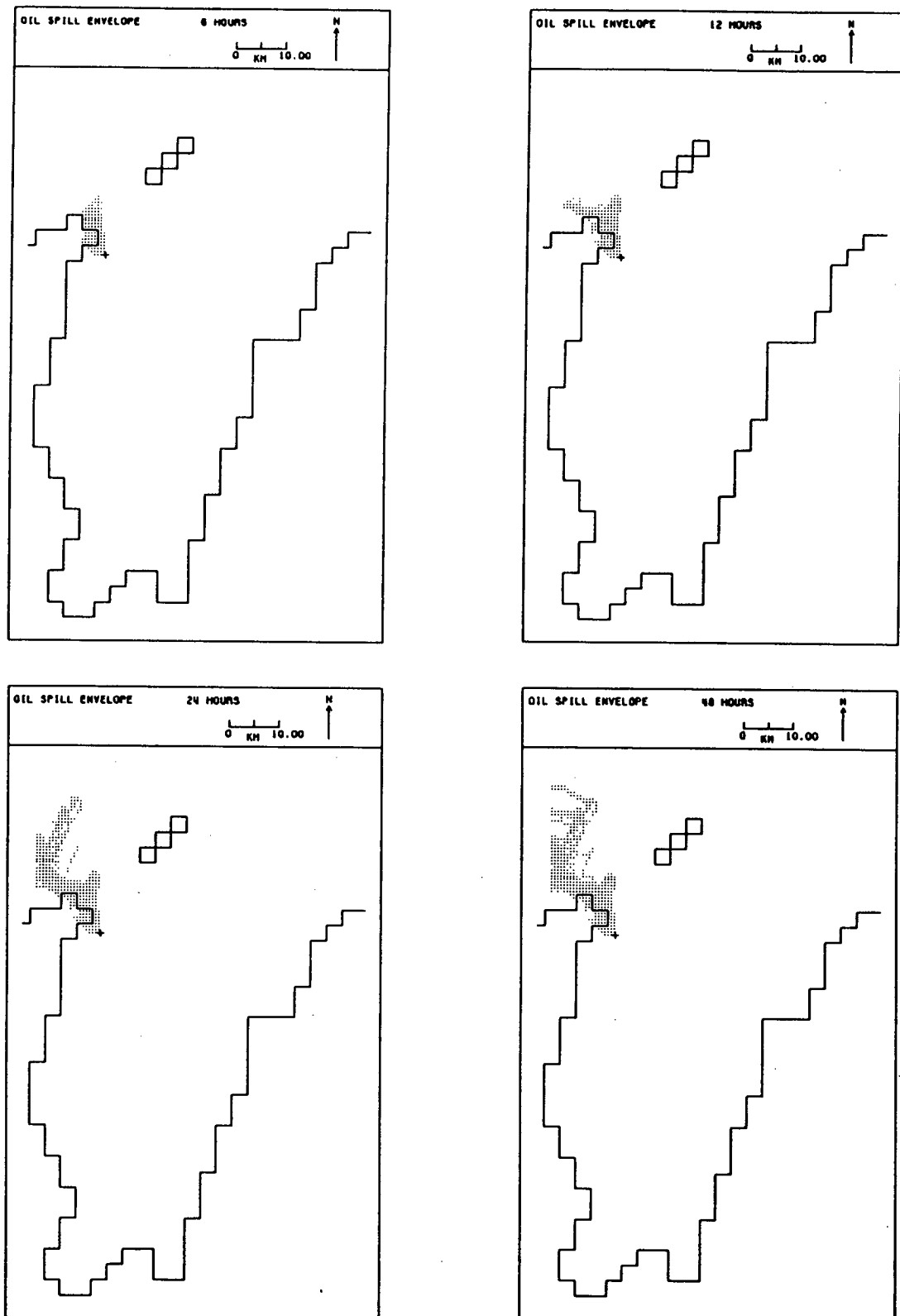


Figure 5.9 Oil spill envelopes for release times of 6, 12, 24 and 48 hours for the case of a 10 m s^{-1} easterly wind during neap tides for Whalebone Prospect.

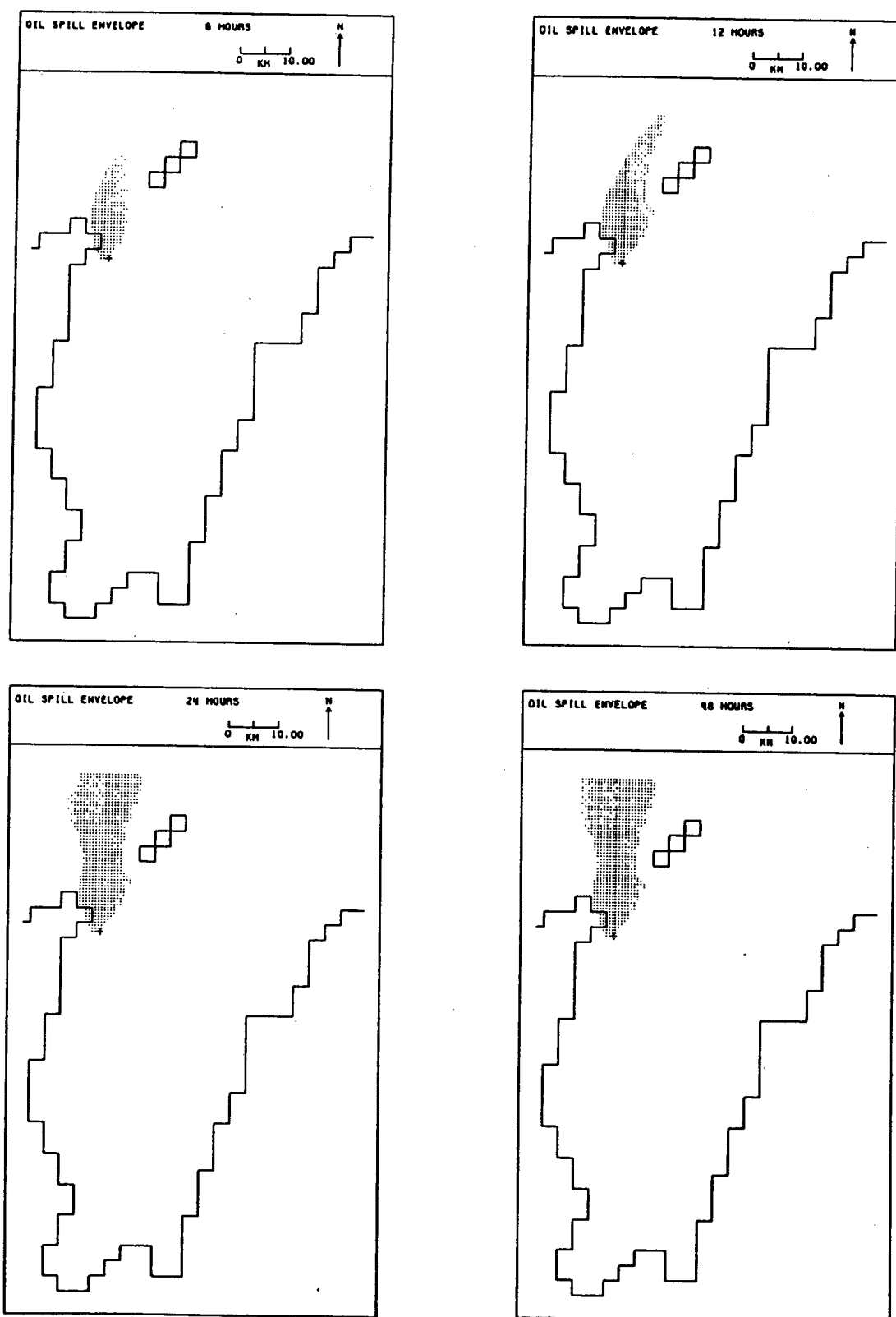


Figure 5.10 Oil spill envelopes for release times of 6, 12, 24 and 48 hours for the case of a 10 m s^{-1} south-easterly wind during spring tides for Whalebone Prospect.

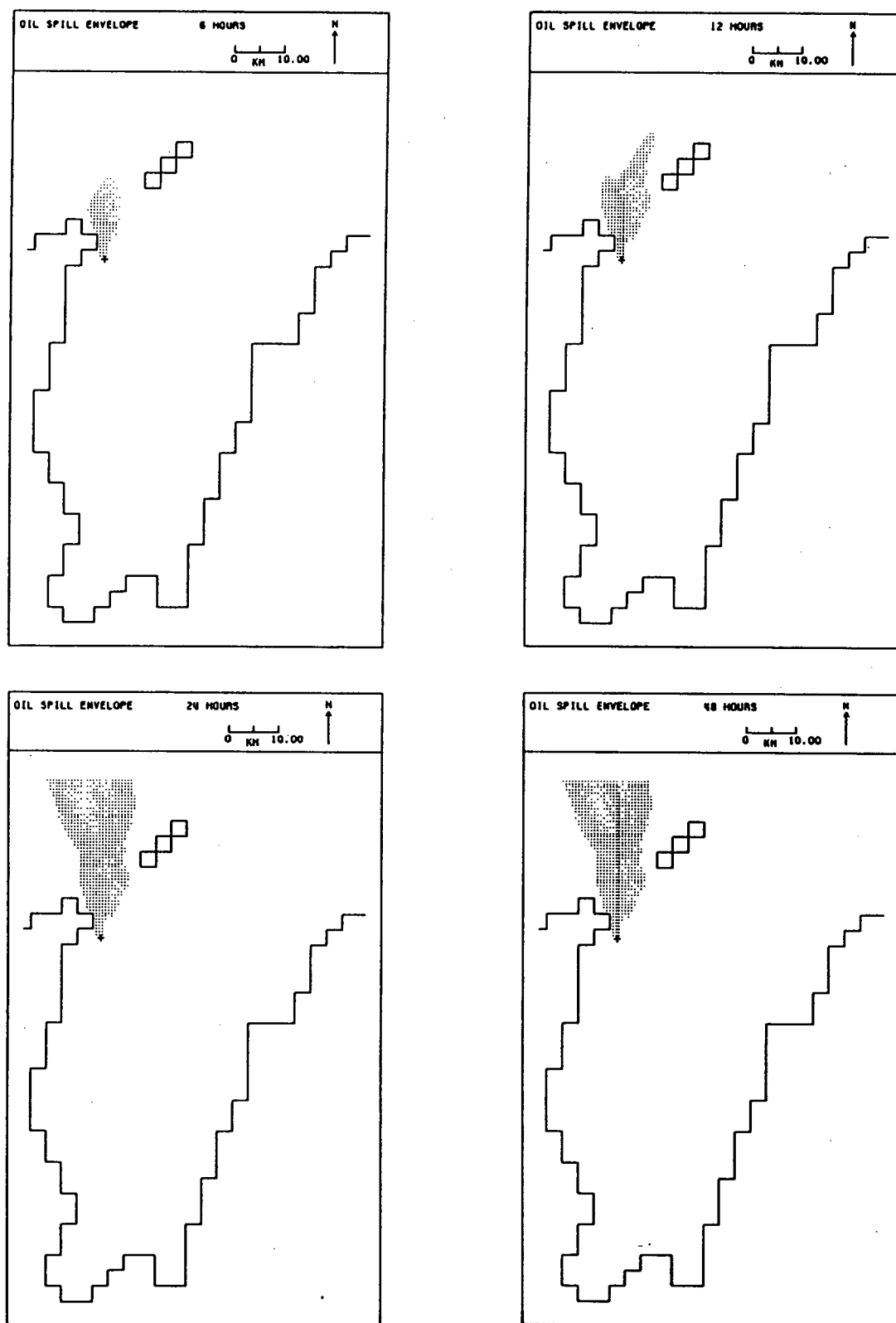


Figure 5.11 Oil spill envelopes for release times of 6, 12, 24 and 48 hours for the case of a 10 m s^{-1} south-easterly wind during neap tides for Whalebone Prospect.

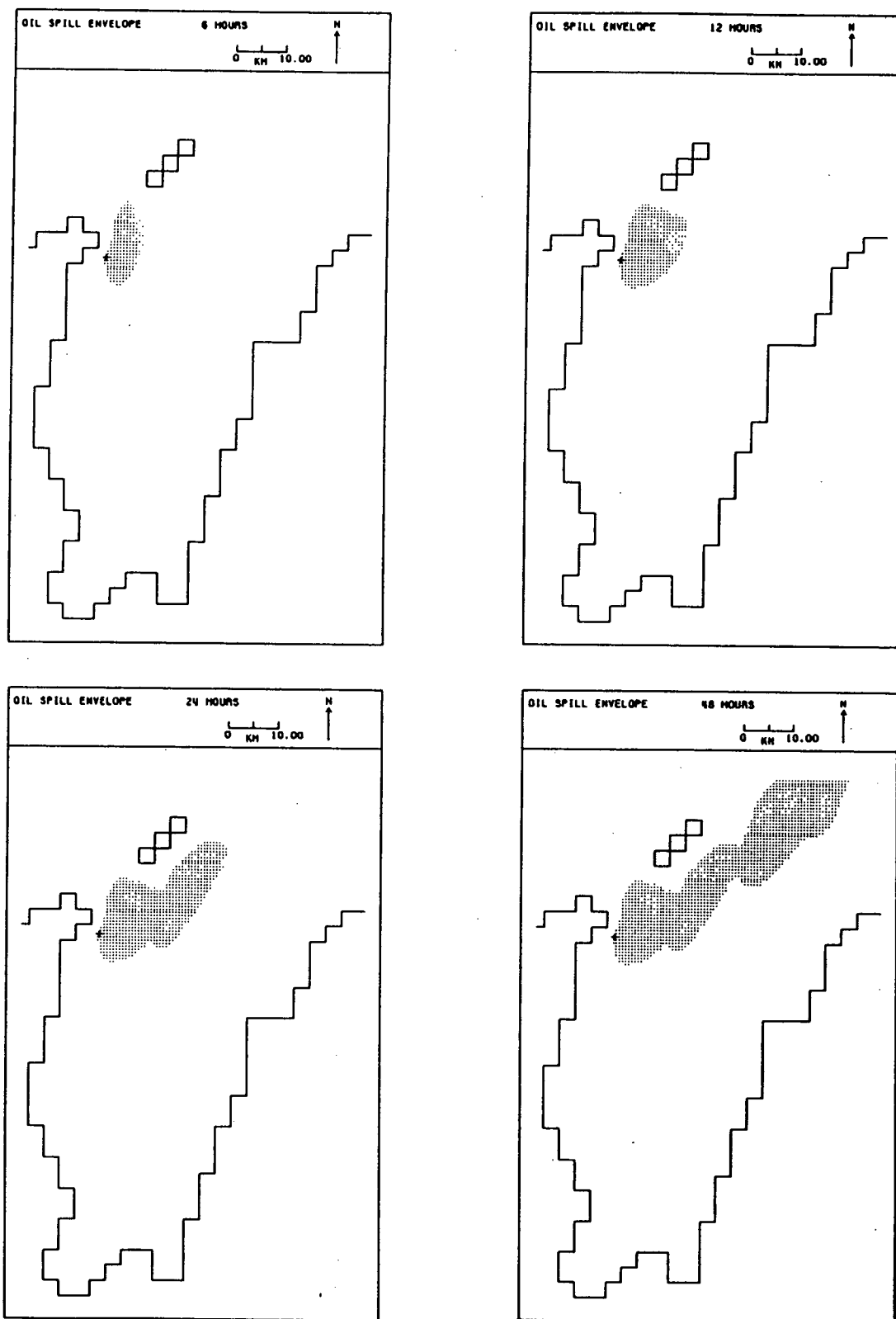


Figure 5.12 Oil spill envelopes for release times of 6, 12, 24 and 48 hours for the case of a 10 m s^{-1} southerly wind during spring tides for Whalebone Prospect.

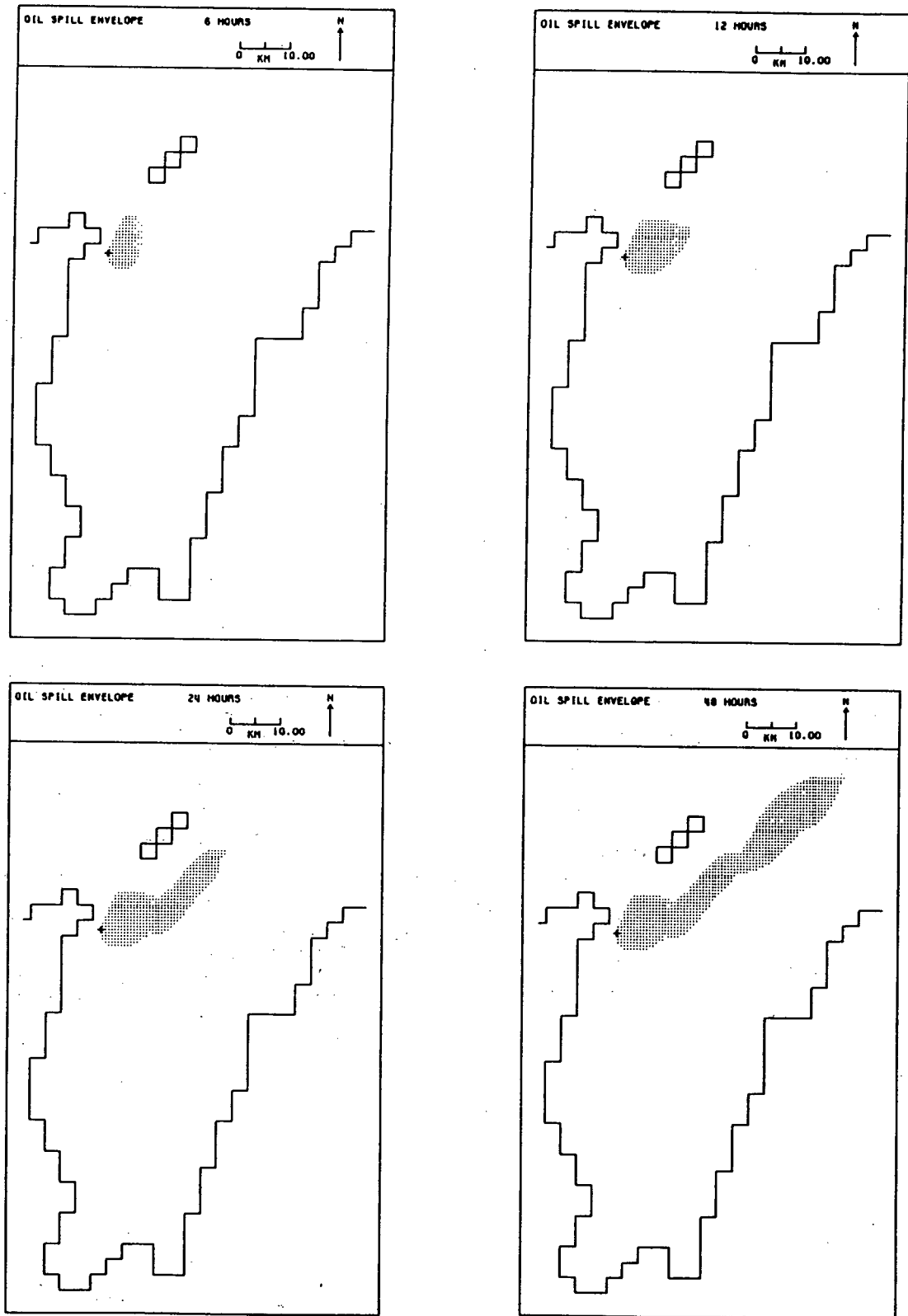


Figure 5.13 Oil spill envelopes for release times of 6, 12, 24 and 48 hours for the case of a 10 m s^{-1} southerly wind during neap tides for Whalebone Prospect.

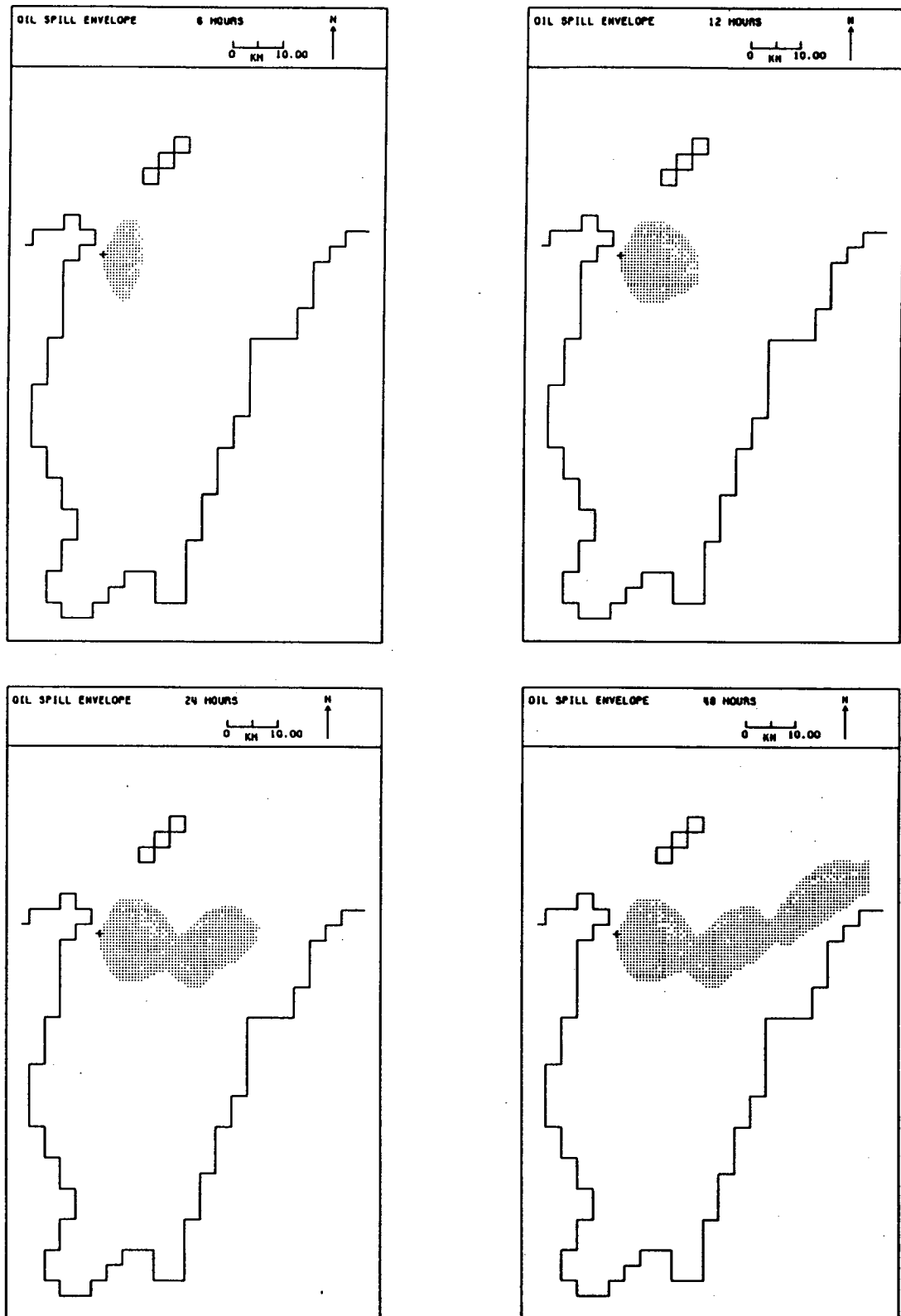


Figure 5.14 Oil spill envelopes for release times of 6, 12, 24 and 48 hours for the case of a 10 m s^{-1} south-westerly wind during spring tides for Whalebone Prospect.

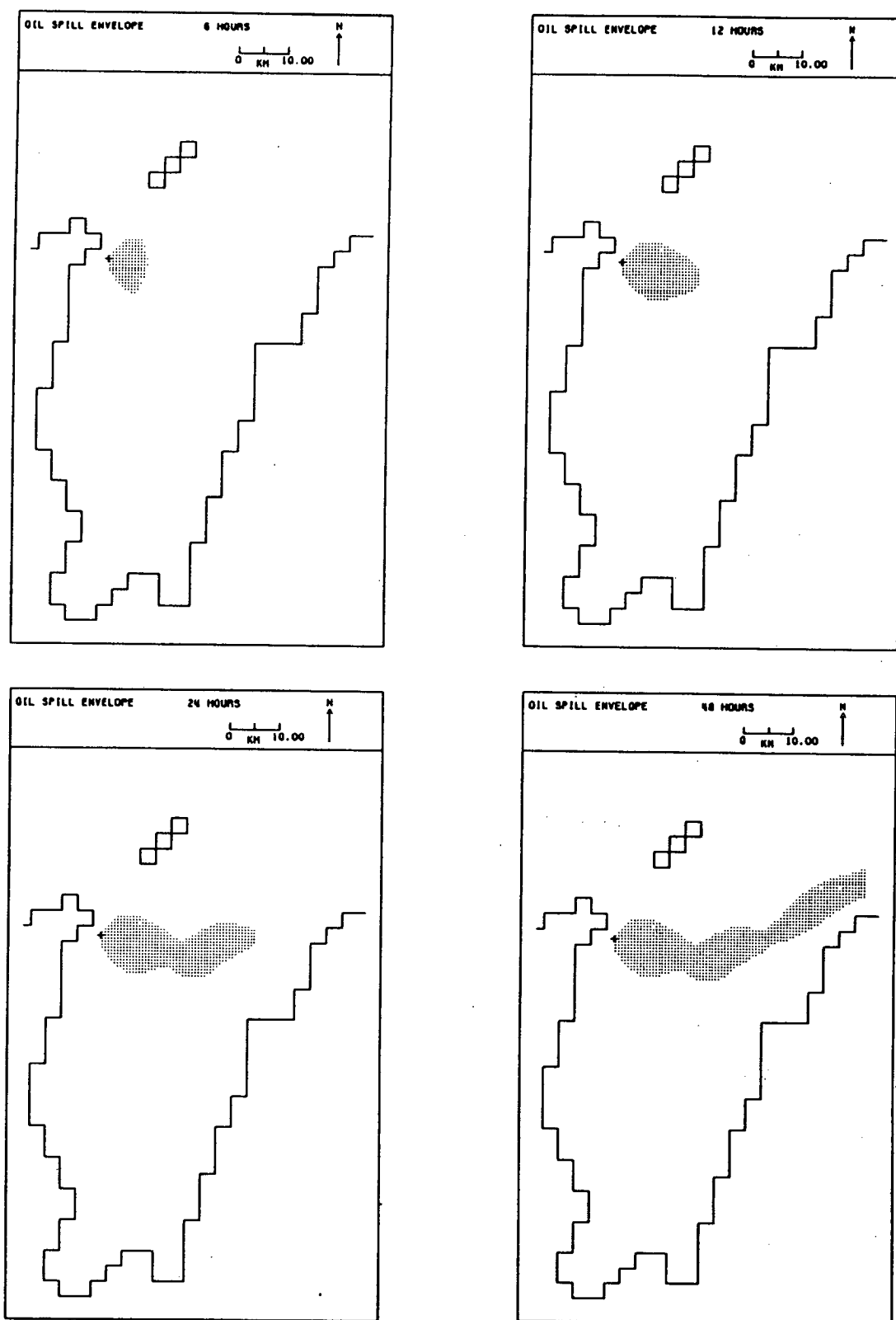


Figure 5.15 Oil spill envelopes for release times of 6, 12, 24 and 48 hours for the case of a 10 m s^{-1} south-westerly wind during neap tides for Whalebone Prospect.

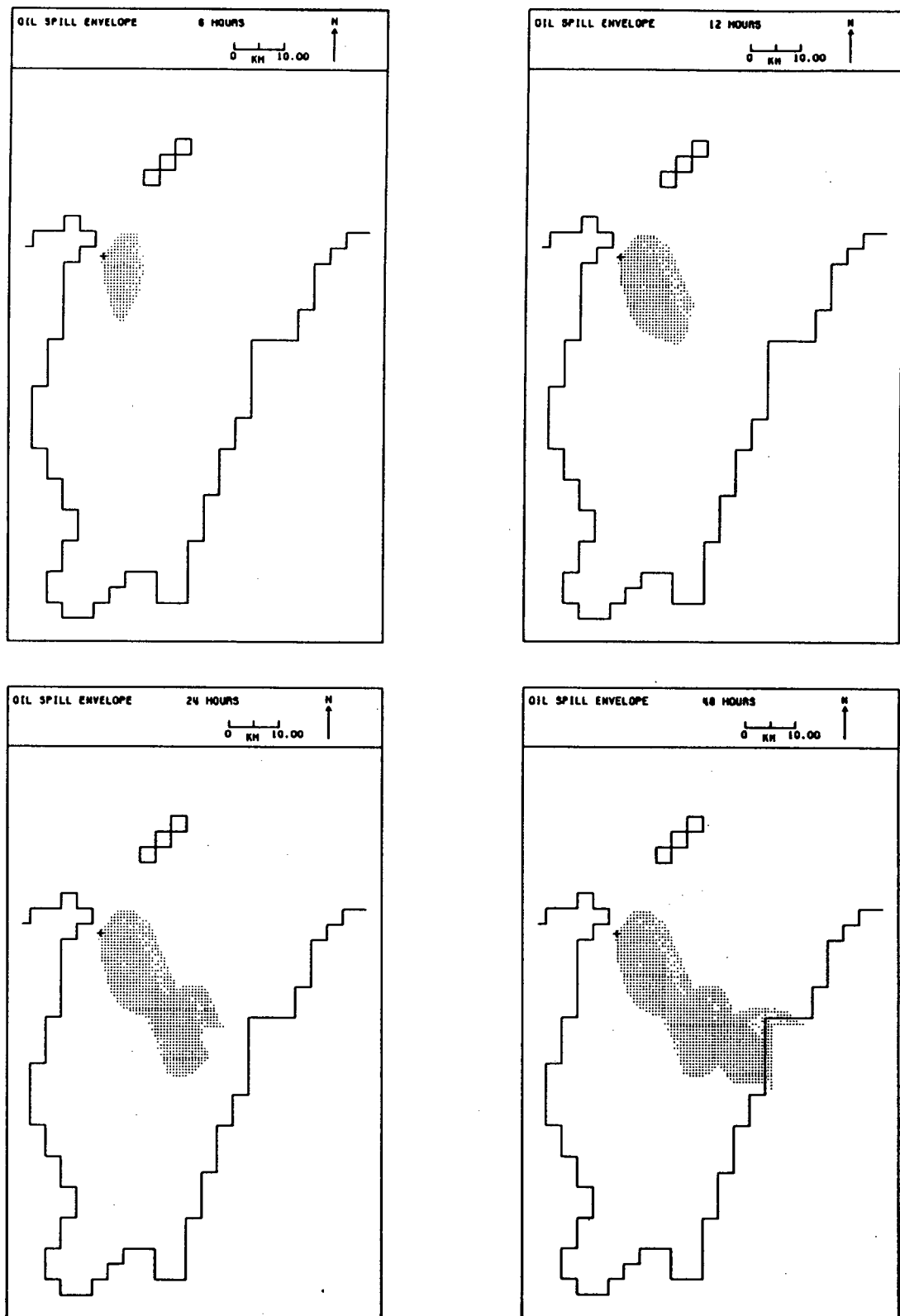


Figure 5.16 Oil spill envelopes for release times of 6, 12, 24 and 48 hours for the case of a 10 m s^{-1} westerly wind during spring tides for Whalebone Prospect.

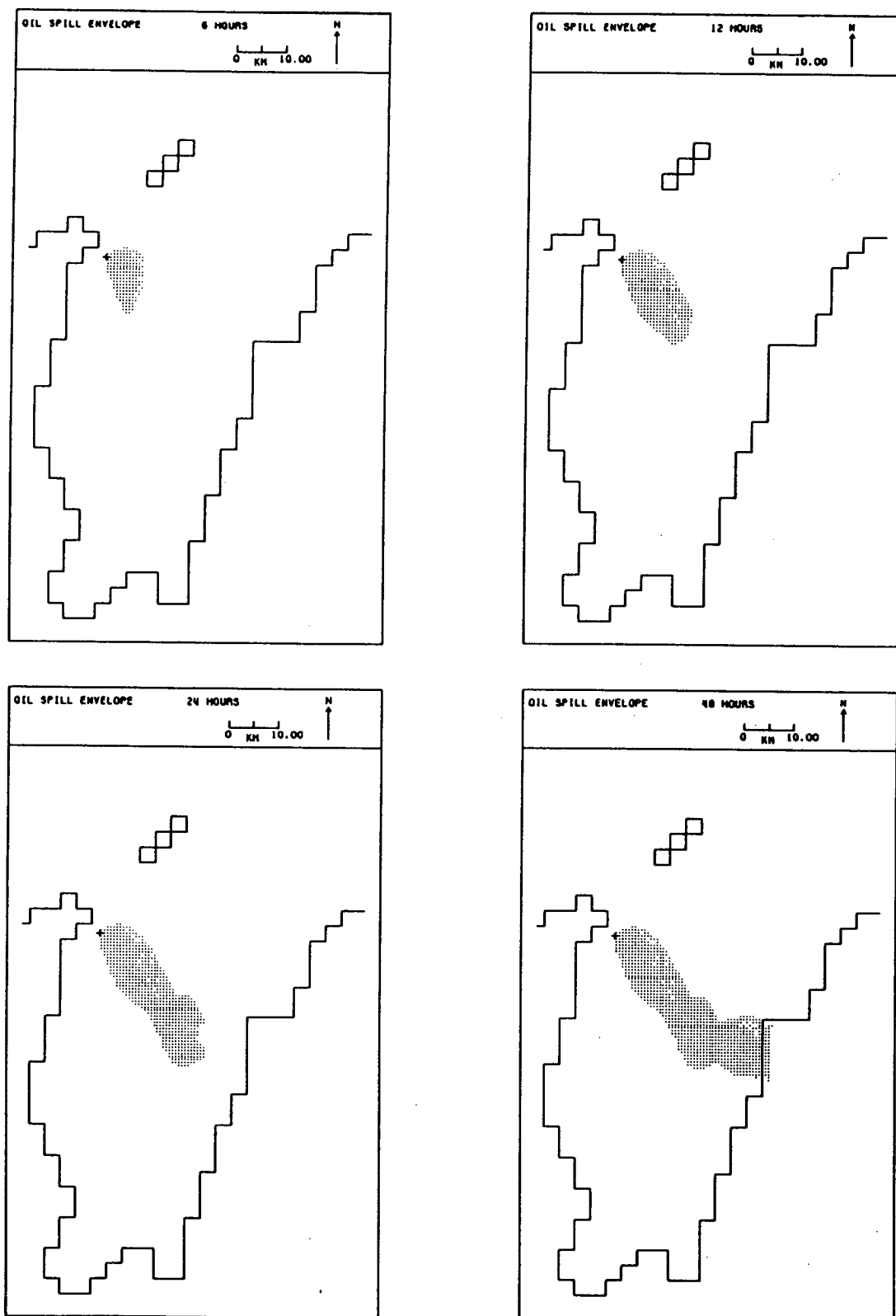


Figure 5.17 Oil spill envelopes for release times of 6, 12, 24 and 48 hours for the case of a 10 m s^{-1} westerly wind during neap tides for Whalebone Prospect.

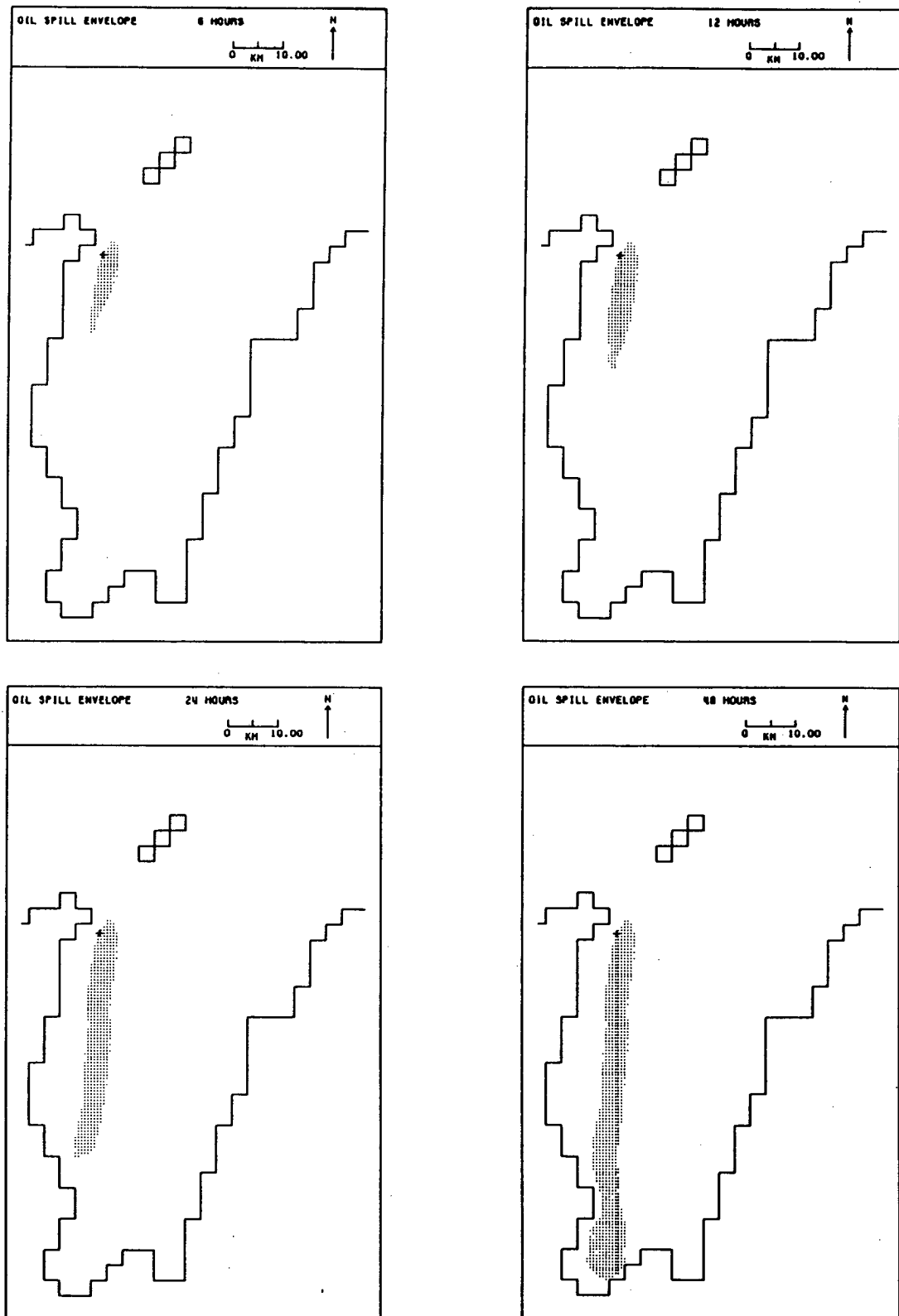


Figure 5.18 Oil spill envelopes for release times of 6, 12, 24 and 48 hours for the case of a 10 m s^{-1} north-westerly wind during spring tides for Whalebone Prospect.

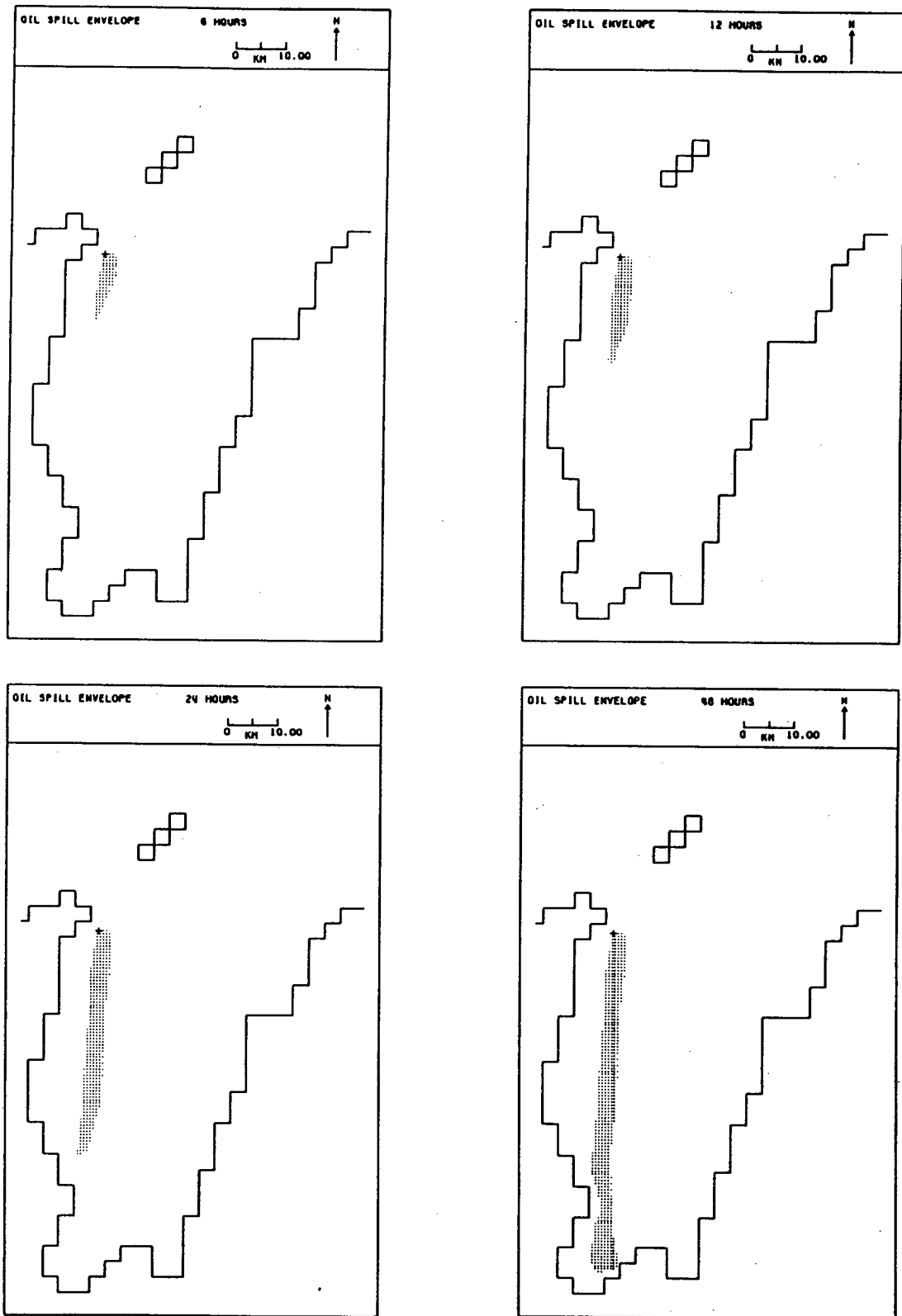


Figure 5.19 Oil spill envelopes for release times of 6, 12, 24 and 48 hours for the case of a 10 m s^{-1} north-westerly wind during neap tides for Whalebone Prospect.

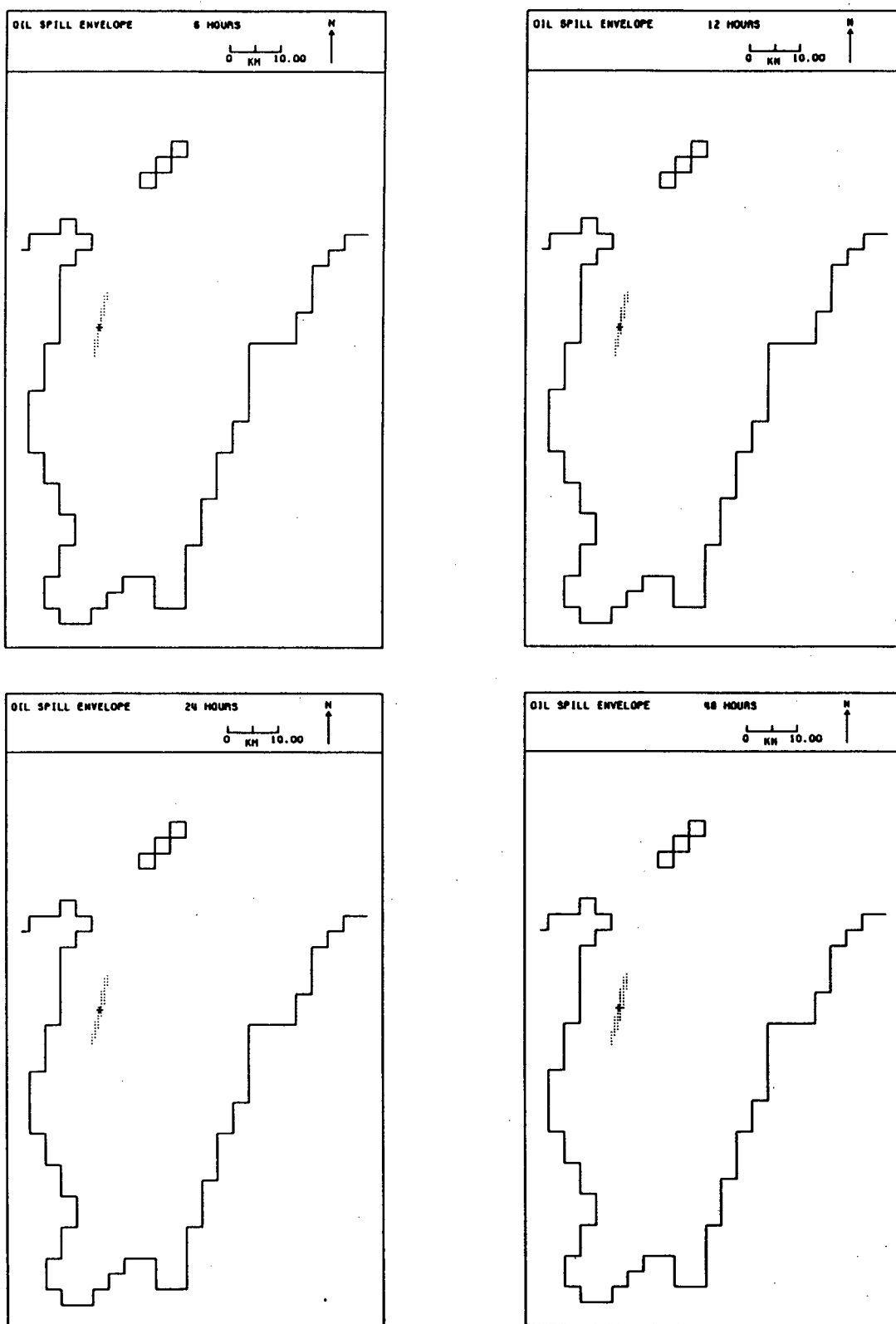


Figure 5.20 Oil spill envelopes for release times of 6, 12, 24 and 48 hours for the case of spring tides only for Rivoli Prospect.

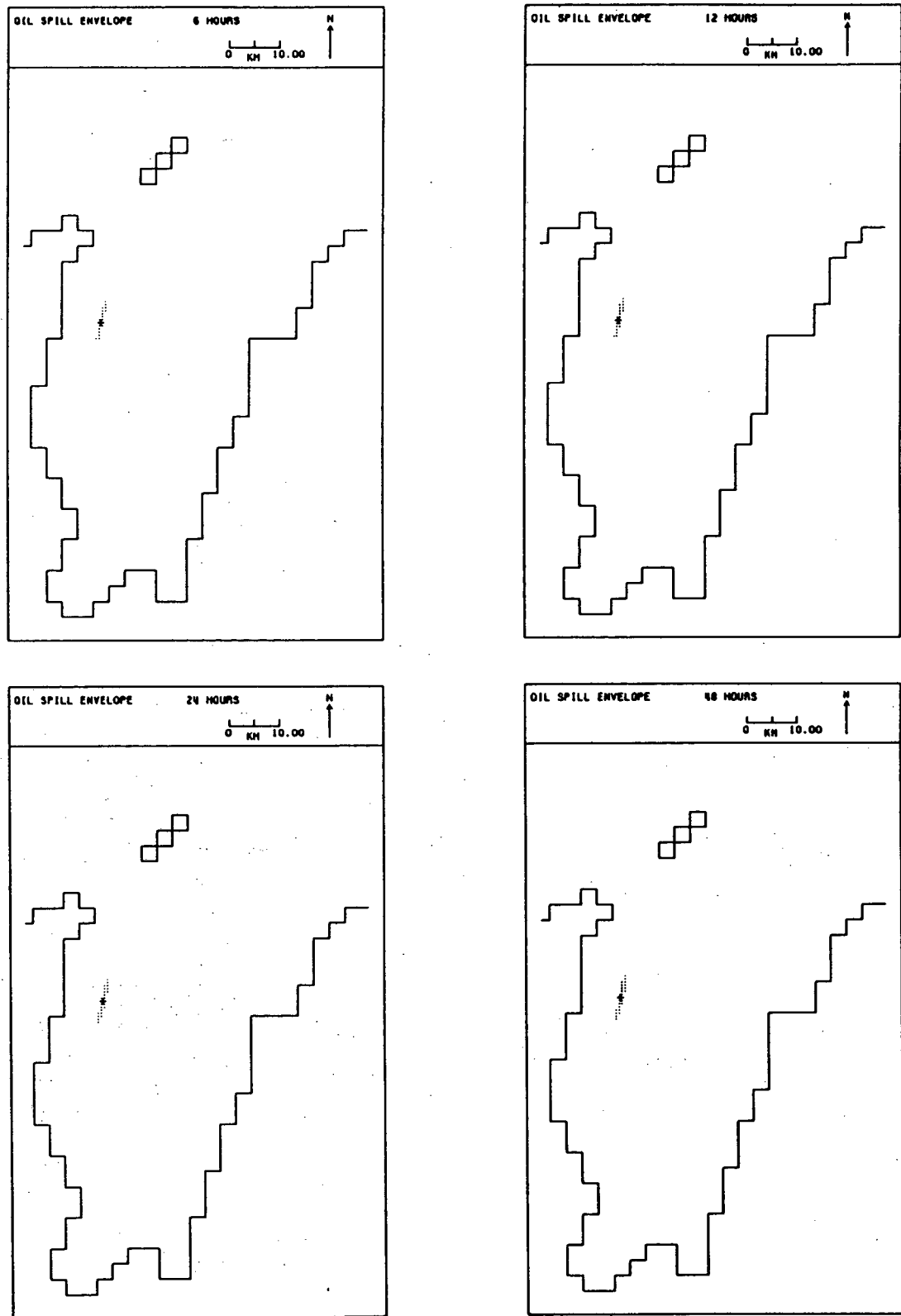


Figure 5.21 Oil spill envelopes for release times of 6, 12, 24 and 48 hours for the case of neap tides only for Rivoli Prospect.

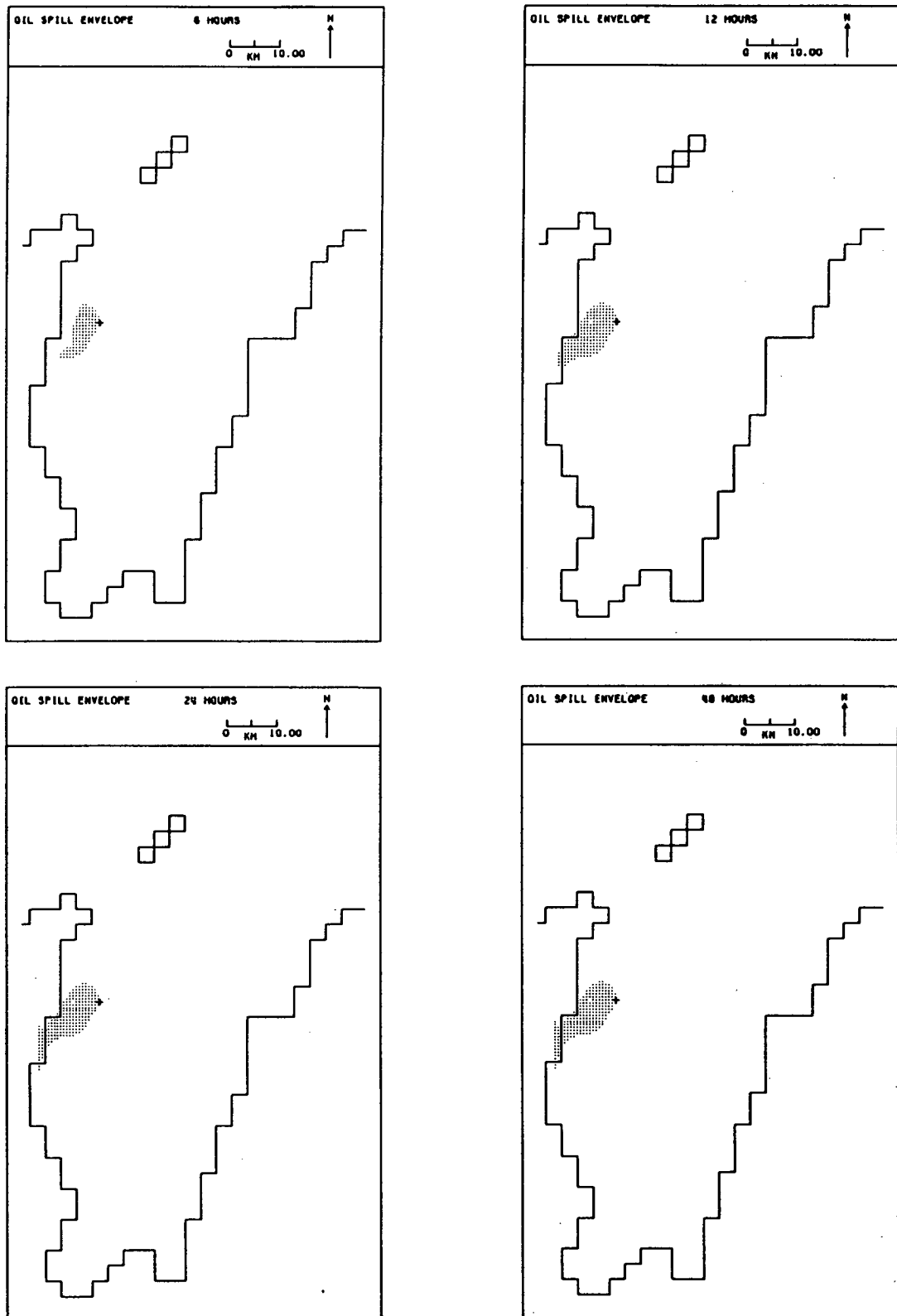


Figure 5.22 Oil spill envelopes for release times of 6, 12, 24 and 48 hours for the case of a 10 m s^{-1} northerly wind during spring tides for Rivoli Prospect.

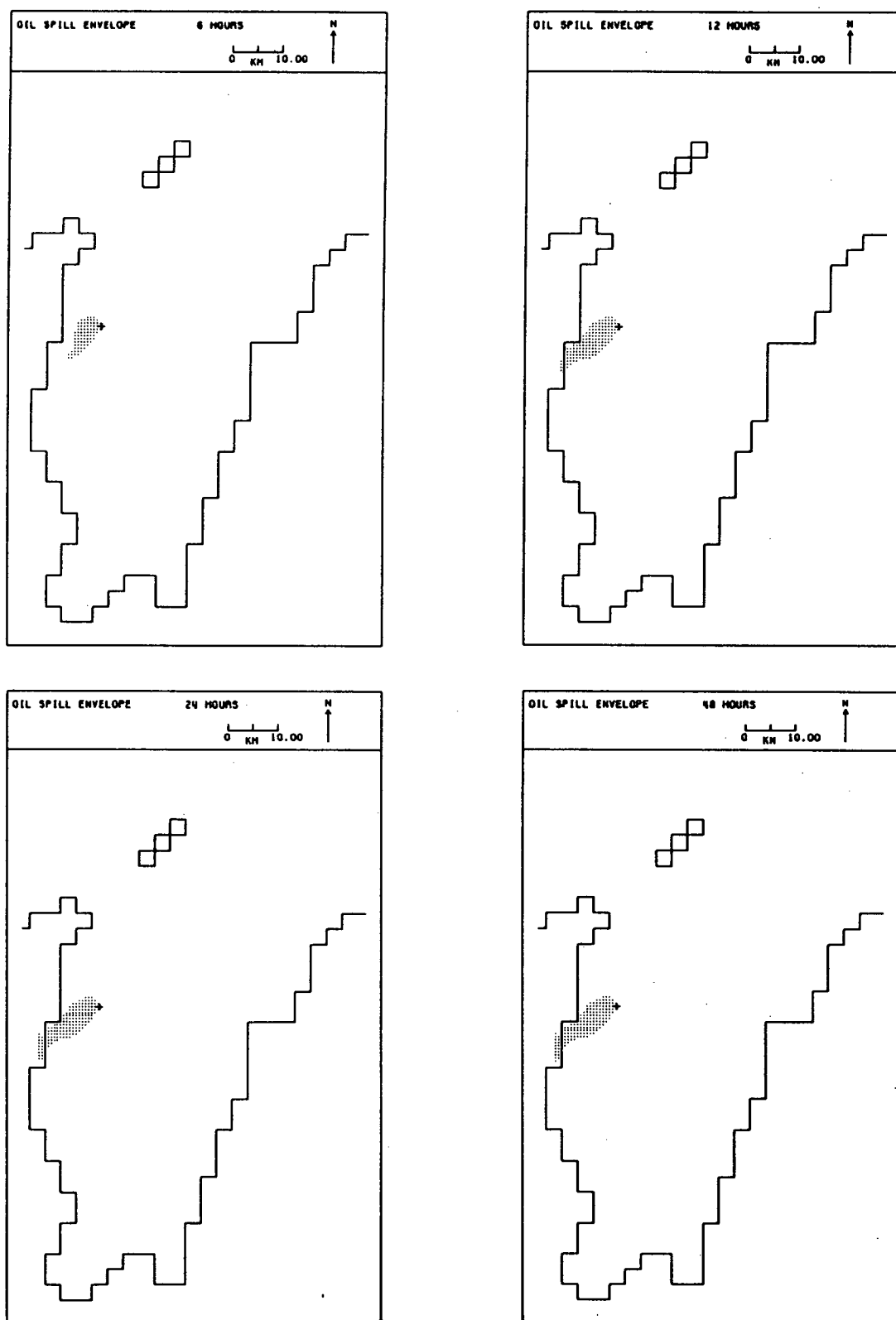


Figure 5.23 Oil spill envelopes for release times of 6, 12, 24 and 48 hours for the case of a 10 m s^{-1} northerly wind during neap tides for Rivoli Prospect.

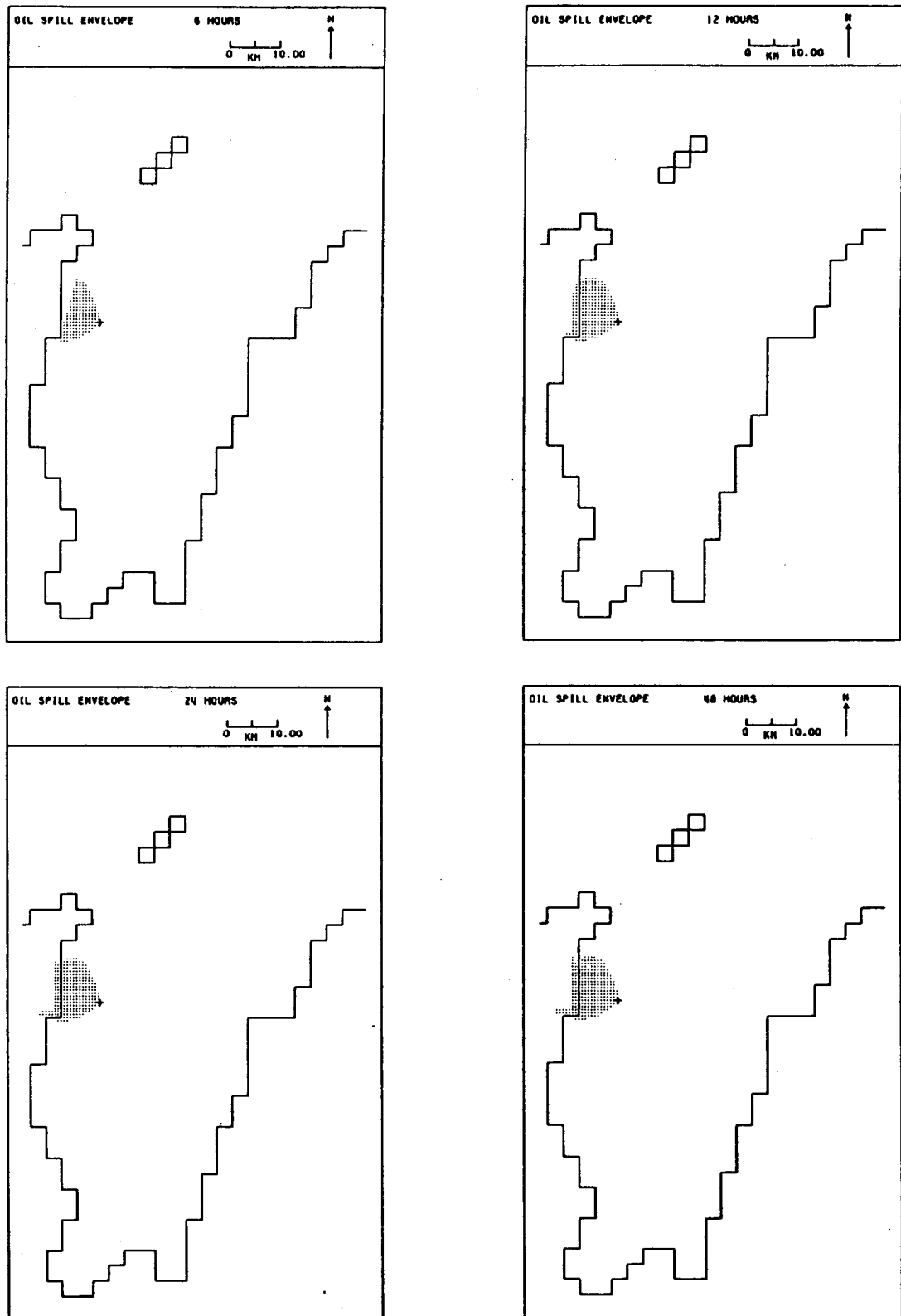


Figure 5.24 Oil spill envelopes for release times of 6, 12, 24 and 48 hours for the case of a 10 m s^{-1} north-easterly wind during spring tides for Rivoli Prospect.

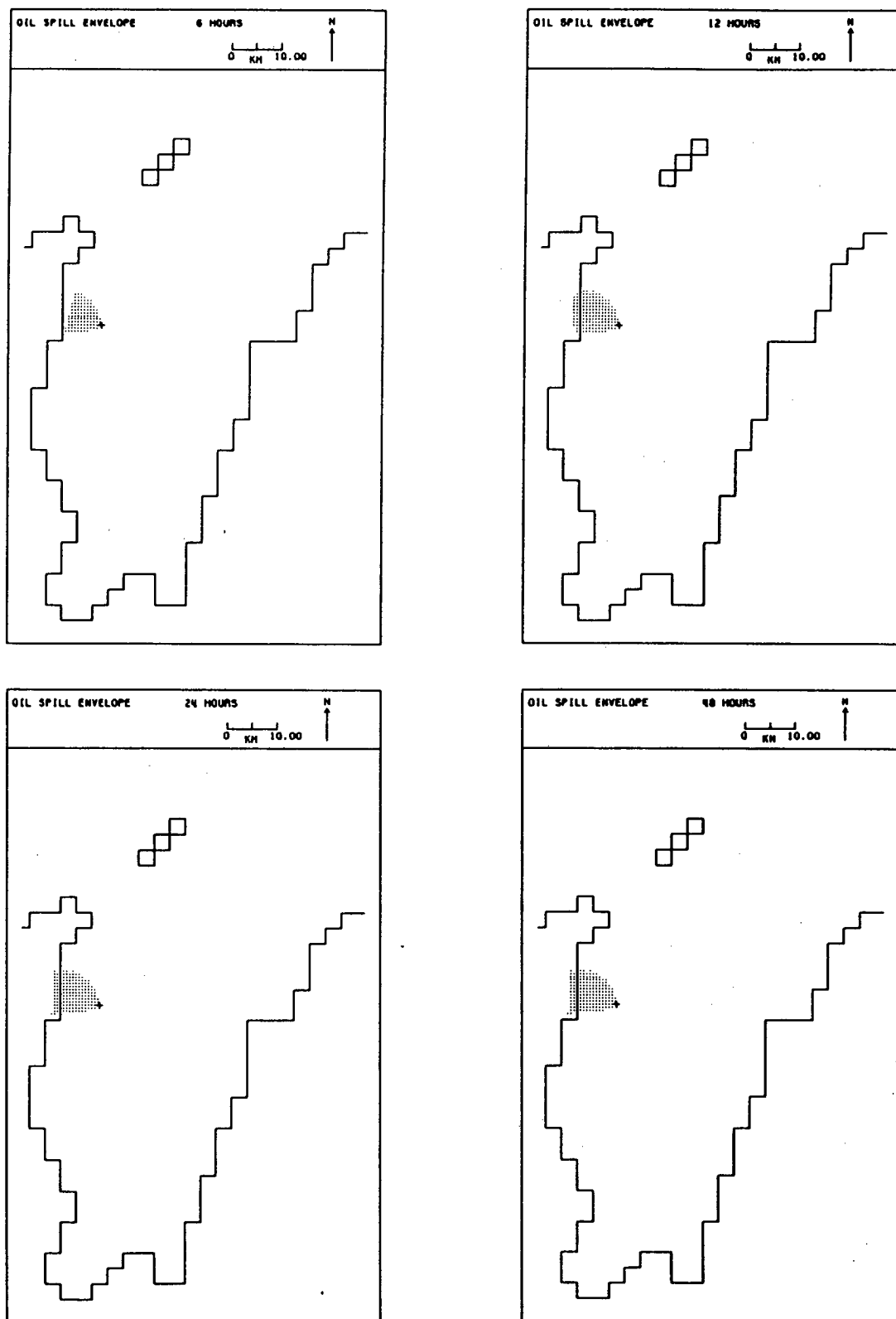


Figure 5.25 Oil spill envelopes for release times of 6, 12, 24 and 48 hours for the case of a 10 m s^{-1} north-easterly wind during neap tides for Rivoli Prospect.

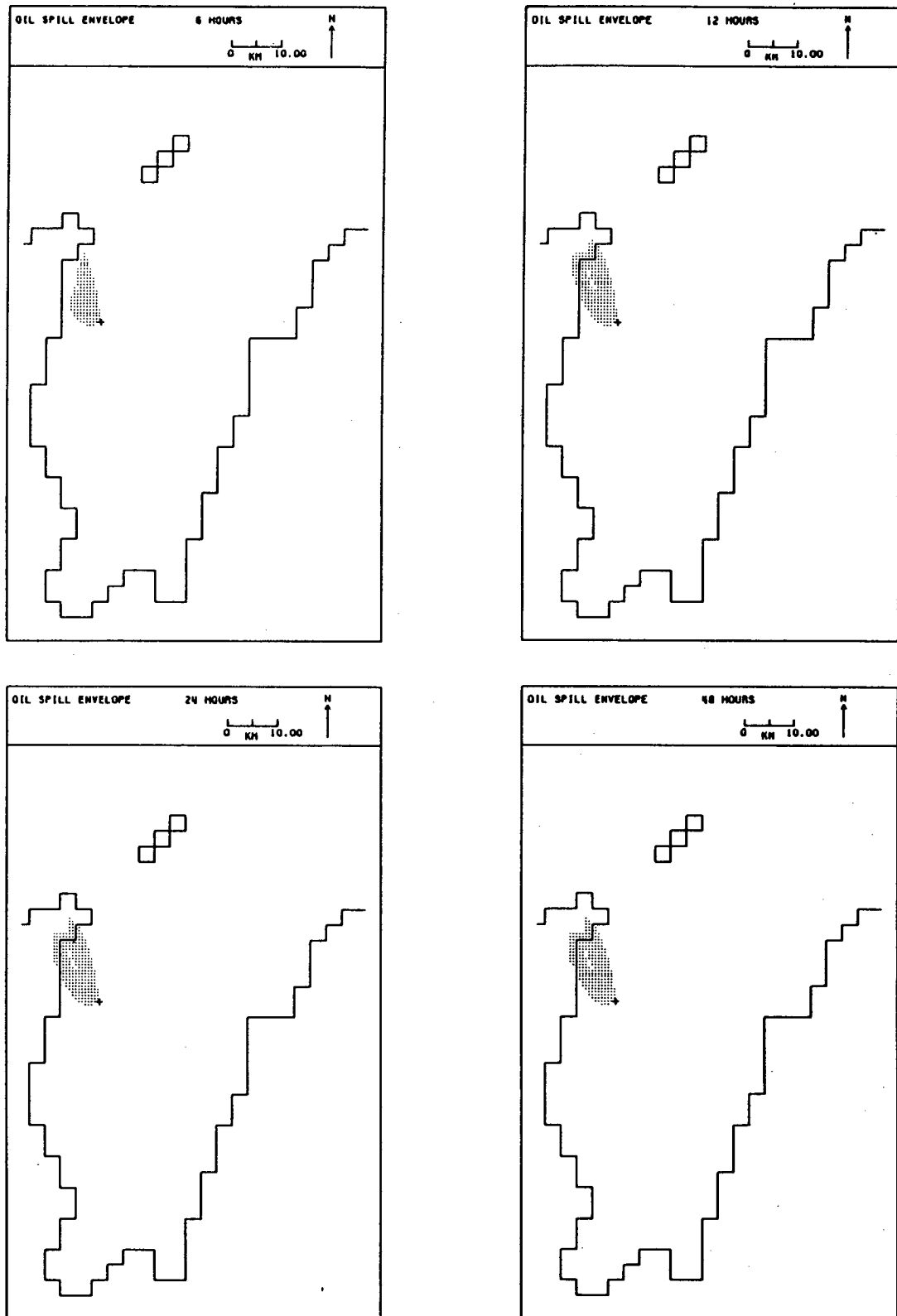


Figure 5.26 Oil spill envelopes for release times of 6, 12, 24 and 48 hours for the case of a 10 m s^{-1} easterly wind during spring tides for Rivoli Prospect.

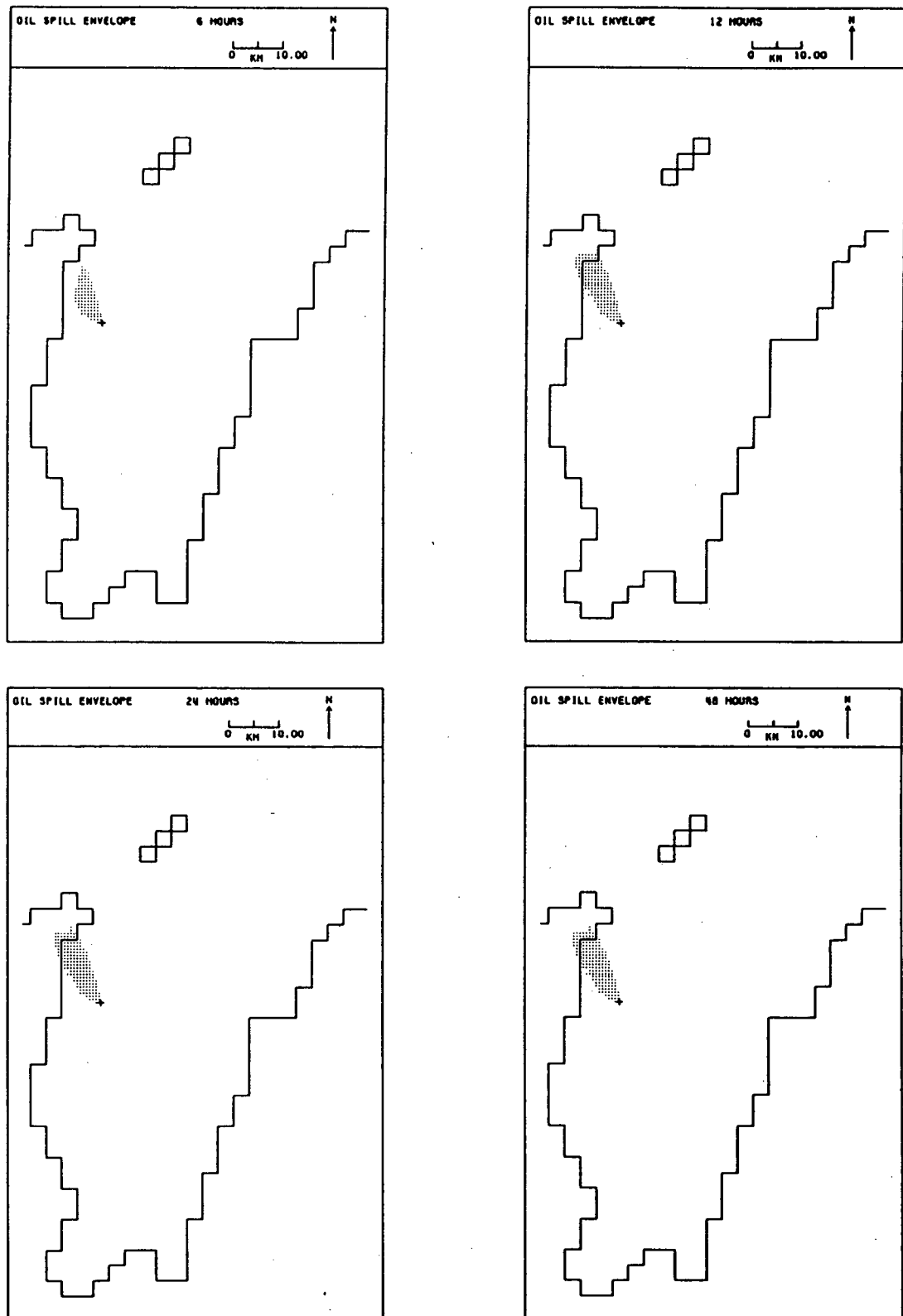


Figure 5.27 Oil spill envelopes for release times of 6, 12, 24 and 48 hours for the case of a 10 m s^{-1} easterly wind during neap tides for Rivoli Prospect.

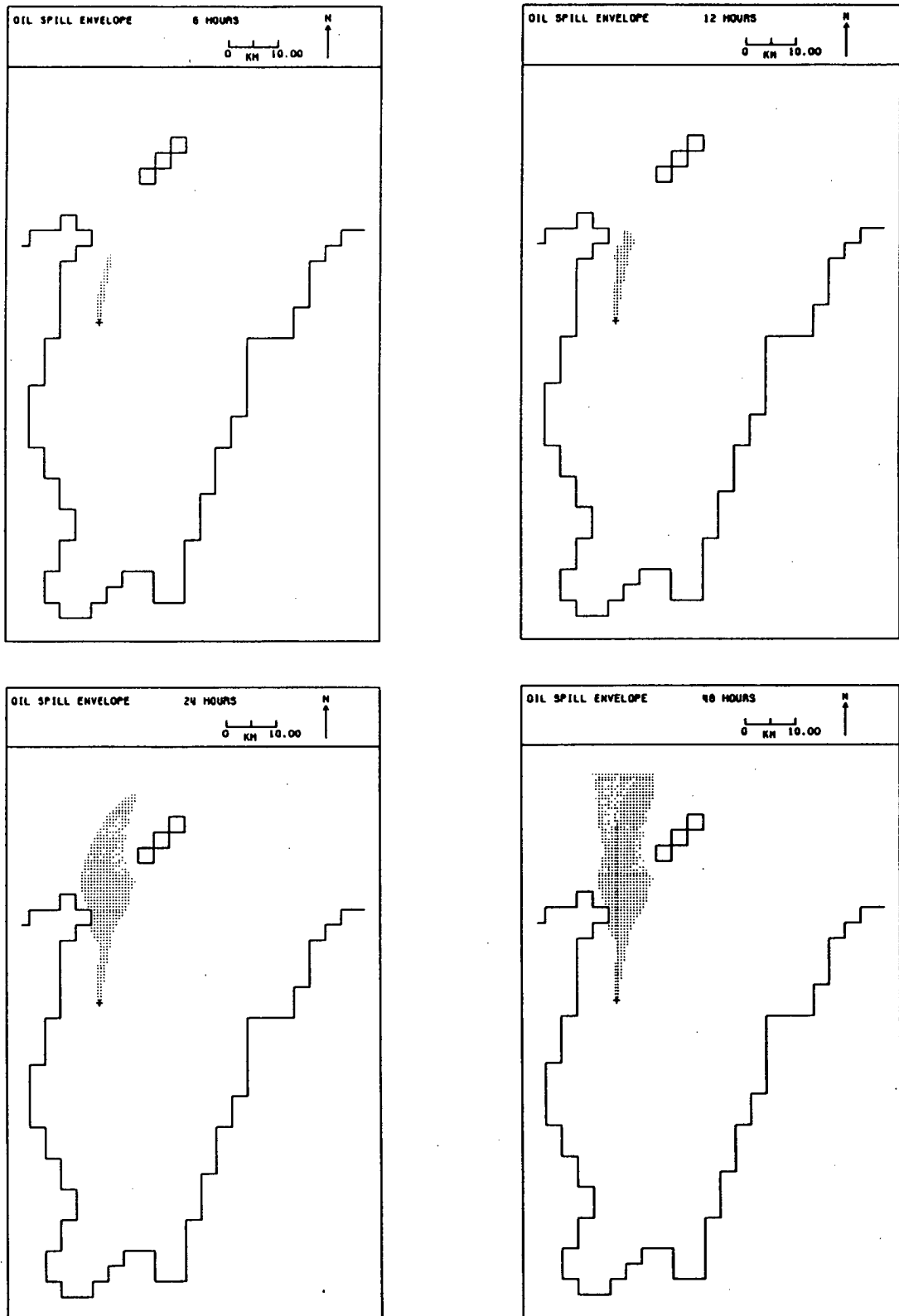


Figure 5.28 Oil spill envelopes for release times of 6, 12, 24 and 48 hours for the case of a 10 m s^{-1} south-easterly wind during spring tides for Rivoli Prospect.

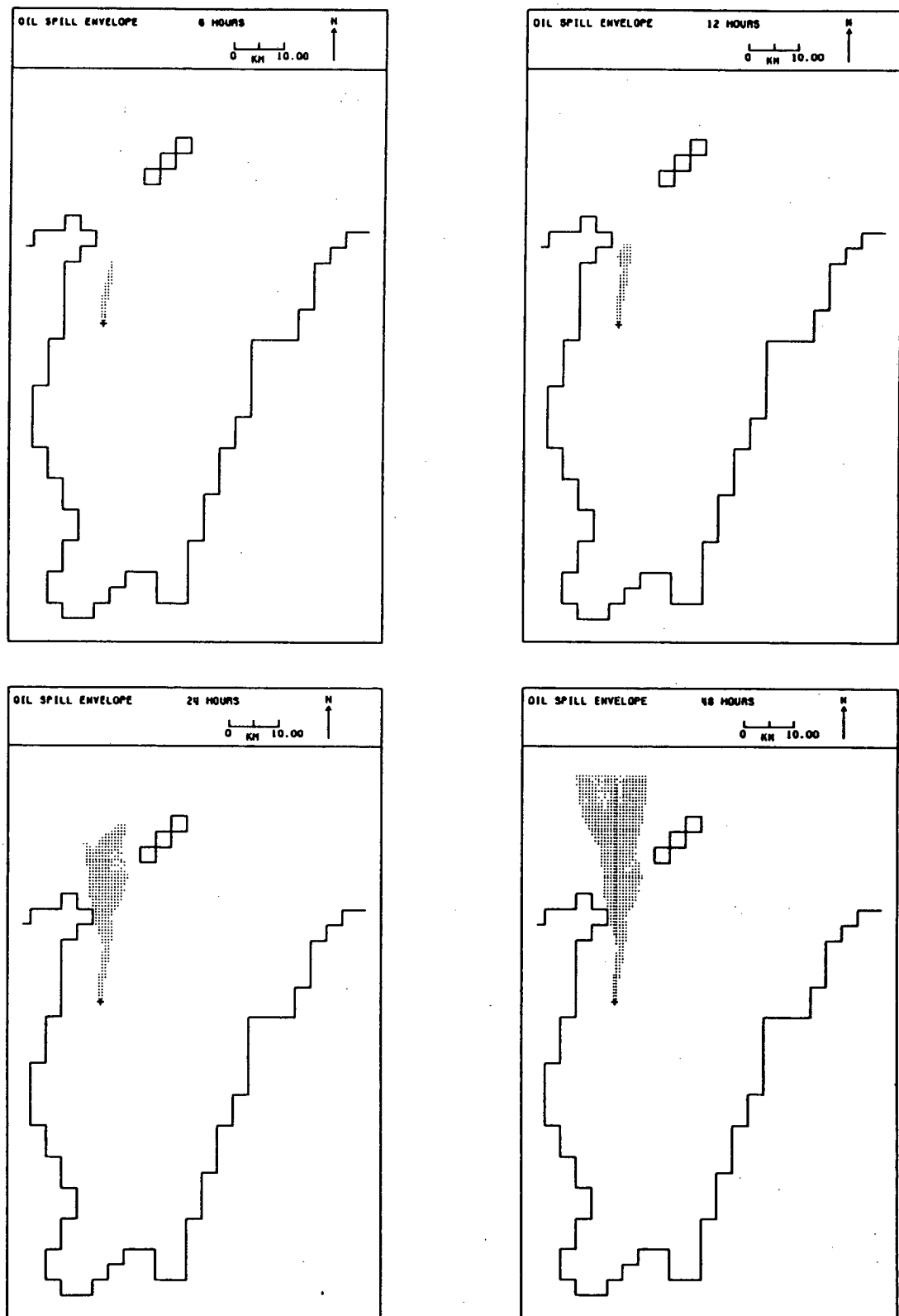


Figure 5.29 Oil spill envelopes for release times of 6, 12, 24 and 48 hours for the case of a 10 m s^{-1} south-easterly wind during neap tides for Rivoli Prospect.

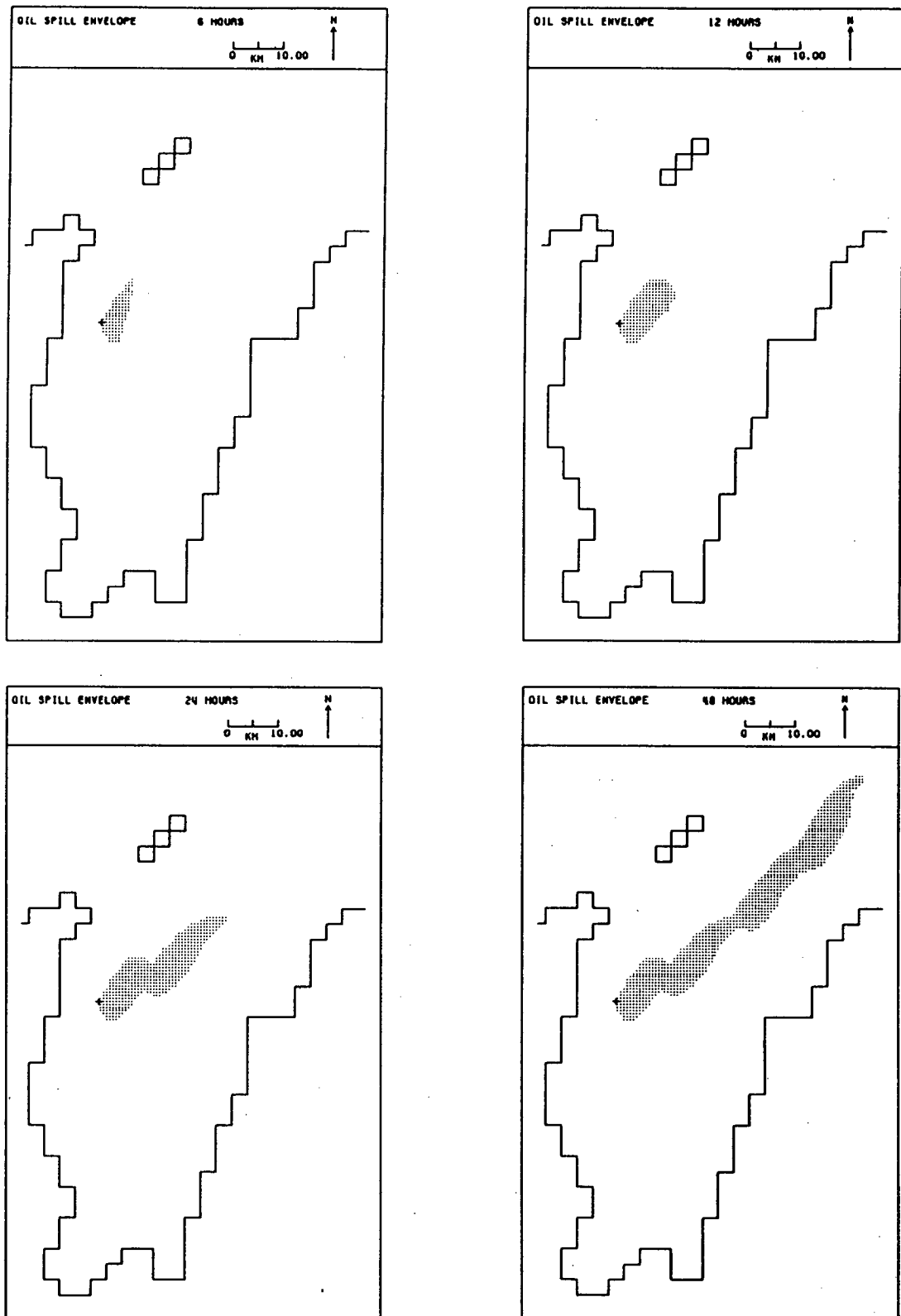


Figure 5.30 Oil spill envelopes for release times of 6, 12, 24 and 48 hours for the case of a 10 m s^{-1} southerly wind during spring tides for Rivoli Prospect.

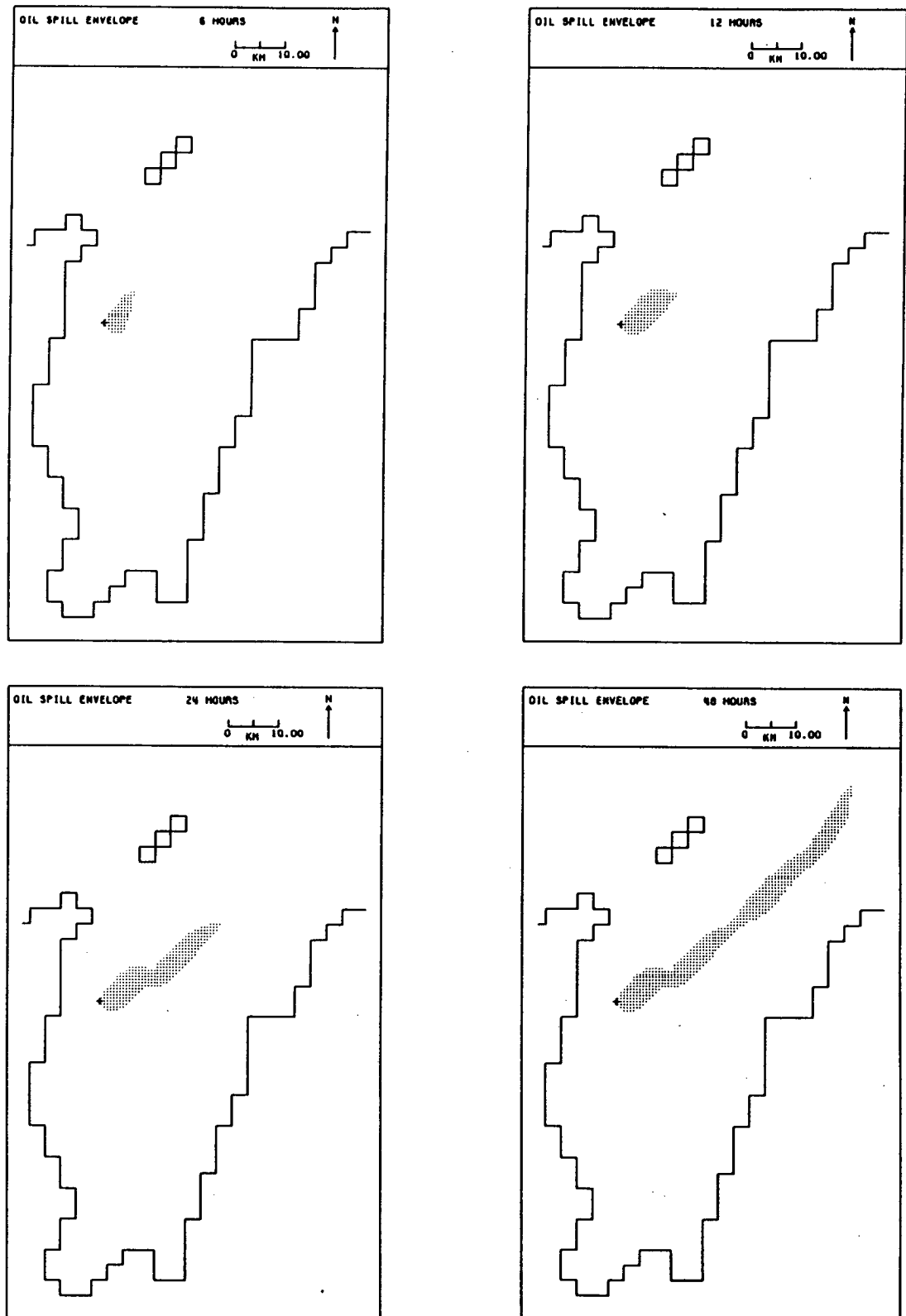


Figure 5.31 Oil spill envelopes for release times of 6, 12, 24 and 48 hours for the case of a 10 m s^{-1} southerly wind during neap tides for Rivoli Prospect.

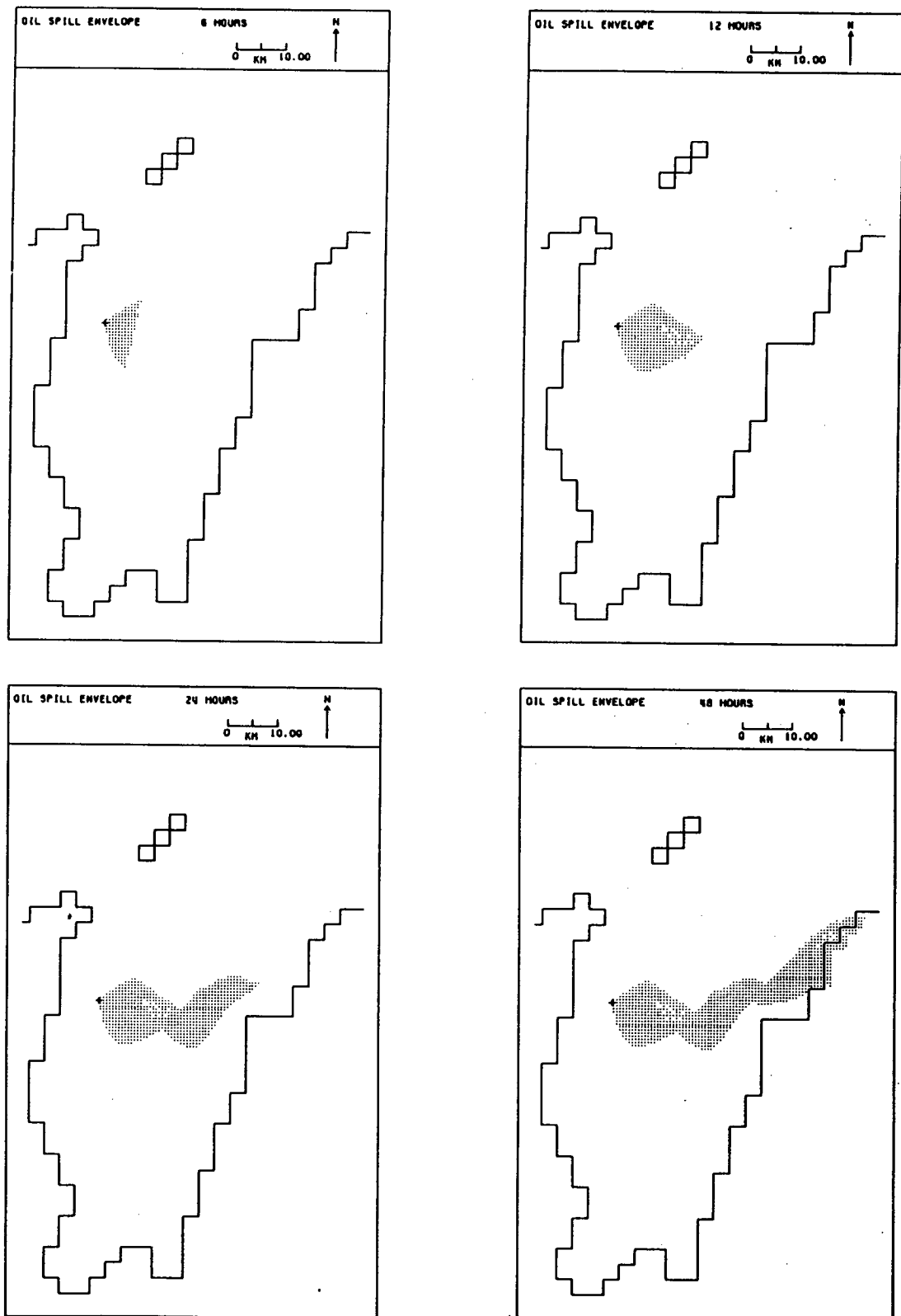


Figure 5.32 Oil spill envelopes for release times of 6, 12, 24 and 48 hours for the case of a 10 m s^{-1} south-westerly wind during spring tides for Rivoli Prospect.

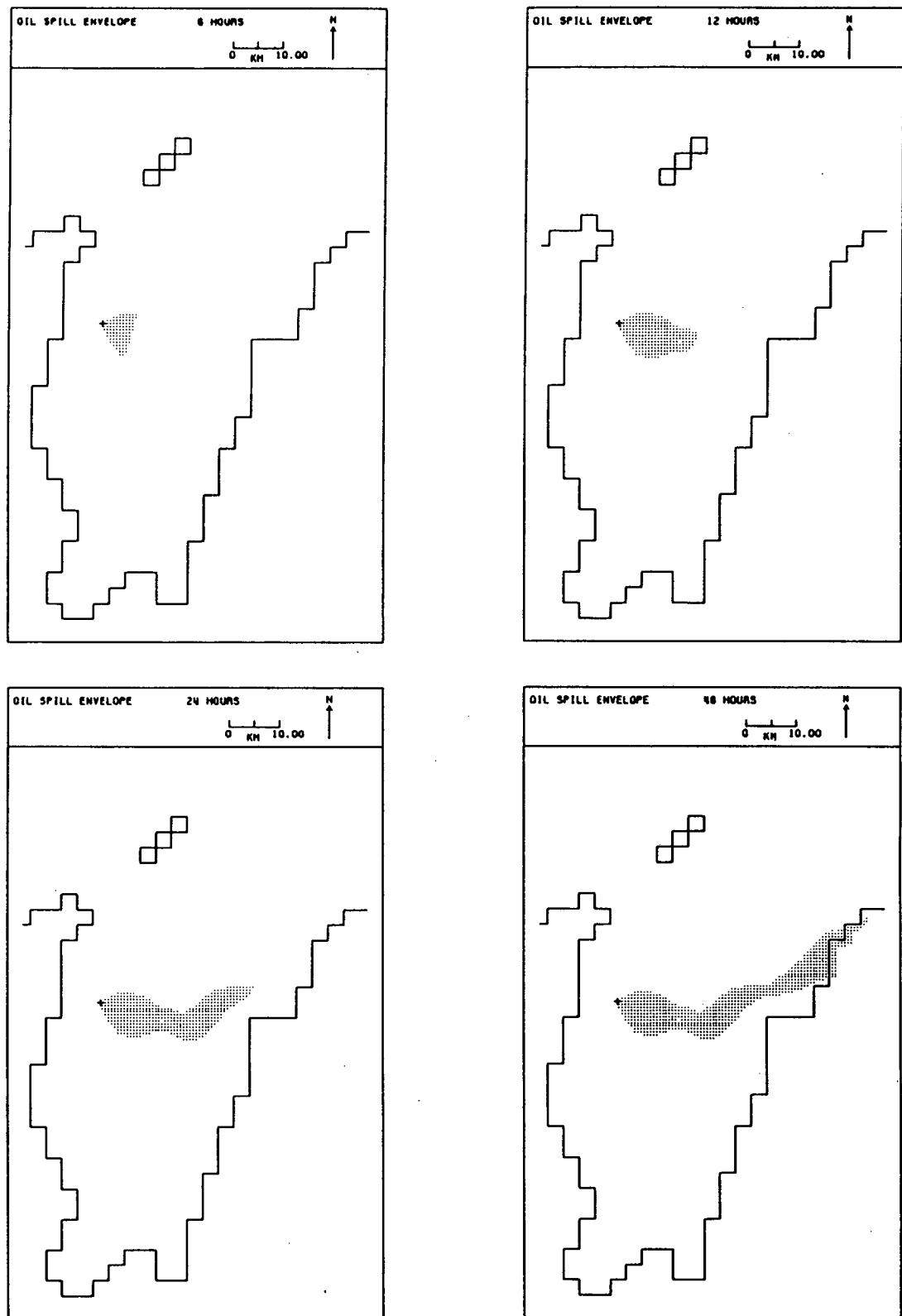


Figure 5.33 Oil spill envelopes for release times of 6, 12, 24 and 48 hours for the case of a 10 m s^{-1} south-westerly wind during neap tides for Rivoli Prospect.

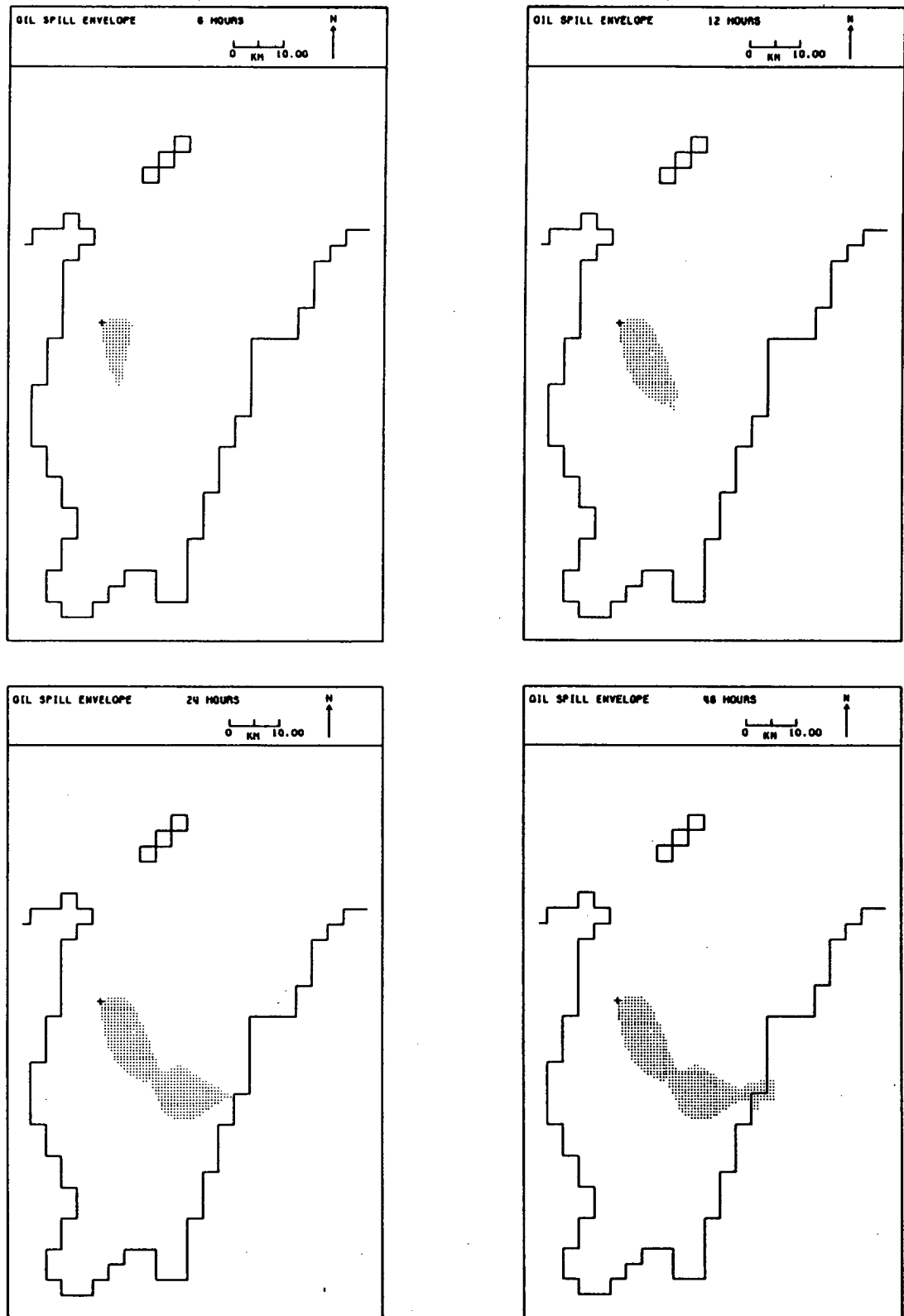


Figure 5.34 Oil spill envelopes for release times of 6, 12, 24 and 48 hours for the case of a 10 m s^{-1} westerly wind during spring tides for Rivoli Prospect.

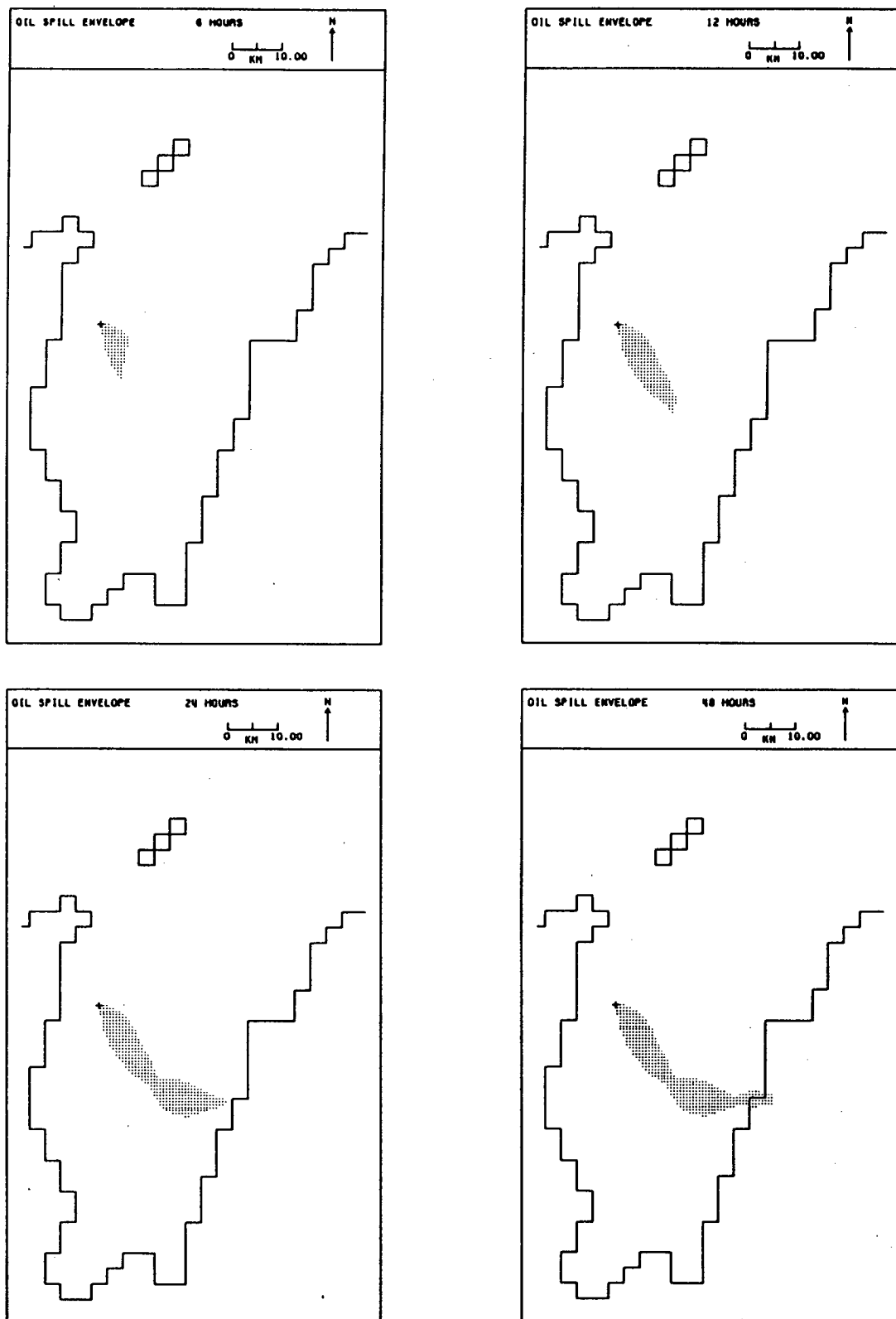


Figure 5.35 Oil spill envelopes for release times of 6, 12, 24 and 48 hours for the case of a 10 m s^{-1} westerly wind during neap tides for Rivoli Prospect.

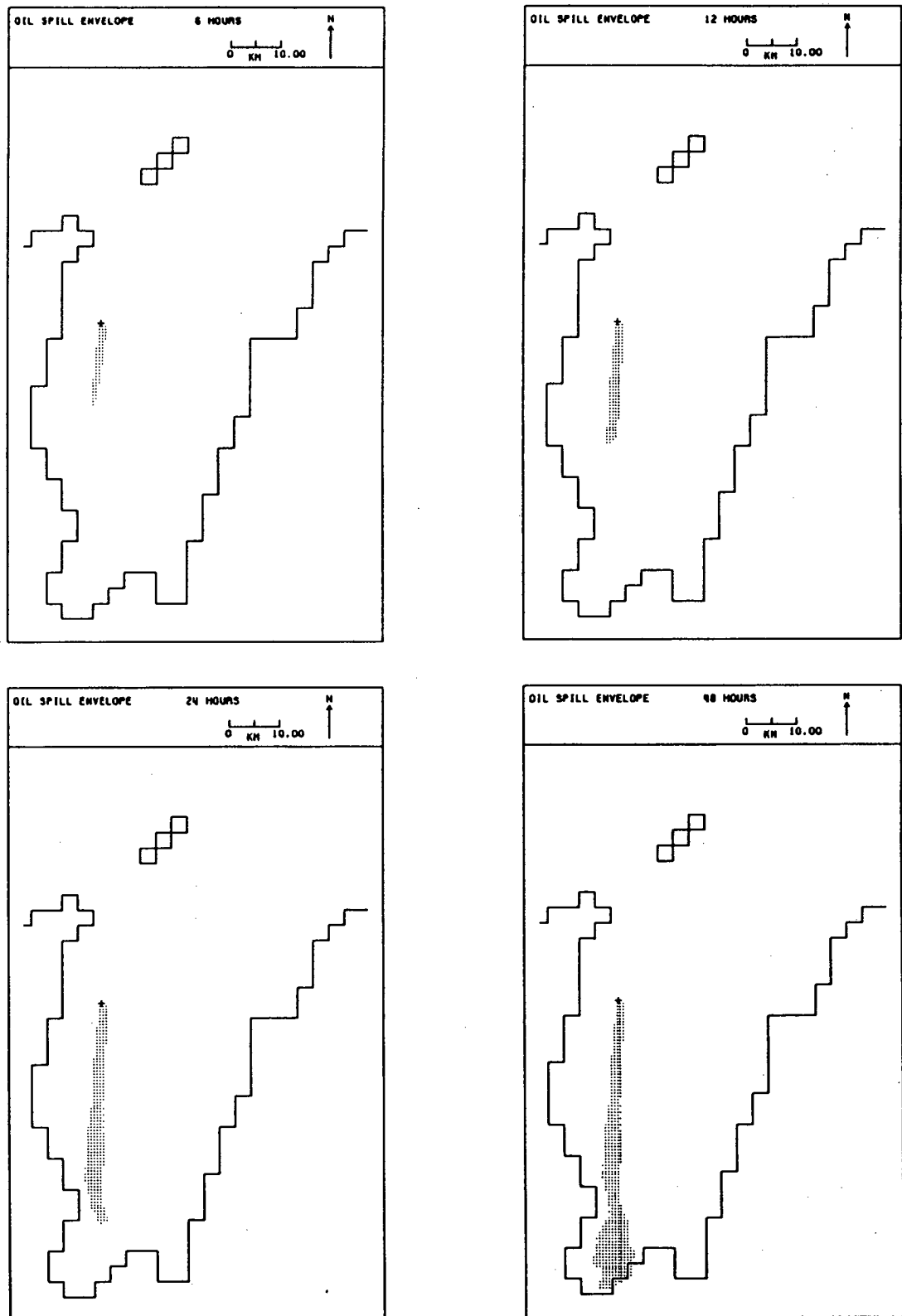


Figure 5.36 Oil spill envelopes for release times of 6, 12, 24 and 48 hours for the case of a 10 m s^{-1} north-westerly wind during spring tides for Rivoli Prospect.

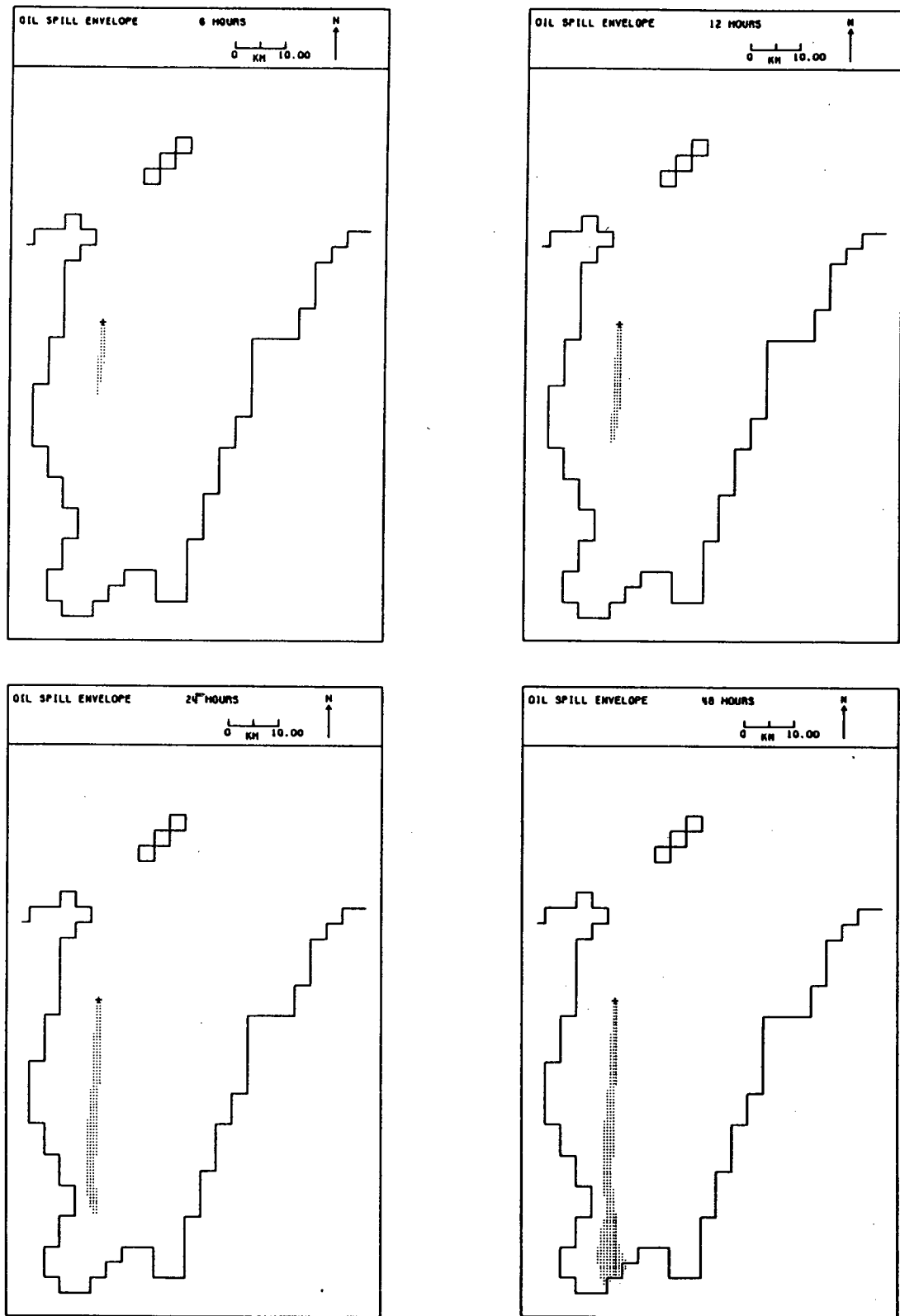


Figure 5.37 Oil spill envelopes for release times of 6, 12, 24 and 48 hours for the case of a 10 m s^{-1} north-westerly wind during neap tides for Rivoli Prospect.

Appendix A

Average Monthly Wind Speed and
Direction Percentage Occurrence Matrices
for Learmonth Meteorological Office and
Exmouth Navy Alpha for the months November through April

STEEDMAN LIMITED

JOB NO. 769

LOCATION: LEARMONTH

WIND SPEED-DIRECTION PERCENTAGE OCCURRENCE MATRIX

=====

LATITUDE: 22 14' 30" S LONGITUDE: 114 5' 36" E

ELEV AHD: ELEV AGL: 10.0 M.

PERIOD: NOVEMBER (1975 TO 1984)

		WIND SPEED (M/S)								TOTALS
		0.1	2.1	4.1	6.1	8.1	10.1	12.1	14.1	
		TO	TO	TO	TO	TO	TO	TO	AND	
		2.0	4.0	6.0	8.0	10.0	12.0	14.0	OVER	
D I R E C T I O N	N	.1	.3	.5	.7		.1			1.8
	NE	.2	.6	1.6	1.1	.6	.1			4.2
	E	.3	1.1	2.4	.6	.1				4.5
	SE	.2	.7	1.0	.5	.5				2.8
	S	.5	2.1	3.6	4.8	2.8	.6			14.4
	SW	1.7	5.3	13.4	20.1	14.1	3.0	.2		57.8
	W	.5	1.1	1.7	4.2	2.9	.3			10.7
	NW		.3	.4	.3					1.1
TOTALS		3.5	11.5	24.6	32.3	20.9	4.3	.2	.0	

OCCURRENCE OF CALMS 2.8%

STATISTICAL SUMMARY

=====

2399 DATA POINTS USED

	MEAN	MAX	S.D.
U - COMP	2.2	10.4	3.3
V - COMP	4.0	11.4	3.6
WIND SPEED	6.3	13.9	2.3

NOTE:

1. SPEEDS IN GROUP 0.1 TO 2.0 IMPLIES $0.0 < S \leq 2.0$, ETC
2. DIRECTION GROUPS 22.5 DEG EITHER SIDE OF SPECIFIED DIRECTION
3. DATA SAMPLE INTERVAL IS 180 MINUTES
4. U - COMP IS +VE EAST, V - COMP IS +VE NORTH
5. DATA SAMPLED 0-2100

Table A.1 Wind speed and direction percentage occurrence matrix for
Learmonth Meteorological Office. Data spans the month November
for the years 1975 to 1984.

STEEDMAN LIMITED

JOB NO. 769

LOCATION: LEARMONTH

WIND SPEED-DIRECTION PERCENTAGE OCCURRENCE MATRIX

LATITUDE: 22 14' 30" S LONGITUDE: 114 5' 36" E
ELEV AHD: ELEV AGL: 10.0 M.

PERIOD: DECEMBER (1975 TO 1984)

		WIND SPEED (M/S)								TOTALS
		0.1	2.1	4.1	6.1	8.1	10.1	12.1	14.1	
		TO	TO	TO	TO	TO	TO	TO	AND	
		2.0	4.0	6.0	8.0	10.0	12.0	14.0	OVER	
D I R E C T I O N	N	.3	.6	.8	.3	.1				2.1
	NE	.2	.8	1.9	1.5	.4				4.7
	E	.1	1.3	2.7	.5	.1	.1			4.7
	SE	.4	.6	.9	.6	.2				2.7
	S	.6	1.9	3.1	4.3	1.7	.4	.1		12.1
	SW	.8	4.9	12.0	19.0	13.6	4.4	.6		55.3
	W	.4	2.0	2.8	5.4	3.3	.5			14.5
	NW	.1	.5	.3	.4	.1				1.4
TOTALS		2.8	12.6	24.5	32.0	19.5	5.5	.7	.0	
OCCURRENCE OF CALMS		2.4%								

STATISTICAL SUMMARY

=====

2478 DATA POINTS USED

	MEAN	MAX	S.D.
U - COMP	2.4	-11.8	3.3
V - COMP	3.9	12.9	3.7
WIND SPEED	6.4	13.4	2.4

NOTE:

1. SPEEDS IN GROUP 0.1 TO 2.0 IMPLIES $0.0 < S \leq 2.0$, ETC
2. DIRECTION GROUPS 22.5 DEG EITHER SIDE OF SPECIFIED DIRECTION
3. DATA SAMPLE INTERVAL IS 180 MINUTES
4. U - COMP IS +VE EAST, V - COMP IS +VE NORTH
5. DATA SAMPLED 0-2100

Table A.2 Wind speed and direction percentage occurrence matrix for Learmonth Meteorological Office. Data spans the month December for the years 1975 to 1984.

STEEDMAN LIMITED

JOB NO. 769

LOCATION: LEARMONTH

WIND SPEED-DIRECTION PERCENTAGE OCCURRENCE MATRIX

=====

LATITUDE: 22 14' 30" S LONGITUDE: 114 5' 36" E

ELEV AHD: ELEV AGL: 10.0 M.

PERIOD: JANUARY (1976 TO 1985)

		WIND SPEED (M/S)								TOTALS
		0.1	2.1	4.1	6.1	8.1	10.1	12.1	14.1	
		TO	TO	TO	TO	TO	TO	TO	AND	
		2.0	4.0	6.0	8.0	10.0	12.0	14.0	OVER	
D I R E C T I O N	N	.3	1.1	1.1	1.2	.2	.1			4.1
	NE	.4	1.2	3.5	2.6	.8	.2	.1	.2	8.9
	E	.3	1.3	2.5	.6	.1			.1	4.9
	SE	.2	.8	.9	.6		.1		.1	2.7
	S	.6	1.5	3.0	3.0	1.7	.3			10.2
	SW	1.1	3.1	9.0	18.6	12.5	3.5	.8		48.8
	W	.3	1.8	2.9	5.6	2.5	1.3	.1		14.5
	NW	.2	.6	.4	.8	.2				2.3
TOTALS		3.3	11.5	23.4	33.1	18.0	5.5	1.1	.4	
OCCURRENCE OF CALMS					3.7%					

STATISTICAL SUMMARY

=====

2479 DATA POINTS USED

	MEAN	MAX	S.D.
U - COMP	2.3	-17.0	3.7
V - COMP	3.1	-15.7	4.4
WIND SPEED	6.4	18.0	2.5

NOTE:

1. SPEEDS IN GROUP 0.1 TO 2.0 IMPLIES $0.0 < S \leq 2.0$, ETC
2. DIRECTION GROUPS 22.5 DEG EITHER SIDE OF SPECIFIED DIRECTION
3. DATA SAMPLE INTERVAL IS 180 MINUTES
4. U - COMP IS +VE EAST, V - COMP IS +VE NORTH
5. DATA SAMPLED 0-2100

Table A.3 Wind speed and direction percentage occurrence matrix for Learmonth Meteorological Office. Data spans the month January for the years 1976 to 1985.

STEEDMAN LIMITED

JOB NO. 769

LOCATION: LEARMONTH

WIND SPEED-DIRECTION PERCENTAGE OCCURRENCE MATRIX

=====

LATITUDE: 22 14' 30" S LONGITUDE: 114 5' 36" E

ELEV AHD: ELEV AGL: 10.0 M.

PERIOD: FEBRUARY (1976 TO 1985)

		WIND SPEED (M/S)								TOTALS
		0.1	2.1	4.1	6.1	8.1	10.1	12.1	14.1	
		TO	TO	TO	TO	TO	TO	TO	AND	
		2.0	4.0	6.0	8.0	10.0	12.0	14.0	OVER	
D I R E C T I O N	N	.2	1.1	1.5	1.0	.5		.1		4.5
	NE	.2	1.4	3.4	2.1	.8	.4	.2	.2	8.8
	E	.4	2.3	3.8	1.5	.6	.2			8.9
	SE	.3	1.1	.9	.4	.2	.1			3.0
	S	.8	2.2	3.6	2.6	.5	.4			10.0
	SW	.9	5.3	10.8	12.9	6.6	1.5	.1		38.0
	W	.7	2.4	5.2	7.5	3.5	1.0			20.2
	NW	.3	.6	.7	.8	.2				2.6
TOTALS		3.8	16.1	29.9	28.7	12.9	3.6	.6	.3	
OCCURRENCE OF CALMS		4.0%								

STATISTICAL SUMMARY

=====

2264 DATA POINTS USED

	MEAN	MAX	S.D.
U - COMP	1.8	-14.2	4.0
V - COMP	2.0	-14.9	4.1
WIND SPEED	5.8	17.0	2.4

NOTE:

1. SPEEDS IN GROUP 0.1 TO 2.0 IMPLIES $0.0 < S \leq 2.0$, ETC
2. DIRECTION GROUPS 22.5 DEG EITHER SIDE OF SPECIFIED DIRECTION
3. DATA SAMPLE INTERVAL IS 180 MINUTES
4. U - COMP IS +VE EAST, V - COMP IS +VE NORTH
5. DATA SAMPLED 0-2100

Table A.4 Wind speed and direction percentage occurrence matrix for Learmonth Meteorological Office. Data spans the month February for the years 1976 to 1985.

STEEDMAN LIMITED

JOB NO. 769

LOCATION: LEARMONTH

WIND SPEED-DIRECTION PERCENTAGE OCCURRENCE MATRIX

=====

LATITUDE: 22 14' 30" S LONGITUDE: 114 5' 36" E

ELEV AHD: ELEV AGL: 10.0 M.

PERIOD: MARCH (1976 TO 1985)

		WIND SPEED (M/S)								TOTALS
		0.1	2.1	4.1	6.1	8.1	10.1	12.1	14.1	
		TO	TO	TO	TO	TO	TO	TO	AND	
		2.0	4.0	6.0	8.0	10.0	12.0	14.0	OVER	
D I R E C T I O N	N	.6	1.4	1.5	.8	.2	.2	.1		4.8
	NE	.4	1.9	3.3	2.4	.7	.2	.2	.3	9.3
	E	.4	2.2	3.5	1.0	.3	.2			7.7
	SE	.5	1.5	1.7	.6	.3	.1			4.7
	S	.8	2.6	4.2	3.7	1.1	.4		.1	12.9
	SW	2.2	8.3	12.3	12.9	5.0	1.2			42.0
	W	1.0	2.3	3.1	3.9	1.0		.1		11.3
	NW	.2	.4	.4	.5					1.7
TOTALS		6.2	20.5	30.0	25.8	8.6	2.3	.5	.4	
OCCURRENCE OF CALMS		5.5%								

STATISTICAL SUMMARY

=====

2480 DATA POINTS USED

	MEAN	MAX	S.D.
U - COMP	1.0	14.7	3.4
V - COMP	2.3	18.5	4.1
WIND SPEED	5.3	20.6	2.5

NOTE:

1. SPEEDS IN GROUP 0.1 TO 2.0 IMPLIES $0.0 < S \leq 2.0$, ETC
2. DIRECTION GROUPS 22.5 DEG EITHER SIDE OF SPECIFIED DIRECTION
3. DATA SAMPLE INTERVAL IS 180 MINUTES
4. U - COMP IS +VE EAST, V - COMP IS +VE NORTH
5. DATA SAMPLED 0-2100

Table A.5 Wind speed and direction percentage occurrence matrix for Learmonth Meteorological Office. Data spans the month March for the years 1976 to 1985.

STEEDMAN LIMITED

JOB NO. 769

LOCATION: LEARMONTH

WIND SPEED-DIRECTION PERCENTAGE OCCURRENCE MATRIX

=====

LATITUDE: 22 14' 30" S LONGITUDE: 114 5' 36" E

ELEV AHD: ELEV AGL: 10.0 M.

PERIOD: APRIL (1976 TO 1985)

		WIND SPEED (M/S)								TOTALS
		0.1	2.1	4.1	6.1	8.1	10.1	12.1	14.1	
		TO	TO	TO	TO	TO	TO	TO	AND	
		2.0	4.0	6.0	8.0	10.0	12.0	14.0	OVER	
D I R E C T I O N	N	.5	1.7	1.5	.6	.2				4.5
	NE	.5	2.3	3.6	2.0	.8	.5			9.8
	E	.7	3.9	3.7	1.0	.3	.3			9.8
	SE	.6	1.5	1.9	1.1	.4				5.6
	S	1.8	4.6	4.0	2.8	.4				13.6
	SW	4.1	12.6	13.2	6.8	1.5	.1			38.4
	W	1.8	2.1	3.0	1.9	.1				8.9
	NW	.4	.4	.4	.3					1.5
TOTALS		10.6	29.1	31.2	16.5	3.8	.9	.0	.0	
OCCURRENCE OF CALMS		7.8%								

STATISTICAL SUMMARY

=====

2396 DATA POINTS USED

	MEAN	MAX	S.D.
U - COMP	.3	-12.9	3.0
V - COMP	1.6	-10.4	3.4
WIND SPEED	4.4	14.4	2.1

NOTE:

1. SPEEDS IN GROUP 0.1 TO 2.0 IMPLIES $0.0 < S \leq 2.0$, ETC
2. DIRECTION GROUPS 22.5 DEG EITHER SIDE OF SPECIFIED DIRECTION
3. DATA SAMPLE INTERVAL IS 180 MINUTES
4. U - COMP IS +VE EAST, V - COMP IS +VE NORTH
5. DATA SAMPLED 0-2100

Table A.6 Wind speed and direction percentage occurrence matrix for Learmonth Meteorological Office. Data spans the month April for the years 1976 to 1985.

STEEDMAN LIMITED

JOB NO. 769

LOCATION: EXMOUTH

WIND SPEED-DIRECTION PERCENTAGE OCCURRENCE MATRIX

=====

LATITUDE: 21 49' 0" S LONGITUDE: 114 10' 0" E

ELEV AHD: ELEV AGL: 10.0 M.

PERIOD: NOVEMBER (1972 TO 1975)

		WIND SPEED (M/S)								TOTALS
		0.1	2.1	4.1	6.1	8.1	10.1	12.1	14.1	
		TO	TO	TO	TO	TO	TO	TO	AND	
		2.0	4.0	6.0	8.0	10.0	12.0	14.0	OVER	
D I R E C T I O N	N		.4	.4	.7	.1				1.5
	NE	.1	.5	.4	.4	.1	.1			1.5
	E		1.0	.6						1.5
	SE	.5	1.0	1.4	.6			.1	.1	3.7
	S	.1	2.1	5.4	9.2	10.4	7.6	4.8	1.3	40.8
	SW	1.1	4.0	4.8	5.8	3.2	3.2	.5		22.6
	W	1.1	2.4	2.4	4.9	3.9	.8	.1		15.6
	NW	.2	.6	1.2	2.0	1.0	.1			5.1
TOTALS		3.1	11.9	16.4	23.6	18.7	11.9	5.5	1.4	
OCCURRENCE OF CALMS										7.5%

STATISTICAL SUMMARY

=====

840 DATA POINTS USED

	MEAN	MAX	S.D.
U - COMP	1.6	11.9	3.5
V - COMP	5.1	16.4	4.7
WIND SPEED	7.3	16.4	3.2

NOTE:

1. SPEEDS IN GROUP 0.1 TO 2.0 IMPLIES $0.0 < S \leq 2.0$, ETC
2. DIRECTION GROUPS 22.5 DEG EITHER SIDE OF SPECIFIED DIRECTION
3. DATA SAMPLE INTERVAL IS 180 MINUTES
4. U - COMP IS +VE EAST, V - COMP IS +VE NORTH
5. DATA SAMPLED 0-2100

Table A.7 Wind speed and direction percentage occurrence matrix for Exmouth Navy Alpha station. Data spans the month November for the years 1972 to 1975.

STEEDMAN LIMITED

JOB NO. 769

LOCATION: EXMOUTH

WIND SPEED-DIRECTION PERCENTAGE OCCURRENCE MATRIX

=====

LATITUDE: 21 49' 0" S LONGITUDE: 114 10' 0" E

ELEV AHD: ELEV AGL: 10.0 M.

PERIOD: DECEMBER (1972 TO 1975)

		WIND SPEED (M/S)								TOTALS
		0.1 TO 2.0	2.1 TO 4.0	4.1 TO 6.0	6.1 TO 8.0	8.1 TO 10.0	10.1 TO 12.0	12.1 TO 14.0	14.1 AND OVER	
D I R E C T I O N	N		1.0	1.0	.2	.3			.1	2.8
	NE	.1	.6	1.5	.9	.1				3.2
	E	.1	.5	.7	.5	.1	.2	.1	.1	2.3
	SE	.1	.8	1.5	.8	.1				3.3
	S	.5	2.8	4.7	8.9	8.4	9.8	3.2	.7	38.9
	SW	.5	3.2	3.2	4.7	2.4	1.5			15.6
	W	.7	2.2	2.5	6.7	4.3	2.3	.2	.2	19.1
	NW	.2	1.3	1.0	2.6	.8				6.0
TOTALS		2.2	12.3	16.2	25.3	16.6	13.8	3.6	1.2	
OCCURRENCE OF CALMS					8.8%					

STATISTICAL SUMMARY

=====

868 DATA POINTS USED

	MEAN	MAX	S.D.
U - COMP	1.8	-14.4	3.9
V - COMP	4.3	-20.9	4.9
WIND SPEED	7.2	22.6	3.1

NOTE:

1. SPEEDS IN GROUP 0.1 TO 2.0 IMPLIES $0.0 < S \leq 2.0$, ETC
2. DIRECTION GROUPS 22.5 DEG EITHER SIDE OF SPECIFIED DIRECTION
3. DATA SAMPLE INTERVAL IS 180 MINUTES
4. U - COMP IS +VE EAST, V - COMP IS +VE NORTH
5. DATA SAMPLED 0-2100

Table A.8 Wind speed and direction percentage occurrence matrix for Exmouth Navy Alpha station. Data spans the month December for the years 1972 to 1975.

STEEDMAN LIMITED

JOB NO. 769

LOCATION: EXMOUTH

WIND SPEED-DIRECTION PERCENTAGE OCCURRENCE MATRIX

LATITUDE: 21 49' 0" S LONGITUDE: 114 10' 0" E
ELEV AHD: ELEV AGL: 10.0 M.

PERIOD: JANUARY (1973 TO 1976)

		WIND SPEED (M/S)								TOTALS
		0.1 TO 2.0	2.1 TO 4.0	4.1 TO 6.0	6.1 TO 8.0	8.1 TO 10.0	10.1 TO 12.0	12.1 TO 14.0	14.1 AND OVER	
D I R E C T I O N	N		1.3	.8	1.3	.2	.2		.6	4.4
	NE		.5	.7	.6	.2	.1		.3	2.4
	E		.5	.5	.8	.2			.5	2.4
	SE		1.8	2.1	1.0	.3	.1	.1	.2	5.8
	S	.5	2.6	4.6	7.0	5.6	4.4	1.8	.2	26.8
	SW	1.2	4.1	5.8	5.0	2.5	2.6	.8	.1	22.1
	W	.7	3.1	3.5	3.1	5.2	2.8	.8		19.1
	NW	.1	.7	1.4	3.9	1.8	.9			8.9
TOTALS		2.4	14.6	19.2	22.7	16.2	11.2	3.6	2.0	
OCCURRENCE OF CALMS		8.1%								

STATISTICAL SUMMARY

=====

868 DATA POINTS USED

	MEAN	MAX	S.D.
U - COMP	2.2	-20.4	4.5
V - COMP	3.1	-21.8	5.1
WIND SPEED	7.0	23.6	3.4

NOTE:

1. SPEEDS IN GROUP 0.1 TO 2.0 IMPLIES $0.0 < S \leq 2.0$, ETC
2. DIRECTION GROUPS 22.5 DEG EITHER SIDE OF SPECIFIED DIRECTION
3. DATA SAMPLE INTERVAL IS 180 MINUTES
4. U - COMP IS +VE EAST, V - COMP IS +VE NORTH
5. DATA SAMPLED 0-2100

Table A.9 Wind speed and direction percentage occurrence matrix for Exmouth Navy Alpha station. Data spans the month January for the years 1973 to 1976.

STEEDMAN LIMITED

JOB NO. 769

LOCATION: EXMOUTH

WIND SPEED-DIRECTION PERCENTAGE OCCURRENCE MATRIX

LATITUDE: 21 49' 0" S LONGITUDE: 114 10' 0" E
ELEV AHD: ELEV AGL: 10.0 M.

PERIOD: FEBRUARY (1973 TO 1976)

		WIND SPEED (M/S)								TOTALS
		0.1	2.1	4.1	6.1	8.1	10.1	12.1	14.1	
		TO	TO	TO	TO	TO	TO	TO	AND	
		2.0	4.0	6.0	8.0	10.0	12.0	14.0	OVER	
D I R E C T I O N	N	.1	.4	1.5	1.1	.5			.4	4.0
	NE	.4	1.4	2.0	.6	.4			.3	5.0
	E		.3	.5	.5	.1	.3	.3	.3	2.1
	SE	.1	.9	2.1	.6	.1				3.9
	S	.6	3.0	6.3	6.2	6.1	4.9	2.1	.4	29.6
	SW	.5	2.6	3.9	3.9	2.0	1.9	.6		15.5
	W	1.1	2.4	3.9	4.5	3.3	2.0	.5	.6	18.4
	NW	.3	1.6	2.3	4.0	1.4		.4	.3	10.2
TOTALS		3.2	12.6	22.6	21.6	13.9	9.1	3.9	2.1	
OCCURRENCE OF CALMS		11.1%								

STATISTICAL SUMMARY

793 DATA POINTS USED

	MEAN	MAX	S.D.
U - COMP	2.0	19.0	4.4
V - COMP	2.9	-18.0	5.2
WIND SPEED	6.9	19.5	3.3

NOTE:

1. SPEEDS IN GROUP 0.1 TO 2.0 IMPLIES $0.0 < S \leq 2.0$, ETC
2. DIRECTION GROUPS 22.5 DEG EITHER SIDE OF SPECIFIED DIRECTION.
3. DATA SAMPLE INTERVAL IS 180 MINUTES
4. U - COMP IS +VE EAST, V - COMP IS +VE NORTH
5. DATA SAMPLED 0-2100

Table A.10 Wind speed and direction percentage occurrence matrix for Exmouth Navy Alpha station. Data spans the month February for the years 1973 to 1976.

STEEDMAN LIMITED

JOB NO. 769

LOCATION: EXMOUTH

WIND SPEED-DIRECTION PERCENTAGE OCCURRENCE MATRIX

LATITUDE: 21 49' 0" S LONGITUDE: 114 10' 0" E
ELEV AHD: ELEV AGL: 10.0 M.

PERIOD: MARCH (1973 TO 1976)

		WIND SPEED (M/S)								TOTALS
		0.1	2.1	4.1	6.1	8.1	10.1	12.1	14.1	
		TO	TO	TO	TO	TO	TO	TO	AND	
		2.0	4.0	6.0	8.0	10.0	12.0	14.0	OVER	
D I R E C T I O N	N		1.3	1.6	.8	.3	.1		.1	4.3
	NE	.2	1.6	2.5	2.2	1.0	.8	.1	.3	8.9
	E	.1	1.3	1.5	1.6	1.4	1.6	.5	.3	8.3
	SE	.3	1.3	2.5	1.8	.1	.3	.2	.2	6.9
	S	.9	2.2	8.2	7.7	6.5	3.7	.5		29.7
	SW	.8	4.3	3.4	1.7	1.0	1.0	.1		12.4
	W	.9	2.3	2.2	4.5	1.0	.5	.1		11.6
	NW	.2	1.0	2.7	3.6	.1	.1		.2	8.0
TOTALS		3.6	15.3	24.6	24.0	11.6	8.2	1.5	1.3	
OCCURRENCE OF CALMS		9.9%								

STATISTICAL SUMMARY

865 DATA POINTS USED

	MEAN	MAX	S.D.
U - COMP	-.1	-26.1	4.6
V - COMP	2.0	-31.3	5.3
WIND SPEED	6.4	33.9	3.4

NOTE:

1. SPEEDS IN GROUP 0.1 TO 2.0 IMPLIES $0.0 < S \leq 2.0$, ETC
2. DIRECTION GROUPS 22.5 DEG EITHER SIDE OF SPECIFIED DIRECTION
3. DATA SAMPLE INTERVAL IS 180 MINUTES
4. U - COMP IS +VE EAST, V - COMP IS +VE NORTH
5. DATA SAMPLED 0-2100

Table A.11 Wind speed and direction percentage occurrence matrix for Exmouth Navy Alpha station. Data spans the month March for the years 1973 to 1976.

STEEDMAN LIMITED

JOB NO. 769

LOCATION: EXMOUTH

WIND SPEED-DIRECTION PERCENTAGE OCCURRENCE MATRIX

=====

LATITUDE: 21 49' 0" S LONGITUDE: 114 10' 0" E

ELEV AHD: ELEV AGL: 10.0 M.

PERIOD: APRIL (1973 TO 1976)

		WIND SPEED (M/S)								TOTALS
		0.1	2.1	4.1	6.1	8.1	10.1	12.1	14.1	
		TO	TO	TO	TO	TO	TO	TO	AND	
		2.0	4.0	6.0	8.0	10.0	12.0	14.0	OVER	
D I R E C T I O N	N	.1	1.3	.8	.4	.2				2.9
	NE	.2	2.6	2.3	1.1	.5	.5	.2		7.5
	E	.1	.8	1.2	1.1	.6	.5	.2		4.6
	SE	.2	1.9	3.4	1.3	.5	1.1	.5		8.9
	S	.6	3.0	9.7	13.0	7.7	5.9	1.6	.6	42.1
	SW	1.7	4.3	4.7	4.0	1.0	.6			16.2
	W	.6	1.2	2.3	2.5	1.0	.1			7.7
	NW	.2	1.2	1.9	1.1	.1				4.6
TOTALS		3.8	16.5	26.3	24.4	11.5	8.7	2.5	.6	
OCCURRENCE OF CALMS		5.6%								

STATISTICAL SUMMARY

=====

832 DATA POINTS USED

	MEAN	MAX	S.D.
U - COMP	-.2	-13.4	3.5
V - COMP	3.7	15.4	4.6
WIND SPEED	6.3	15.4	2.8

NOTE:

1. SPEEDS IN GROUP 0.1 TO 2.0 IMPLIES $0.0 < S \leq 2.0$, ETC
2. DIRECTION GROUPS 22.5 DEG EITHER SIDE OF SPECIFIED DIRECTION
3. DATA SAMPLE INTERVAL IS 180 MINUTES
4. U - COMP IS +VE EAST, V - COMP IS +VE NORTH
5. DATA SAMPLED 0-2100

Table A.12 Wind speed and direction percentage occurrence matrix for Exmouth Navy Alpha station. Data spans the month April for the years 1973 to 1976.

Appendix B

Theory of Wind and Tide Driven Depth-averaged
Coastal Circulation

B1 WATER LEVEL AND OCEAN CURRENT MODELSB1.1 Introduction

The subject of coastal circulation and water levels is well developed, both theoretically and experimentally (e.g. Csanady, 1982). The theoretical models, based on the equations of fluid motion, have been related to observed currents, sea level variations and water properties. Quantitative parameters such as average current movement and water levels can be estimated within reasonable bounds of error.

Numerical coastal water level and circulation models allowing for time varying wind forcing, irregular coastlines, variable bathymetry and various flows (mass transport $\text{m}^3 \text{s}^{-1}$) associated with changes of sea levels about the model boundaries are in regular use. The models fall into two main classes: vertically integrated, two-dimensional (2-D) models, and three-dimensional (3-D) models. The two-dimensional models generally have a homogeneous water density field (barotropic motion, e.g. Leendertse, 1970; Flather, 1979; Heaps, 1969; Fandry, 1982; Steedman and Craig, 1983; Davies, 1985). Water levels and vertically integrated currents are calculated by these models.

Three-dimensional models may have a homogeneous water density field (e.g. Heaps, 1974; Forristall, 1974; Fandry, 1983), or be inhomogeneous with stratification (i.e. baroclinic, e.g. Leendertse et al. 1973). The water levels, and currents may also be calculated by these models.

In general the vertically integrated model produces first order estimates of the mean currents and water levels (at relatively small costs). The more specialized 3-D models may be used where there is adequate data (to test the model) and large fast computers.

The following addresses the theory of 2-D numerical models.

B1.2 The Equations of Motion

The linear depth integrated equations of a homogeneous ocean on an f-plane and written in Cartesian coordinates (e.g. Heaps, 1969; Csanady, 1982) are

$$\partial \eta / \partial t + \partial (Hu) / \partial x + \partial (Hv) / \partial y = 0 \quad , (B1.1)$$

$$\partial u / \partial t - fv = -\partial p / \partial x - ku(u^2 + v^2)^{1/2} / H + \tau_x / (\rho H) \quad , (B1.2)$$

$$\partial v / \partial t + fu = -\partial p / \partial y - kv(u^2 + v^2)^{1/2} / H + \tau_y / (\rho H) \quad , (B1.3)$$

where x and y are horizontal coordinates; t is time; p is the pressure; u and v are components of depth averaged flow corresponding to x and y ; the total water depth $H = h + \eta$, where η is elevation of the sea surface and h is the undisturbed depth; f is the Coriolis parameter, assumed constant; g is gravitational acceleration; ρ is density of water; k is the coefficient of quadratic bottom friction and takes a value of 0.003; and τ_x and τ_y are components of wind stress corresponding to x and y .

The depth averaged currents u and v are defined by

$$u = 1/H \int_{-h}^{\eta} u' dz, \quad v = 1/H \int_{-h}^{\eta} v' dz,$$

where u' and v' are the horizontal components of current at the depth z from the sea surface whose equilibrium position is taken as $z = 0$.

B1.3 Model Assumptions

The following assumptions have been made in deriving equations (B1.1) to (B1.3):

- (i) hydrostatic balance is maintained in the vertical direction;
- (ii) horizontal shear stresses are negligible;
- (iii) non-linear advective terms in the horizontal momentum equations are negligible;
- (iv) the fluid density is horizontally uniform;
- (v) bottom friction is related directly to the component of depth averaged velocity;
- (vi) the variation of the boundary at the coast, with changes in the tidal elevation, will be of negligible importance.

Assumptions (iii) and (iv) are regarded as the most questionable, but may be justified under the following circumstances. In the absence of shallow water regions within the basin the non linear advective terms usually make only small contributions to the dynamics (Heaps, 1969). In open coastal situations without river outfalls and ground water inflows the densities may be reasonably uniform. Unless observations show otherwise it is assumed these horizontal density gradients are negligible and do not contribute to the pressure gradients.

B2 ATMOSPHERIC FORCING AND BOTTOM FRICTION

B2.1 Atmospheric Forcing

The surface atmospheric pressure forcing enters the equations of motion (B1.2) and (B1.3) through the terms $\partial p / \partial x$ and $\partial p / \partial y$. The water column pressure p is the sum of two parts

$$p = \rho g (h + \eta) + p_a,$$

one caused by the disturbance of the water level η by the storm, and the second caused by changes in the atmospheric pressure p_a . For small scale storms such as tropical cyclones p_a often is calculated at each grid point across the model for each change in position of the tropical cyclone with respect to the model grid. In the present applications it is assumed that p_a is constant across the model and therefore does not enter the driving forces.

The mean surface wind stress components τ_x and τ_y (B1.2 and B1.3) are given by

$$\tau_x = c_d \rho_a |U_{10}| U_{10} \quad , \quad (B2.1)$$

$$\tau_y = c_d \rho_a |V_{10}| V_{10} \quad , \quad (B2.2)$$

where c_d is an empirical drag coefficient, ρ_a the density of air, and U_{10} and V_{10} are the wind velocity components at 10 m above mean sea level, in the x and y directions respectively. Note the wind stress axis convention is also positive to the east and north. The magnitude of the wind speed $|S_{10}|^2 = U_{10}^2 + V_{10}^2$.

The drag coefficient c_d is reasonably well understood at wind speeds $< 20 \text{ m s}^{-1}$ and for long fetch conditions (e.g. Wu, 1969, 1980, 1981; Smith and Banke, 1975; Smith, 1980; Large and Pond, 1982). Even so, there is considerable variation in the magnitude of c_d for a given wind speed.

Figure B1.1 shows the range of c_d from various determinations. At a given wind speed of say 15 m s^{-1} the c_d may vary from about 1.4×10^{-3} to 2.0×10^{-3} , which will greatly influence the model results. Further, most of these estimates have been determined for extra-tropical cyclonic conditions of the North Atlantic.

Estimates of c_d at higher wind speeds (Wu, 1980) and under the fetch conditions associated with tropical cyclones are not available. It remains to be seen whether the disintegrated air/sea surface with intensive breaking and spray can still be described by the roughness length.

It is assumed Wu's (1980) wind stress coefficient to be the most applicable. In a slightly modified form, this becomes

$$c_d = \begin{cases} (0.8 + 0.065 U_{10}) \times 10^{-3} , & 1 < U_{10} < 20 \text{ m s}^{-1} \\ 2.1 \times 10^{-3} , & U_{10} > 20 \text{ m s}^{-1} \end{cases} \quad (B2.3)$$

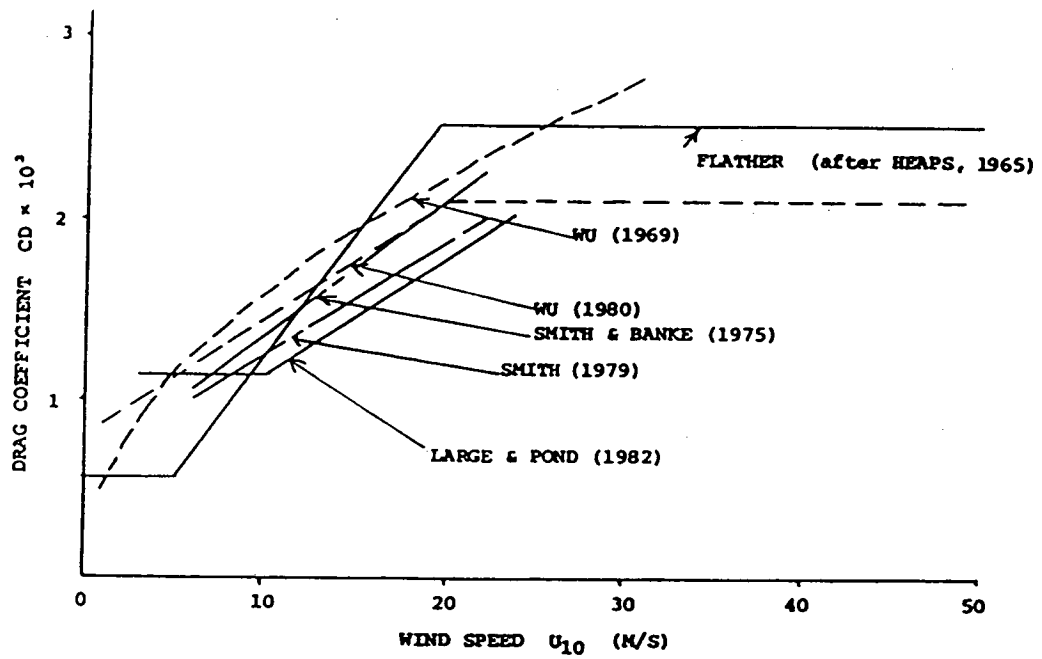


Figure B1.1 Different relationships for variations of drag coefficient with wind velocity.

where we have limited the c_d at larger wind speeds due to the change in nature of the sea surface (cf. Wu, 1969).

The wind stress is input to each model grid point using equations (B2.1) and (B2.2).

B2.2 Bottom Friction

Bottom friction was incorporated in the numerical circulation model by using a quadratic bottom friction law as in equations (B1.2) and (B1.3). This form is well accepted in the literature (Heaps, 1969; Fandry, 1982) but a range of values for the bottom friction coefficient have been found by various authors (see table B2.1). In the absence of data it is usual to set the bottom friction coefficient at a constant value of $k = 0.003$.

B3 BOUNDARY CONDITIONS

To complete the integration of the equations of motion the tidal conditions and the coastal and open sea boundary conditions must be specified at the coastal boundaries.

B3.1 Closed or Coastal Boundary

The normal component of depth averaged flow is zero, i.e.

$$\underline{v} \cdot \underline{\hat{n}} = 0 ,$$

where $\underline{\hat{n}}$ is the unit normal vector and \underline{v} is the velocity vector.

B3.2 Open Boundaries - Wind Driven Flow

The problem of the open boundary conditions under wind driven flow has received much attention (for a summary, see Fandry, 1981 and 1982), but still remains a difficulty with these models. For purely wind-driven flow, the initial condition

$$\eta = 0, \underline{v} = 0 , \text{ at } t = 0 ,$$

is set and continuity of flow is used to determine the normal flow across the boundaries. Once the elevation is prescribed along an open boundary, continuity may be used to determine the normal flow across the boundary.

Alternatively, other boundary conditions are easily implemented, for example a radiation condition given by

$$U = \sqrt{gh} \, \eta$$

or zero normal flow gradient across an open boundary.

Mean Value $k \times 10^3$	Range of Values $k \times 10^3$	Location	Water Depth (m)	Reference
2.4	1.60 - 3.00	Irish Sea		Taylor (1918)
1.8	0.57 - 2.04	Wharf Bay Anglesey		Bowden & Fairbain (1952)
2.6	-			Heaps (1978)
2.6	-	Irish Sea		Heaps & Jones (1979)
2.5	-	North Sea		Flather (1979)
5.0	-	North Sea		Davies (1985)
3.3	-	-		Ramming & Kowalik (1980)
-	1.96 - 3.35	-		Johns (1983)
-	4.80 - 10.50	Off North	90	Grant, Williams & Glenn (1984)
-	3.3 - 4.4	California	90	Grant, Williams & Glenn (1984)

Table B2.1 A range of values for the bottom friction coefficient, k , to be used in the quadratic bottom friction term of the numerical circulation model.

B4 NUMERICAL PROCEDUREB4.1 Finite Difference Scheme

The equations (B1.1) to (B1.3) are integrated over the model region using an explicit Arakawa C type finite differencing scheme (with forward time and central space differences) in which three types of grid points exist (Mesinger and Arakawa, 1976). A basic mesh element consists of a rectangle of dimensions Δx , Δy in the x and y directions respectively, with points at which u is evaluated are denoted by + at the midpoint of the y-directed sides, points at which v is evaluated are denoted by x at the midpoint of the x-directed sides and the points at which η is evaluated are denoted by o in the centre (figure B4.1). Each element of the finite difference network is identified by pairs of integers i, j corresponding to the coordinates x, y respectively. All the variables corresponding to the ijth element are denoted by the subscript ij, e.g. η_{ij} .

The land and open sea boundaries of the model are traced out on the grid approximately as closely as possible to those of the region of interest. The coastal sea under consideration is then covered by a rectangular array of elements $i = 1, n$ and $j = 1, m$ (e.g. Fandry, 1981). Only those variables within the boundary are calculated.

B4.2 Finite Difference Equations

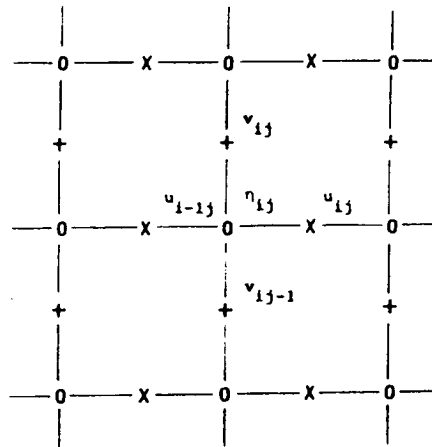
Equations (B1.1) to (B1.3) may be approximated as:

$$\begin{aligned} [\eta_{ij}(t+\Delta t) - \eta_{ij}(t)]/\Delta t = & \\ -[d_{ij}(t)u_{ij}(t) - d_{i-1j}(t)u_{i-1j}(t)]/\Delta x & \\ -[e_{ij}(t)v_{ij}(t) - e_{ij-1}(t)v_{ij-1}(t)]/\Delta y & , \end{aligned} \quad (B4.1)$$

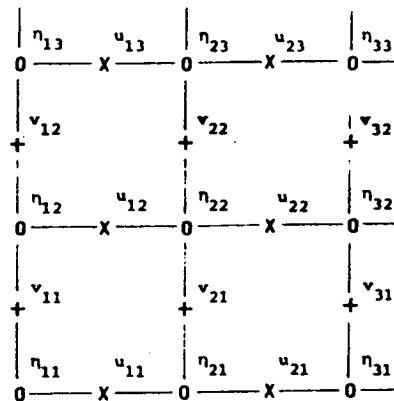
$$\begin{aligned} [u_{ij}(t+\Delta t) - u_{ij}(t)]/\Delta t = & \\ f\bar{v}_{ij}(t) - k u_{ij}(t+\Delta t) [\bar{u}_{ij}^2(t) + \bar{v}_{ij}^2(t)]^{1/2} / d_{ij}(t+\Delta t) & \\ -g [\eta_{i+1j}(t+\Delta t) - \eta_{ij}(t+\Delta t)]/\Delta x + \tau_{ij}^x / \rho d_{ij}(t+\Delta t), & \end{aligned} \quad (B4.2)$$

and

$$\begin{aligned} [v_{ij}(t+\Delta t) - v_{ij}(t)]/\Delta t = & \\ -f\bar{u}_{ij}(t+\Delta t) - k v_{ij}(t+\Delta t) [\bar{u}_{ij}^2(t+\Delta t) + \bar{v}_{ij}^2(t)]^{1/2} / e_{ij}(t+\Delta t) & \\ -g [\eta_{ij+1}(t+\Delta t) - \eta_{ij}(t+\Delta t)]/\Delta y + \tau_{ij}^y / \rho e_{ij}(t+\Delta t), & \end{aligned} \quad (B4.3)$$



- (a) interior grid network; the depths h_{ij} are located the η_{ij} points and the lines represent the model grid.



- (b) bottom left hand corner showing the boundaries; the depths h_{ij} are located at the η_{ij} points, $i, j = 1, 2, 3$.

Figure B4.1 The staggered grid geometry for the finite difference scheme (used by 2DWT.FLOW).

where

$$d_{ij} = 0.5 (H_{ij} + H_{i+1j}) ,$$

$$e_{ij} = 0.5 (H_{ij} + H_{ij+1}) ,$$

$$H_{ij} = h_{ij} + \eta_{ij} ,$$

$$\bar{v}_{ij} = [H_{ij}(v_{ij} + v_{ij-1}) + H_{i+1j}(v_{i+1j} + v_{i+1j-1})]/4H_{ij}$$

$$\bar{u}_{ij} = [H_{ij}(u_{ij} + u_{i-1j}) + H_{ij+1}(u_{ij+1} + u_{i-1j+1})]/4 H_{ij}$$

and Δt is the time increment.

Together with the appropriate boundary conditions, equations (B4.1) to (B4.3) represent an explicit system which, taken in the above order, may be solved to determine η_{ij} , u_{ij} , v_{ij} respectively at time $t+\Delta t$ from known values at the earlier time t , thereby advancing the solution one time step. The iterative procedure is carried out for the desired number of time steps starting from an initial state of rest represented by the initial conditions

$$\eta_{ij}(0) = u_{ij}(0) = v_{ij}(0) = 0 .$$

B4.3 Open Boundary Conditions for Tidal Flow

When the elevation is prescribed along an open boundary the continuity equation may be used to determine the normal flow across the boundary. For example, along an open western boundary, the normal component of transport across the boundary may take the form

$$\begin{aligned} u_{1j}(t+\Delta t) = & u_{2j}(t) + (\Delta x/\Delta y) [v_{2j}(t) - v_{2j-1}(t)] \\ & + (\Delta x/\Delta t) [\eta_{2j}(t+\Delta t) - \eta_{2j}(t)] \end{aligned}$$

B4.4 Open Boundary Conditions for Wind Driven Flow

For wind driven flow the surface elevation is set to zero.

For the radiation boundary condition, the normal flow across a boundary takes the form, e.g. for an open western boundary:

$$u_{1j}(t+\Delta t) = -[0.5g(h_{1j} + h_{2j} + \eta_{2j}(t))]^{1/2} \eta_{2j}(t) ,$$

For zero normal flow on a western boundary, the condition takes the form

$$u_{1j}(t+\Delta t) = u_{2j}(t)$$

B4.5 Stability Condition - Time Step, Δt

The time step Δt has to be chosen according to the Courant-Freidricks-Levy stability criterion given by

$$\Delta t < \min(\Delta x, \Delta y) (2g h_{\max})^{-1/2}$$

B5 REFERENCES

- Csanady, G.T., 1982. Circulation in the Coastal Ocean. D. Reidel Publishing Company (Holland).
- Davies, A.M., 1985. Application of sigma coordinate sea model to calculation of wind induced currents. Continental Shelf Res., 4, 389-423.
- Fandry, C.B., 1981. Development of a numerical model of tidal and wind driven circulation in Bass Strait. Aust. J. Freshwater Res., 32, 9-29.
- Fandry, C.B., 1982. A numerical model of the wind-driven transient motion in Bass Strait. J. Geophys. Res., 87, 499-517.
- Fandry, C.B., 1983. A model for the three-dimensional structure of wind driven and tidal circulation in Bass Strait. Australian J. Mar. and Freshw. Res., 34, 121-141.
- Flather, R.A. and N.S. Heaps, 1975. Tidal compensations for Morecomb Bay. Geophys. J.R. Astron. Soc, 42, 389-517.
- Forristall, G.Z., 1974. Three-dimensional structure of storm generated currents. J. Geophys. Res., 79, 2721-2729.
- Grant, W.D., A.J. Williams and S.M. Glenn, 1984. Bottom stress estimates and their prediction on the Northern California continental shelf during CODE-1: The Importance of Wave-Current Interaction. J. Phy. Oceanogr., 14, 506-527.
- Heaps, N.S., 1969. A two-dimensional numerical sea model. Phil Trans. Roy. Soc., A 265, 93-197.
- Heaps, N.S., 1974. Development of a three-dimensional numerical model of the Irish Sea. Rapp. P. -v. Reun. Cons. int. Explor. Mer., 167, 147-162.

- Heaps, N.S., 1978. Linearised vertically-integrated equations for residual circulation in coastal seas. *Deutsche Hydrographische Zeitschrift*, 31(5) : 147-169.
- Heaps, N.S., and Jones, J.E., 1979. Recent storm surges in the Irish Sea. In : *Marine Forecasting Predictability and Modelling in Ocean Hydrodynamics* edited by Elsevier Scientific Publishing Company (Amsterdam), pp285-319.
- Jelesnianski, C.P., 1970. Bottom Stress Time History in Linearized Equations of Motion for Storm Surges. *Mon. Weather Rev.* 98, 462-78.
- Leendertse, J.J., 1970. A water quality simulation model for well-mixed estuaries and coastal seas: Volume I, Principles of Computation. Publication number RM-6230-RC, Rand Corporation (Santa Monica).
- Leendertse, J.J., R.C. Alexander, S. Liu, 1978. A three dimensional model for estuaries and coastal seas : Volume 1 Principles of Computation. Publication number R1417-OWRR, Rand Corporation (Santa Monica).
- Mesinger, F. and A. Arakawa, 1976. Numerical methods used in atmospheric models. GARP Publ. Ser. 17, ICUS/WMO, Geneva, Switzerland.
- Nihoul, J.C.J. (edit.), 1979. *Marine Forecasting Predictability and Modelling in Ocean Hydrodynamics*. Proc. 10th International Liege Colloquium on Ocean Hydrodynamics. Elsevier Scientific Publishing Co. (Amsterdam), pp 493.
- Nihoul, J.C.J. (edit.), 1982. *Hydrodynamics of Semi-enclosed Seas*. Proc. 13th International Liege Colloquium on Ocean Dynamics. Elsevier Scientific publishing Company (Amsterdam), pp 555.
- Ramming, H.G. and Kowalik, Z., 1980. *Numerical Modelling of Marine Hydrodynamics, Applications to Dynamic Physical processes*. Elsevier Scientific Publishing Company (Amsterdam).
- Smith, S.D., 1980. Wind stress and heat flux over the ocean in gale force winds. *J. Phys. Oceanogr.*, 10, 709-726.
- Smith, S.D. and E.G. Banke, 1975. Variation of the sea surface drag coefficient with wind speed. *Quart. J. Roy. Meteor. Soc.*, 101, 655-673.
- Steedman, R.K. and P.D. Craig, 1983. Wind driven circulation of Cockburn Sound. *Aust. J. Freshw. Mar. Sci.*, 34, 187-212.
- Taylor G.I., 1918. Tidal friction in the Irish Sea. *Phil. Trans. Roy. Soc.(A)*, 220, 1-21.

- Wu, J., 1969. Froude number scaling of wind stress coefficients. J. Atmos. Sci., 26, 308-413.
- Wu, J., 1980. Wind stress coefficients over sea surface near neutral conditions - a revisit. J. Phys. Oceanogr., 10, 727-740.
- Wu, J., 1981. On critical roughness Reynolds numbers of the atmospheric surface layer. J. Geophys. Res., 86, 6661-6665.

Appendix C

Extension of Depth-Averaged Circulation
to Include Vertical Structure

C1.1 Introduction

Appendix B describes the theory of 2-D coastal circulation developed by Heaps (1969) and implemented by Fandry (1982). A numerical model, 2DWT.FLOW, based on that technique has been written by Andrewartha and Steedman (1987). Following several other authors, Fandry (1983) has extended the 2-D concept to include vertical structure by combining it with an analytical solution of the Ekman equations, to provide time dependent flow at any selected depth in terms of a convolution integral over the sea surface slope and wind stress.

The following is a description of the theory described by Fandry (1983) and used in 3DWT.FLOW.

C1.2 Equations of Motion

The linearized, 3-D equations of motion for homogeneous, hydrostatic flow on an f-plane are:

$$\frac{\partial u}{\partial t} - fv = -g \frac{\partial \eta}{\partial x} + \frac{\partial}{\partial z} \left(v \frac{\partial u}{\partial z} \right) \quad (C1.1)$$

$$\frac{\partial v}{\partial t} + fu = -g \frac{\partial \eta}{\partial y} + \frac{\partial}{\partial z} \left(v \frac{\partial v}{\partial z} \right) \quad (C1.2)$$

$$\frac{\partial u}{\partial x} + \frac{\partial v}{\partial y} + \frac{\partial w}{\partial z} = 0 \quad (C1.3)$$

where t is time; x and y the horizontal and z the vertical coordinates, respectively; u, v and w the corresponding velocity components; η the sea-surface elevation; f is the Coriolis parameter; g the gravitational acceleration; and v the coefficient of vertical eddy viscosity.

The depth-integrated versions of the equations are given by equations B1.1 to B1.3.

C1.3 Vertical Structure

Following Jelesnianski (1970), equations C1.1 and C1.2 are written in complex form,

$$\frac{\partial q}{\partial t} + ifq = -\phi + \frac{\partial}{\partial z} \left(v \frac{\partial q}{\partial z} \right) \quad (C1.4)$$

$$\text{where } q = u + iv \quad (C1.5)$$

$$\phi = g \left(\frac{\partial \eta}{\partial x} + i \frac{\partial \eta}{\partial y} \right) + \frac{1}{\rho} \left(\frac{\partial p}{\partial x} + i \frac{\partial p}{\partial y} \right) \quad (C1.6)$$

In this treatment, v is assumed to be constant with depth, thus providing equation B1.4 with a simple solution. More complicated solutions have been derived but are not treated here.

For evaluation of the eddy viscosity, Fandry uses an expression similar to that of Bowden (1967), i.e.

$$v = k e^{-1} h (\bar{u}^2 + \bar{v}^2)^{1/2}$$

where \bar{u} and \bar{v} are readily obtained from the depth-integrated calculations and k is the bottom drag coefficient.

The following boundary conditions are applied:

$$q = 0 \quad \text{at} \quad t = 0 \quad (C1.7)$$

$$v \frac{\partial q}{\partial z} = \tau_s \quad \text{at} \quad z = 0 \quad (C1.8)$$

$$q = 0 \quad \text{at} \quad z = -h \quad (C1.9)$$

where $\tau_s = \tau_s^x + i \tau_s^y$ is the complex form of the wind stress.

The numerical solution of the depth-integrated equations provides the history of the sea-surface slope, $\phi(t)$ at each point of a finite-difference grid. The solution of equation C1.4, together with the boundary conditions C1.7 to C1.9, becomes

$$q(z, t) = \frac{2}{h} \sum_{n=0}^{\infty} \cos \left[\left(n + \frac{1}{2} \right) \frac{\pi z}{h} \right] \int_0^t \left[\tau_s(t - \tau) - \frac{(-1)^n \phi(t - \tau)}{(n + \frac{1}{2}) \pi / h} \right] e^{s_n \tau} d\tau \quad (C1.10)$$

$$\text{where } s_n = -if - v(n + \frac{1}{2})^2 \pi^2 / h^2 \quad (C1.11)$$

The complex velocity in equation C1.10 is seen to consist of two parts: the first term is due to the wind stress and represents the 'drift current', the second term is due to the sea-surface slope and represents the 'slope current'.

The infinite series in equation C1.10 is uniformly and absolutely convergent and allows the interchange of summation and integration, a step which is implemented in the following section which details the numerical calculation of equation C1.10.

C1.4 Numerical Calculation of the Complex Velocity

The wind stress term in equation C1.10 can be integrated by parts as

$$\int_0^t \tau_s(t - \tau) e^{s_n \tau} d\tau$$

$$\begin{aligned}
&= \frac{e^{\frac{s}{s_n} \tau}}{s_n} \tau_s(t-\tau) \Big|_0^t - \int_0^t \frac{e^{\frac{s}{s_n} \tau}}{s_n} \frac{\partial \tau_s}{\partial \tau} (t-\tau) d\tau \\
&= \frac{1}{s_n} \left[e^{\frac{s}{s_n} t} \tau_s(0) - \tau_s(t) \right] - \frac{1}{s_n} \int_0^t e^{\frac{s}{s_n} \tau} \frac{\partial \tau_s}{\partial \tau} (t-\tau) d\tau .
\end{aligned}$$

Equation C1.10 then becomes,

$$\begin{aligned}
q(z,t) = \frac{2}{h} \sum_{n=0}^{\infty} \cos\left[\left(n + \frac{1}{2}\right) \frac{\pi z}{h}\right] \left\{ \frac{1}{s_n} \left[e^{\frac{s}{s_n} t} \tau_s(0) - \tau_s(t) \right] \right. \\
\left. + \int_0^t \left[-\frac{1}{s_n} \frac{\partial \tau_s}{\partial \tau} (t-\tau) - \frac{(-1)^n \phi(t-\tau)}{\left(n + \frac{1}{2}\right) \pi/h} \right] e^{\frac{s}{s_n} \tau} d\tau \right\} .
\end{aligned}$$

Changing variable, $t' = t - \tau$, gives

$$\begin{aligned}
q(z,t) = \frac{2}{h} \sum_{n=0}^{\infty} \cos\left[\left(n + \frac{1}{2}\right) \frac{\pi z}{h}\right] \left\{ \frac{1}{s_n} \left[e^{\frac{s}{s_n} t} \tau_s(0) - \tau_s(t) \right] \right. \\
\left. + \int_0^t \left[\frac{1}{s_n} \frac{\partial \tau_s}{\partial t'} (t') - \frac{(-1)^n \phi(t')}{\left(n + \frac{1}{2}\right) \pi/h} \right] e^{\frac{s}{s_n} (t-t')} dt' \right\}
\end{aligned}$$

Interchange summation and integration, and separate out the time-varying term gives

$$\begin{aligned}
q(z,t) = \frac{2}{h} \sum_{n=0}^{\infty} \cos\left[\left(n + \frac{1}{2}\right) \frac{\pi z}{h}\right] \frac{1}{s_n} \left[e^{\frac{s}{s_n} t} \tau_s(0) - \tau_s(t) \right] \\
+ \frac{2}{h} \int_0^t \sum_{n=0}^{\infty} \cos\left[\left(n + \frac{1}{2}\right) \frac{\pi z}{h}\right] \left[\frac{1}{s_n} \frac{\partial \tau_s}{\partial t'} (t') - \frac{(-1)^n \phi(t')}{\left(n + \frac{1}{2}\right) \pi/h} \right] \\
e^{\frac{s}{s_n} (t-t')} dt' \quad (C1.12)
\end{aligned}$$

The first term above is due to the wind stress at time = 0 and time = t and may therefore be calculated independently of the numerical time-stepping loop.

The second term is the convolution integral of the wind stress and surface slope terms.

For the numerical implementation of equation C1.12 put

$$c_n = (n + \frac{1}{2}) \frac{\pi}{h} \quad . \quad (C1.13)$$

Then,

$$\begin{aligned} \frac{1}{s_n} &= - \frac{1}{if + v c_n^2} \\ &= (v c_n^2 - if) / Q_n \end{aligned} \quad (C1.14)$$

$$\text{where } Q_n = -[v^2 c_n^4 + f^2] .$$

Therefore,

$$\frac{1}{s_n} e^{s_n t} = e^{-v c_n^2 t} [R_1 - i R_2] / Q_n , \quad (C1.15)$$

$$\text{where } R_1 = (v c_n^2 \cos ft - f \sin ft)$$

$$R_2 = (f \cos ft + v c_n^2 \sin ft) .$$

Also,

$$e^{s_n(t-t')} = [\cos f(t-t') - i \sin f(t-t')] e^{-v c_n^2(t-t')}$$

which implies

$$\frac{1}{s_n} e^{s_n(t-t')} = [S_1 - i S_2] e^{-v c_n^2(t-t')}$$

$$\text{where } S_1 = (v c_n^2 \cos f(t-t') - f \sin f(t-t')) / Q_n$$

$$S_2 = (f \cos f(t-t') + v c_n^2 \sin f(t-t')) / Q_n$$

and

$$\begin{aligned} \frac{1}{s_n} e^{s_n(t-t')} \frac{\partial \tau}{\partial t'} &= [(S_1 \frac{\partial \tau^x}{\partial t'} + S_2 \frac{\partial \tau^y}{\partial t'}) + i(S_1 \frac{\partial \tau^y}{\partial t'} - S_2 \frac{\partial \tau^x}{\partial t'})] \\ &\quad e^{-v c_n^2(t-t')} . \end{aligned} \quad (C1.16)$$

Also, on substitution of equation C1.6,

$$e^{s_n(t-t')} \frac{(-1)^n \phi(t')}{c_n} = \frac{(-1)^n q}{c_n} [(\eta_x \cos f(t-t') + \eta_y \sin f(t-t')) + i(\eta_y \cos f(t-t') - \eta_x \sin f(t-t'))] e^{-vc_n^2(t-t')} \quad (C1.17)$$

where

$$\eta_x = \frac{\partial \eta}{\partial x}, \quad \eta_y = \frac{\partial \eta}{\partial y}.$$

Substitution of equations C1.14 to C1.17 into C1.12 leads to the final expanded equation

$$\begin{aligned} q(z, t) = & \frac{2}{h} \sum_{n=0}^{\infty} \frac{\cos(c_n z)}{Q_n} \{ [R_1 \tau^x(0) + R_2 \tau^y(0)] e^{-vc_n^2 t} - [vc_n^2 \tau^x(t) + f \tau^y(t)] \\ & + i([R_1 \tau^y(0) - R_2 \tau^x(0)] e^{-vc_n^2 t} - [vc_n^2 \tau^y(t) - f \tau^x(t)]) \} \\ & + \frac{2}{h} \int_0^t \sum_{n=0}^{\infty} \cos(c_n z) e^{-vc_n^2(t-t')} \{ [s_1 \frac{\partial \tau^x}{\partial t'} + s_2 \frac{\partial \tau^y}{\partial t'}] \\ & - \frac{(-1)^n q}{c_n} [\eta_x \cos f(t-t') + \eta_y \sin f(t-t')] \} \\ & + i([s_1 \frac{\partial \tau^y}{\partial t'} - s_2 \frac{\partial \tau^x}{\partial t'}] - \frac{(-1)^n q}{c_n} [\eta_y \cos f(t-t') - \eta_x \sin f(t-t')]) dt' \quad (C1.18) \end{aligned}$$

Upon numerical calculation of $q(z, t)$ the x-component of velocity at depth z and time t is given by the real component of q , while the y-component of velocity is given by the imaginary component.

C1.5 Properties of the Solution

The solution given by equation C1.10 does not in general satisfy physical boundary conditions along a coastline. That is, the normal component of the depth-dependent currents is not constrained to be zero. This problem could be overcome by including a horizontal viscosity, however, in the simplified solution given here, the results are deemed valid only outside a narrow region adjacent to the coast.

Another property of the solution is that the vertical current profile at a given time, is determined by the past history of the wind field and the sea-surface slope. However, the exponential term in equation C1.10 ensures that past events beyond a certain limit do not contribute to any significant extent. This limit is given approximately by $T = 4h^2/v\pi^2$.

C2 REFERENCES

- Andrewartha, J.R. and Steedman, R.K. 1987. 2DWT.FLOW and 2DP.DISP Software Library and Reference Manual. Software for coastal numerical circulation and dispersion from a point source, written in Fortran-77. Computer Applications CA28, Steedman Limited, Perth, W.A.
- Bowden, K.F., 1967. Stability effects on mixing in tidal currents. Phys. Fluids Suppl., 10, 5278-80.
- Fandry, C.B., 1982. A numerical model of the wind-driven transient motion in Bass Strait. J. Geophys. Res., 87, 499-517.
- Fandry, C.B., 1983. Model for the three-dimensional structure of wind-driven and tidal circulation in Bass Strait. Aust. J. Mar. Freshw. Res., 34, 121-141.
- Heaps, N.S., 1969. A two dimensional numerical sea model. Phil. Trans. Roy. Soc., A265, 98-137.
- Jelesnianski, C.P., 1970. Bottom stress time history in linearized equations of motion for storm surges. Mon. Weather Rev., 98, 462-478.

ENVIRONMENTAL PROTECTION AUTHORITY
1100/11 STREET, PERTH